

For Reference

NOT TO BE TAKEN FROM THIS ROOM

Ex LIBRIS
UNIVERSITATIS
ALBERTAEISIS





Digitized by the Internet Archive
in 2023 with funding from
University of Alberta Library

<https://archive.org/details/Gauthier1973>

THE UNIVERSITY OF ALBERTA

RELEASE FORM

NAME OF AUTHOR : Luce Gauthier

TITLE OF THESIS: Test of Resonance Recognition
Criteria in Potential Scattering.

DEGREE FOR WHICH THESIS WAS PRESENTED : Ph.D.

YEAR THIS DEGREE GRANTED : 1973

Permission is hereby granted to THE UNIVERSITY OF ALBERTA LIBRARY to reproduce single copies of this thesis and to lend or sell such copies for private, scholarly or scientific research purposes only.

The author reserves other publication rights, and neither the thesis nor extensive extracts from it may be printed or otherwise reproduced without the author's written permission.

THE UNIVERSITY OF ALBERTA

TEST OF RESONANCE RECOGNITION CRITERIA
IN POTENTIAL SCATTERING

by



Luce Gauthier

A THESIS

SUBMITTED TO THE FACULTY OF GRADUATE STUDIES AND RESEARCH
IN PARTIAL FULFILLMENT OF THE REQUIREMENTS FOR THE DEGREE
OF DOCTOR OF PHILOSOPHY

IN

THEORETICAL PHYSICS

DEPARTMENT OF PHYSICS

EDMONTON, ALBERTA

FALL 1973

THE UNIVERSITY OF ALBERTA

FACULTY OF GRADUATE STUDIES AND RESEARCH

The undersigned certify that they have read, and recommend to the Faculty of Graduate Studies and Research, for acceptance, a thesis entitled TEST OF RESONANCE RECOGNITION CRITERIA IN POTENTIAL SCATTERING submitted by Luce Gauthier in partial fulfillment of the requirements for the degree of Doctor of Philosophy in Theoretical Physics.

ABSTRACT

The resonance recognition criteria are tested in three different soluble models of potential scattering. Exact solutions are obtained for the partial wave scattering amplitude in the single as well as in the two-channel cases. Resonances are forced in those models and resonance energies are determined theoretically through the definition $\text{Re } \det[D] = 0$, where $\det[D]$ is the Fredholm determinant.

The values of $\text{Im } F_{11}$, $|F_{11}|$, $\text{vel } F_{11}$ (F_{11} being the elastic channel scattering amplitude) and the elasticity parameter η (where applicable) are obtained both for the un-coupled and the coupled cases. The resonances are then identified through the criteria

- i) $\max \text{Im } F_{11}$
- ii) $\max |F_{11}|$
- iii) $\max \text{vel } F_{11}$, where $\text{vel } F_{11}$ is the velocity of F_{11} on the Argand diagram;
- iv) $\min \eta$.

The resonance energies are then compared with the theoretically defined location of resonances.

It is found that the $\max \text{Im } F_{11}$ and $\max |F_{11}|$ criteria produce by and large the most accurate resonance energies while the $\max \text{vel } F_{11}$ criterion works better as signalling the presence of resonances though

the location of resonance is usually not accurately predicted. The results on the min η criterion are difficult to conclude but suggest that it might be interesting for the study of highly inelastic problems.

ACKNOWLEDGEMENT

I would like to thank my supervisor, Professor A.N. Kamal, for his concern and constant help throughout the course of this work. I am very grateful to him for his patience and his learned comments have been most appreciated.

I would also like to take this opportunity to thank Professor M. Razavy who acted as my supervisor while Professor Kamal was on sabbatical leave. His judicious advices and his enthusiasm have been most beneficial to me.

I am furthermore indebted to Mr. R. Teshima who has done the computer programming required for this work.

My thanks also go to Mrs. M. Yiu who has typed the manuscript of this thesis.

It is my pleasure to acknowledge the warm hospitality received at the University of Alberta.

I would finally like to thank the Department of Physics for financial assistance and the National Research Council of Canada for a post-graduate scholarship.

CONTENTS

	Page
CHAPTER I : Introduction	1
The partial wave scattering amplitude	3
Resonance poles	8
Resonance parameters	12
Argand diagrams	17
Resonance recognition criteria	21
Aim of the work	29
Solution of the general two channel model	30
The $[N] [D^{-1}]$ representation for the scattering matrix	36
Techniques	38
 CHAPTER II:	
A. S-wave scattering from a separable δ -function potential	40
- single channel problem	43
- two channel problem	49
B. S-wave scattering from a separable exponential potential	62
- single channel problem	65
- two channel problem	71
C. P-wave scattering from a separable exponential potential	82
- single channel problem	84
- two channel problem	88
Summary	108

CONTENTS (continued)

	Page
REFERENCES	115
APPENDIX 1 : Numerical calculation related to section II.B	117
APPENDIX 2 : Evaluation of an integral appearing in section II.C	119

LIST OF TABLES

Table		Page
2A.1	Resonance positions and the corresponding coupling constants for the single channel case. $v(r) = \delta(r-a)$, $\ell = 0$.	48
2A.2	Resonance positions defined by $\text{Re det}[D] = 0$.	51
2A.3	Resonance widths.	52
2A.4	Resonance positions as given by the various resonance recognition criteria. Single channel problem.	53
2A.5	Resonance positions as given by the various resonance recognition criteria. Two-channel problem.	54
2B.1	Resonance positions as given by the various resonance recognition criteria and as defined by $\text{Re } D = 0$. Single channel problem $v(r) = e^{-mr}$, $\ell = 0$.	70
2B.2	Resonance positions as given by the various resonance recognition criteria and as defined by $\text{Re det}[D] = 0$. Two-channel problem.	77
2C.1	Resonance energies and corresponding coupling strengths for the single channel case. $v(r) = e^{-mr}$, $\ell = 1$.	87
2C.2	Resonance positions defined by $\text{Re det}[D] = 0$.	90
2C.3	Resonance positions defined by $\text{Re det}[D] = 0$.	91
2C.4	Resonance widths	92
2C.5	Resonance widths	93
2C.6	Resonance positions as given by the various resonance recognition criteria. Single channel problem.	94

LIST OF TABLES (continued)

Table		Page
2C.7	Resonance positions as given by the various resonance recognition criteria. Two-channel problem.	95
2C.8	Resonance positions as given by the various resonance recognition criteria. Two-channel problem.	96

LIST OF FIGURES

Figure		Page
2A.1	Im F, F and vel F for $g'_{11} = 8.17$, $g'_{12}^2 = 16$ and $k'_o{}^2 = 11.56$. Argand diagrams for $g'_{12}^2 = 0$ and 16.	55
2A.2	Argand diagrams for $g'_{11} = 16.94$, $k'_o{}^2 =$ 11.56 , $g'_{12}^2 = 0$ and 16.	56
2A.3	Im F, F , vel F and η for $g'_{11} = 16.94$, $g'_{12}^2 = 16$ and $k'_o{}^2 = 11.56$.	57
2A.4	Im F, F and vel F for $g'_{11} = -9.82$, $g'_{12}^2 = 16$ and $k'_o{}^2 = 11.56$. Argand diagrams for $g'_{12}^2 = 0$ and 16.	58
2A.5	Argand diagrams for $g'_{11} = -33.34$, $k'_o{}^2 = 11.56$, $g'_{12}^2 = 0$ and 16.	59
2A.6	Im F, F , vel F and η for $g'_{11} = -33.34$, $g'_{12}^2 = 16$ and $k'_o{}^2 = 11.56$.	60
2A.7	The absolute value of the scattering amplitude for a) $g'_{11} = -9.82$, $g'_{12}^2 = 0$ and 16 b) $g'_{11} = 8.17$, $g'_{12}^2 = 0$ and 16.	61
2B.1	Argand diagram, Im F, F and vel F for $g_{11} = 18 \text{ m}^3$ and $g_{12}^2 = 0$.	78
2B.2	Argand diagram, Im F, F and vel F for $g_{11} = 0$, $g_{22} = -18 \text{ m}^3$, $g_{12}^2 = 1 \text{ m}^6$ and $(k_o/m)^2 = 8$.	79
2B.3	Argand diagram, Im F, F and vel F for $g_{11} = 0$, $g_{22} = -18 \text{ m}^3$, $g_{12}^2 = 9 \text{ m}^6$ and $(k_o/m)^2 = 8$.	80

LIST OF FIGURES (continued)

Figure		Page
2B.4	Argand diagram, $\text{Im } F$, $ F $ and vel F for $g_{11} = 0$, $g_{22} = -18 \text{ m}^3$, $g_{12}^2 = 16 \text{ m}^6$ and $(k_o/m)^2 = 8$.	81
2C.1	$\text{m}^3 \text{ Re } G_{11}$ vs $E' \equiv (k/m)^2$.	97
2C.2	$\text{Im } F$, $ F $ and vel F for $g_{11} = -10.420 \text{ m}^3$, $g_{12}^2 = 1.2 \text{ m}^6$ and $(k_o/m)^2 = .05$. Argand diagrams for $g_{12}^2 = 0$ and 1.2 m^6 .	98
2C.3	$\text{Im } F$, $ F $ and vel F for $g_{11} = -9.800 \text{ m}^3$, $g_{12}^2 = 1.2 \text{ m}^6$ and $(k_o/m)^2 = .05$. Argand diagrams for $g_{12}^2 = 0$ and 1.2 m^6 .	99
2C.4	$\text{Im } F$, $ F $ and vel F for $g_{11} = -10.129 \text{ m}^3$, $g_{12}^2 = 1.2 \text{ m}^6$ and $(k_o/m)^2 = .10$. Argand diagrams for $g_{12}^2 = 0$ and 1.2 m^6 .	100
2C.5	$\text{Im } F$, $ F $ and vel F for $g_{11} = -9.370 \text{ m}^3$, $g_{12}^2 = 1.2 \text{ m}^6$ and $(k_o/m)^2 = .10$. Argand diagrams for $g_{12}^2 = 0$ and 1.2 m^6 .	101
2C.6	a) Argand diagram for $g_{11} = -10.420 \text{ m}^3$, $g_{12}^2 = 4 \text{ m}^6$ and $(k_o/m)^2 = .005$. b) Argand diagram for $g_{11} = -9.800 \text{ m}^3$, $g_{12}^2 = 6 \text{ m}^6$ and $(k_o/m)^2 = .005$.	102
2C.7	$\text{Im } F$, $ F $, vel F and η for $g_{11} =$ -10.420 m^3 , $g_{12}^2 = 4 \text{ m}^6$ and $(k_o/m)^2 =$.005.	103
2C.8	$\text{Im } F$, $ F $, vel F and η for $g_{11} = -9.800 \text{ m}^3$, $g_{12}^2 = 6 \text{ m}^6$ and $(k_o/m)^2 = .005$.	104

LIST OF FIGURES (continued)

Figure		Page
2C.9	a) Argand diagram for $g_{11} = -10.129 \text{ m}^3$, $g_{12}^2 = 4 \text{ m}^6$ and $(k_o/m)^2 = .01$. b) Argand diagram for $g_{11} = -9.370 \text{ m}^3$, $g_{12}^2 = 6 \text{ m}^6$ and $(k_o/m)^2 = .01$.	105
2C.10	$\text{Im } F$, $ F $, vel F and η for $g_{11} = -10.129 \text{ m}^3$, $g_{12}^2 = 4 \text{ m}^6$ and $(k_o/m)^2 = .01$.	106
2C.11	$\text{Im } F$, $ F $, vel F and η for $g_{11} = -9.370 \text{ m}^3$, $g_{12}^2 = 6 \text{ m}^6$ and $(k_o/m)^2 = .01$.	107

CHAPTER I

Introduction

During the past decade or so phase shift analysis has become an increasingly important tool to analyse experimental data on two body particle scattering. The method endeavours to find the partial wave amplitudes at a given energy to fit the data on differential cross-section (and polarization if applicable). These analyses have proved very successful in allowing recognition of resonances which were not seen on total cross-section plots (Donnachie 1968). However phase shift analyses are neither simple nor in general unique since more than one value of the phase shift, δ , and the elasticity parameter, η , can successfully fit the data (Salmeron 1970). Once an ambiguity free analysis has been done one has to define resonance recognition criteria in order to identify resonances.

The criteria (see the following section for details) are generally abstracted from the study of the Breit-Wigner form of the amplitude. The main criterion is that the partial wave amplitude should trace out a counter clockwise circle in the complex plane (Real part of the amplitude vs the imaginary part of the amplitude) as the energy is increased (Murphy 1966). The location of the resonance is then known through one of the following criteria (Plano 1970)

max Im F
max |F|
max vel F
min η

where F is the partial wave amplitude.

In view of the fact that the energy assigned to a resonance may depend on the criterion used it becomes important to know the reliability of these criteria. One way to do so would be to set up soluble models for two body scattering in a given partial wave and test the resonance recognition criteria against the theoretical definition of the resonance.

Very few such tests have to our knowledge been carried out. Collins et al. (1967) have shown the failure of the max ImF criterion in a specific Veneziano model. Phillips and Ringland (1969) who have done a more extensive study with a similar model, have found that for prominent resonances all criteria were working well while for overlapping resonances only the velocity criterion was consistently good.

The purpose of this thesis is to present soluble models of potential scattering in the coupled channel case and test the resonance recognition criteria in these models. The details are presented in the following sections.

The partial wave scattering amplitude

It has been proven that for potential satisfying the constraints

1) Local, analytic and energy independent

$$2) \int_0^\infty r |v(r)| dr < \infty$$

$$3) \int_0^\infty r^2 |v(r)| dr < \infty$$

the partial wave scattering amplitude $F_\ell(E)$ is the limit, as $k^2 \rightarrow E + i\epsilon$, of a function $F_\ell(k^2)$ which is a real analytic function in the complex k^2 -plane except for a certain number of isolated singularities, and that, from the requirement of conservation of probability flux, this function $F_\ell(k^2)$ must satisfy the unitarity condition in the physical region.

$$\text{Thus } F_\ell(E) = \lim_{k^2 \rightarrow E+i\epsilon} F_\ell(k^2) \quad [1.1]$$

$$\text{where } F_\ell(k^2) = F_\ell^*(k^{2*}) \quad [1.2]$$

and is analytic in the complex k^2 -plane except for a certain number of isolated singularities, and

$$\text{Im } F_\ell(E) = |F_\ell(E)|^2 \quad [1.3]$$

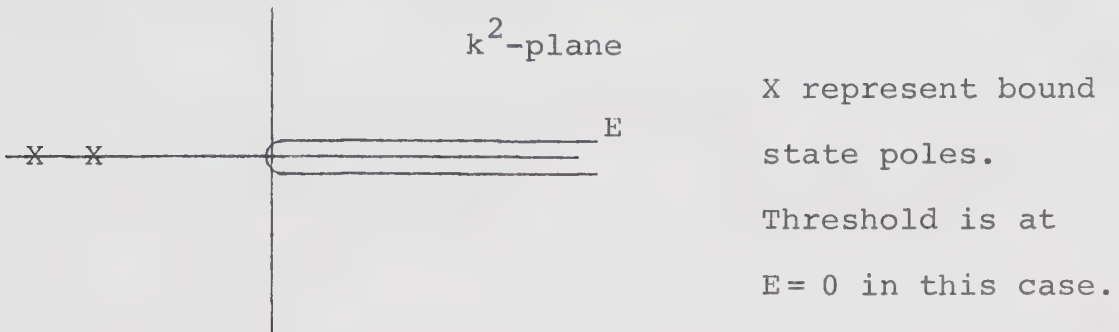
in the physical region.

From property [1.2], there will be a cut for $F_\ell(k^2)$ on the real axis except where the function is real. The discontinuity will be of

$$F_\ell(k^2+i\epsilon) - F_\ell(k^2-i\epsilon) = F_\ell(k^2+i\epsilon) - F_\ell^*(k^{2*}+i\epsilon) = 2i \text{Im } F_\ell(k^2+i\epsilon). \quad [1.4]$$

From property [1.3], unless the amplitude should identically vanish there, the function will not be real in the physical region. Thus, from [1.2] and [1.3], there should be a cut on the real axis of the k^2 -plane from threshold to infinity and the domain of analyticity of the function $F_\ell(k^2)$ will be this cut plane, except for isolated singularities or poles of $F_\ell(k^2)$. The poles of $F_\ell(k^2)$ for $k^2 = E < 0$, that is for negative energies, are the bound state poles.

Domain of analyticity of the function $F_\ell(k^2)$



There also exists an analytic continuation $F'_\ell(k^2)$, of the function $F_\ell(k^2)$, through the cut onto a second k^2 sheet such that

$$F'_\ell(E \pm i\epsilon) = F_\ell(E \mp i\epsilon) . \quad [1.5]$$

The required function $F'(k^2)$ can be found from properties [1.2], [1.3] and [1.5]

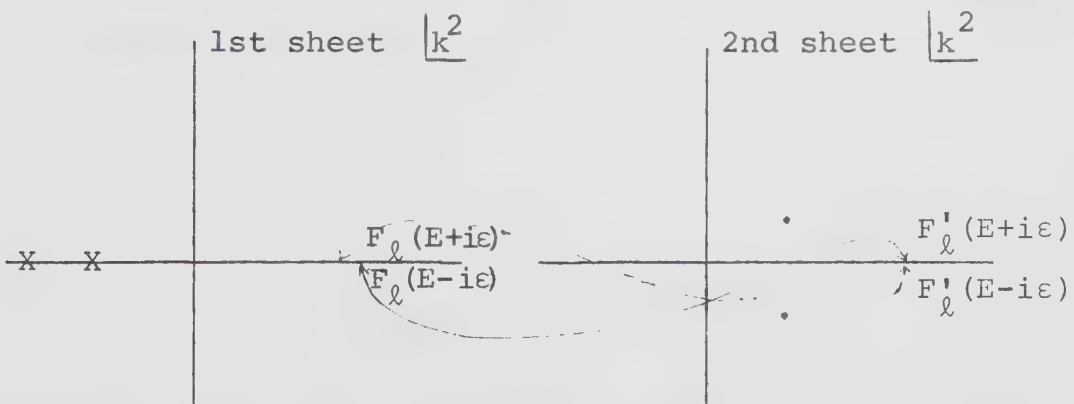
$$F'_\ell(E \pm i\varepsilon) = F_\ell(E \mp i\varepsilon) = F_\ell^*(E \pm i\varepsilon) = + \frac{\text{Im } F_\ell(E \pm i\varepsilon)}{F_\ell(E \pm i\varepsilon)} \quad [1.6]$$

so that

$$F'(k^2) = + \frac{\text{Im } F_\ell(k^2)}{F_\ell(k^2)} . \quad [1.7]$$

The analytic structure of $F_\ell(k^2)$ on the second sheet can thus be read off from eq. [1.7]. The bound state poles have disappeared but new poles have been created, corresponding to the first sheet k^2 values for which $F_\ell(k^2) = 0$ and $\text{Im } F_\ell(k^2) \neq 0$. The poles of $F_\ell(k^2)$ for $k^2 > 0$ on the second Riemann sheet define the resonance poles.

The two-sheeted Riemann surface



X represent bound state poles

- represent resonance poles

Because of the Schwartz reflection property [1.2], the resonance poles will always come in pairs since if

$$F_\ell(\operatorname{Re} k^2 + i \operatorname{Im} k^2) = 0$$

so is

$$F_\ell^*(\operatorname{Re} k^2 + i \operatorname{Im} k^2) = F_\ell(\operatorname{Re} k^2 - i \operatorname{Im} k^2) .$$

Hence if $F_\ell(\operatorname{Re} k^2 + i \operatorname{Im} k^2) = 0$, $F_\ell(\operatorname{Re} k^2 - i \operatorname{Im} k^2) = 0$, and two poles on the second sheet correspond to those zeros. However, from condition [1.1], only the pole nearer to the real axis will have a physical significance, that is the lower one on the second sheet (Frautschi 1963).

Mapping the two Riemann sheets onto the k -plane, it is found that since

$$k^2 = r e^{i\theta}$$

so that

$$k = \sqrt{r} e^{i\theta/2} ,$$

the first sheet will map onto the upper half of the k -plane ($\operatorname{Im} k > 0$), and the second sheet will map onto the lower half of the k -plane ($\operatorname{Im} k < 0$).

Hence, from this discussion, a unified definition of bound states and resonances has emerged

a bound state is a pole* of $F_\ell(k^2)$ for $\text{Im } k > 0$ and $\text{Re } k = 0$

[1.8]

a resonance is a pole of $F_\ell(k^2)$ for $\text{Im } k < 0$. [1.9]

In the case of a multi-channel problem, the function $F_\ell(k^2)$ becomes a square matrix and each of its elements can be analytically continued. $[F_\ell(k^2)]$ will have a pole when one or many of its elements become infinite for some value of k^2 . The conditions [1.2] and [1.3] will be generalized to $F(k^2) = F^\dagger(k^{2*})$ and $F(E) - F^\dagger(E) = +F^\dagger(E)F(E)$ (Messiah 1964).

When the properties [1.2] and [1.3] cannot be established because of a lack of knowledge about the matrix $[F_\ell]$, they are always assumed so that the definitions [1.8] and [1.9] are always applicable and form a basic theoretical framework to describe physical phenomena.

* Examples are knowned, (S-wave scattering through a central exponential potential) where only one pole of $F_\ell(k^2)$ is to be identified with the bound state and the others are simply the left hand cut degenerated to extra poles. The poles of $F_\ell(k^2)$ in the present thesis will be interpreted as the zeros of the Fredholm determinant and the above difficulty does not arise.

Resonance poles

Let us consider an element $f'_{\ell}(k^2)$ of the scattering matrix $[F'_{\ell}]$ which becomes infinite for $k^2 = \alpha$. α being a pole of the analytic function $f'_{\ell}(k^2)$, it is possible to expand this function, around α , in a Laurent series

$$f'_{\ell}(k^2) = e^{i\phi_{\ell}(k^2)} \sum_{n=-\infty}^{+\infty} a_{n\ell} (k^2 - \alpha)^n \quad [1.10]$$

the coefficients $a_{n\ell}$ of negative index not being all zero and $\phi_{\ell}(k^2)$ being an arbitrary phase. If the pole is of first order, as it will be assumed throughout, eq. [1.10] becomes

$$f'_{\ell}(k^2) = \frac{e^{i\phi_{\ell}(k^2)} a_{-1\ell}(\alpha)}{k^2 - \alpha} + e^{i\phi_{\ell}(k^2)} \sum_{n=0}^{\infty} a_{n\ell} (k^2 - \alpha)^n \quad [1.11]$$

where

$$\alpha = k_R^2 - i \frac{\Gamma(\alpha)}{2} \quad [1.12]$$

is the complex resonance energy, k_R^2 and $\Gamma(\alpha)$ being real and positive. The radius of convergence of the series will be equal to the distance between α and the nearest singularity of $f'_{\ell}(k^2)$.

If the nearest singularity of $f'_{\ell}(k^2)$ lies far enough from α , the expression [1.11] for $f'_{\ell}(k^2)$ will converge in a circle including the real axis so that

$$f'_\ell(E) = f_\ell(E) = \frac{e^{i\phi_\ell(E)}}{E - \alpha} + e^{i\phi_\ell(E)} \sum_{n=0}^{\infty} a_{n\ell} (E - \alpha)^n$$

[1.13]

where $f_\ell(E)$ is the physical amplitude. Expansion [1.13] will be valid only for well isolated poles and the poles of $f'_\ell(k^2)$ which will not meet this condition will define resonances which will not necessarily be experimentally observable (Newton 1966). We shall exclude from our study the consideration of resonance multipoles (Coleman 1969) which is merely a refinement of the theory to allow for the observation of two or more closely spaced resonances.

When the poles are sufficiently isolated to allow the expansion [1.13] for $f_\ell(E)$, a resonance will thus be reflected by the following form for the physical amplitude

$$f_\ell(E) = \frac{e^{i\phi_\ell(E)}}{E - k_R^2 + i \frac{\Gamma(\alpha)}{2}} + e^{i\phi_\ell(E)} \sum_{n=0}^{\infty} a_{n\ell} (E - k_R^2 + i \frac{\Gamma(\alpha)}{2})^n$$

[1.14]

where α is given by eq. [1.12]. But α can also be written

$$\alpha = k_R^2 - i \frac{\Gamma[k_R^2(1 - i \frac{\Gamma(\alpha)}{2k_R^2})]}{2} \quad [1.15]$$

so that if $\Gamma(\alpha)$ is small (Dalitz 1963), or more precisely if $\Gamma(\alpha)/2k_R^2 \ll 1$, eq. [1.15] for α becomes

$$\alpha = k_R^2 - i \frac{\Gamma(k_R^2)}{2} \quad [1.16]$$

and α is a function only of the real parameter k_R^2 .

Using this approximation in eq. [1.14], we get

$$f_\ell(E) = \frac{e^{i\phi_\ell(E)} a_{-1\ell}(k_R^2)}{E - k_R^2 + i \frac{\Gamma(k_R^2)}{2}} + e^{i\phi_\ell(E)} \sum_{n=0}^{\infty} a_{n\ell}(E - k_R^2 + i \frac{\Gamma(k_R^2)}{2})^n \quad [1.17]$$

so that for E near $k_R^2 \equiv E_R$

$$f_\ell(E) = \frac{e^{i\phi_\ell(E)} a_{-1\ell}(E_R)}{E - E_R + i \frac{\Gamma}{2}} + B_\ell(E) \quad [1.18]$$

where we have set

$$B_\ell(E) = e^{i\phi_\ell(E)} \sum_{n=0}^{\infty} a_{n\ell}(E - k_R^2 + i \frac{\Gamma(k_R^2)}{2})^n .$$

Eq. [1.18] is thus a Breit-Wigner formula. The resonance width is defined by the parameter Γ and the condition

$$\frac{\Gamma(\alpha)}{2k_R^2} \approx \frac{\Gamma(k_R^2)}{2k_R^2} \ll 1$$

is the condition for narrow resonance. Under this condition

$$\frac{\alpha}{k_R^2} = 1 - i \frac{\Gamma(k_R^2)}{2k_R^2} \approx 1$$

and the resonance energy is $\alpha = k_R^2 = E_R$.

The quantity $a_{-1\ell}$, the residue of $f_\ell'(k^2)$ at the pole, can be complex. Its norm will be related to the elastic and the reaction width. The quantity $B_\ell(E)$ represents the non-resonating background and will sometimes vanish.

Hence a resonance, defined as a second sheet pole of $f_\ell(k^2)$, produces a physical amplitude which has a Breit-Wigner shape whenever

i) the pole is sufficiently isolated [1.19]

ii) and the resonance width sufficiently narrow. [1.20]

Resonances which do not satisfy the first of these two conditions may not be resolved and therefore may not be observable. For broad resonances, when the second condition is not met, it is an open question, if not a basically insoluble problem (Burkhardt 1969) to know how to define their parameters. The definition of the resonance energy used in the present thesis is given in eq.[1.30].

Resonance parameters

Since only real energies are accessible to experiment it is necessary to reformulate the definition of the parameters of a resonance through conditions on the real k^2 axis, that is on $F_\ell(E)$ rather than on $F_\ell(k^2)$. This can be achieved consistently by requiring that the conditions imposed on $F_\ell(E)$ to produce the Breit-Wigner formula [1.18], define the resonance parameters.

Among the possible expressions for $F_\ell(E)$ in the neighbourhood of the resonance energy, we will choose to use the N_ℓ/D_ℓ representation for $F_\ell(E)$ and to expand $\text{Re } D_\ell(E)$ around E_R in a Taylor series. (The subscript ℓ will now be dropped to simplify the writing.) Writing $F(k^2)$ such that

$$F(k^2) = \frac{N(k^2)}{D(k^2)} \quad [1.21]$$

where $N(k^2)$ and $D(k^2)$ have the following properties (de Alfaro and Regge 1965), (Goldberger and Watson 1967):

- a) $N(k^2)$ has only a left cut;
- b) $D(k^2)$ has only a right cut and has simple zeros at the poles of $F(k^2)$;
- c) $N(k^2) = 0$ as $|k^2| \rightarrow \infty$; [1.22]
- d) $D(k^2) \rightarrow 1$ as $|k^2| \rightarrow \infty$;

e) $D(k^2)$ is real for $k^2 < 0$;

f) $N(k^2)$ is real for k^2 greater than the energy
of the cut;

one obtains $F(E) = \frac{N(E)}{D(E)} + \text{background terms, if any.}$ [1.23]

The background terms will arise if conditions [1.22]

cannot be met to satisfy eq. [1.21]. It has been proved
that the representation [1.21] for $F_\ell(k^2)$ is possible
for local potential satisfying the conditions on page
3 and the conditions for separable potentials are laid
out in Bertero (1968).

Around the resonance energy, eq. [1.23] becomes:

$$f_{\text{res}}(E) = \frac{N(E_R)}{\text{Re } D(E_R) + (E - E_R) \left. \frac{d \text{Re } D(E)}{dE} \right|_{E_R} + i \text{Im } D(E_R)} + B(E)$$

[1.24]

provided that the higher order terms of the expansion
for $\text{Re } D(E)$ and $\text{Im } D(E)$ are negligible. The background,
if present, should of course be a non-resonating func-
tion of E around E_R .

To get the Breit-Wigner formula [1.18] from eq.
[1.24], it must be required that

$$\text{Re } D(E_R) = 0 \quad [1.25]$$

$$\left. \frac{\text{Im } D(E)}{d \text{Re } D(E)} \right|_{E_R} = \frac{\Gamma}{2} > 0 \quad . \quad [1.26]$$

The conditions [1.25] and [1.26] shall thus be taken as the defining equations for the resonance parameters.

When the approximation $\text{Im } D(E) = \text{Im } D(E_R)$ is not possible, that is if the resonance is not narrow, one still has:

$$f_{\text{res}}(E) = \frac{N(E)}{\text{Re } D(E_R) + (E - E_R) \left. \frac{d \text{Re } D(E)}{dE} \right|_{E_R} + i \text{Im } D(E)} + B(E)$$

which through eq. [1.18] allows us to define the resonance position by

$$\text{Re } D(E_R) = 0 .$$

The following definition will also be taken for the resonance width, namely

$$\left. \frac{\text{Im } D(E)}{\frac{d \text{Re } D(E)}{dE}} \right|_{E_R} = \frac{\Gamma(E)}{2} > 0 .$$

Those two conditions will ensure the presence of a second sheet pole the real part of which will define the resonance position.

Before going into the multi-channel generalization of the definitions [1.25] and [1.26], let us see what they imply for the phase shift behaviour when this parametrization is used for the amplitude. Consistent with elastic unitarity one can write,

$$F(E) = \frac{1}{\cotg \delta - i} \quad [1.27]$$

and from [1.23], $\cotg \delta = \text{Re } D(E)/N(E) = \text{Re } D(E)/-\text{Im } D(E)$.

So that from [1.25],

$$\cotg \delta|_{E_R} = 0 \quad \text{and} \quad \delta|_{E_R} = \pi/2 \quad (\text{modulo } \pi) \quad [1.28]$$

and from [1.26]

$$\begin{aligned} \frac{\Gamma}{2} &= \frac{\text{Im } D(E)}{\frac{d}{dE} \text{Re } D(E)} \Big|_{E_R} = \frac{1}{\frac{d}{dE} \left(\frac{\text{Re } D(E)}{\text{Im } D(E)} \right)} \Big|_{E_R} = \\ &= \frac{-1}{\frac{d}{dE} \cotg \delta|_{E_R}} = \frac{1}{\csc^2 \delta \frac{d\delta}{dE}|_{E_R}} = \frac{1}{\frac{d\delta}{dE}|_{E_R}} \quad \text{and} \quad \frac{d\delta}{dE}|_{E_R} > 0. \end{aligned} \quad [1.29]$$

Hence, at resonance, the phase shift must pass through $\pi/2$ (modulo π), from below.

For a multi-channel problem, the definitions [1.25] and [1.26] are generalized to (Zachariasen and Zemach 1962)

$$\text{Re } \det[D(E_R)] = 0 \quad \text{resonance energy} \quad [1.30]$$

$$\frac{\text{Im } \det[D(E)]}{\frac{d}{dE} \text{Re } \det[D(E)]} \Big|_{E_R} = \frac{\Gamma_T}{2} > 0 \quad \text{resonance total width,} \quad [1.31]$$

where $F = [N][D^{-1}]$, $\text{Im}[D] = -[N]$ and $[D]$ is normalized to the unit matrix as $k^2 \rightarrow \infty$. Each element of the matrix $[N]$ must satisfy conditions [1.22a] and [1.22f]

and each element of the matrix [D] must satisfy conditions [1.22b] and [1.22e] (Bjorken 1960). The definition [1.31] should be changed to

$$\left. \frac{\text{Im} \det[D(E)]}{\text{Re} \det[D(E)]} \right|_{E_R} = \frac{\Gamma(E)}{2} > 0$$

for a broad resonance.

Each element $f(E)$ of $[F]$ will then have the form,

$$f(E) = \frac{C(E)}{\text{Re} \det[D] + i \text{Im} \det[D]} + B(E)$$

where $C(E)$ is a complex function of E and $B(E)$ should be non-resonating if it does not vanish. The conditions [1.30] and [1.31] will generate the following Breit-Wigner formula

$$f_{\text{res}}(E) = \frac{\left. \frac{C(E)}{\text{Re} \det[D]} \right|_{E_R} + B(E)}{E - E_R + i \frac{\Gamma_T}{2}} = e^{i\phi_C(E)} \frac{\left(\frac{|C(E_R)|}{\text{Im} \det[D(E_R)]} \right) \frac{\Gamma_T}{2}}{E - E_R + i \frac{\Gamma_T}{2}} + B(E) \quad [1.32]$$

where $\phi_C(E)$ is the phase of $C(E)$.

$$\left(\frac{|C(E_R)|}{\text{Im} \det[D(E_R)]} \right) \frac{\Gamma_T}{2} \quad [1.33]$$

will be identified with $\Gamma_{\text{el}}/2$ ($\sqrt{\Gamma_{\text{el}} \Gamma_{\text{reaction}}}/2$) if $f(E)$ is a diagonal (non-diagonal) matrix element of $[F]$, Γ_{el} and Γ_{reaction} being respectively the elastic and reaction width.

Argand diagrams

Experimentally, measurements are made on total cross-sections, differential cross-sections and polarization. The question arises: how does one recognise a resonance and determine its parameters? One has to set up some resonance recognition criteria and the clue to set up these criteria is the Breit-Wigner formula [1.18]. We will see how such criteria can be derived and it will be the purpose of this work to test their validity both below and above the inelastic threshold. We shall come back to this point later on.

One of the ways to test data for the presence of resonances is through the Argand diagram for the partial wave amplitude. $f_l(E)$ being a complex quantity, it is possible to represent it by a vector in the complex plane. As a function of the energy, the vector will describe a curve on this plane. This is the Argand diagram. Because such a plot requires the knowledge of both the imaginary and real part of the partial wave scattering amplitude, it goes without saying that in practice it is a difficult analysis to do (Salmeron 1970). It is nonetheless a very powerful and thus a widely used technique.

To analyse the special properties exhibited by a resonating Argand plot, let us go back to the expression [1.18] for the partial wave scattering amplitude. Defining,

$$\varepsilon = (E_R - E) \frac{2}{\Gamma_T} \quad \text{and} \quad A = |a_{-1\ell}(E_R)| \frac{2}{\Gamma_T} \quad [1.34]$$

eq. [1.18] becomes:

$$f_\ell(E) = e^{i\phi'_\ell(E)} \frac{A}{\varepsilon - i} + B_\ell(E) \quad [1.35]$$

where A is real and positive and $\phi'_\ell(E) = \phi_\ell(E) + \text{phase of } a_{-1\ell}(E_R) + \pi$.

For the one channel case, from eq. [1.27], this expression reduces to

$$f_\ell(E) = \frac{1}{(E - E_R)(-\frac{2}{\Gamma_T}) - i} = \frac{1}{\varepsilon - i} \quad [1.36]$$

and $A = 1$. From eq. [1.33], $\Gamma_{el}/2 = \Gamma_T/2$. The functions $\phi'_\ell(E)$ and $B_\ell(E)$ are thus arising from the presence of reaction channels and are interpreted as a non-resonating background phase and amplitude for the partial wave ℓ .

Because $\phi'_\ell(E)$ and $B_\ell(E)$ are unknown functions of energy, we will first look at the resonant Argand plot for the single-channel case [eq. 1.36]; we will then indicate what are the modifications to be expected due to the presence of reaction channels.

Letting $\phi'_\ell(E) = 0$ and $B_\ell(E) = 0$ in eq. [1.35], one gets

$$f_\ell(E) = \frac{A}{\varepsilon - i} = \frac{A\varepsilon}{\varepsilon^2 + 1} + i \frac{A}{\varepsilon^2 + 1} = \operatorname{Re} f + i \operatorname{Im} f \quad [1.37]$$

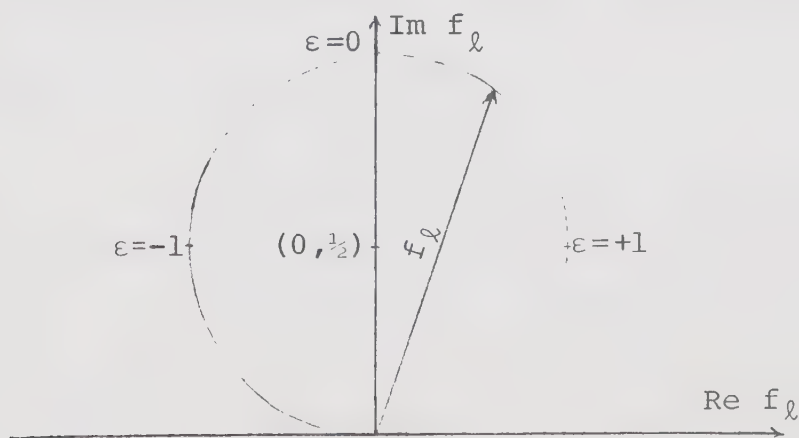
and $\operatorname{Re} f$ and $\operatorname{Im} f$ satisfy the following equation

$$(\operatorname{Re} f)^2 + (\operatorname{Im} f - \frac{A}{2})^2 = (\frac{A}{2})^2 \quad . \quad [1.38]$$

This is the equation of a circle centered at $(0, A/2)$ and of radius $A/2$.

As the energy changes from $E_R - \Gamma/2$ to $E_R + \Gamma/2$, ε goes from $\varepsilon = +1$ to $\varepsilon = -1$, eq. [1.34], and the vector representing the partial wave amplitude describes rapidly an arc in a counter clockwise direction on the upper half part of this circle. This characteristic of the resonating Argand plot serves as a main criterion to detect the presence of a resonance.

For one channel scattering, since $A = 1$, the circle is unitary and lies entirely in the upper half part of the complex plane, its center being at $(0, 1/2)$. Resonating Argand diagram for single channel scattering



When reaction channels are present such that the background functions do not vanish, the resonant circle will be rotated ($\phi'_\ell(E) \neq 0$), and its center will be displaced ($B_\ell(E) \neq 0$). If the functions $\phi'_\ell(E)$ and $B_\ell(E)$ are not slowly varying in energy, the circle could also be distorted. The hope is, of course, that the background phase and amplitude will be slowly varying in comparison with the variation in energy of the resonance amplitude (Donnachie 1970).

Resonance recognition criteria

A main criterion for the existence of resonance has thus been derived from the properties of the Argand diagram for the partial wave amplitude. Other criteria are also actually used either in connection with this one or independently. The hint for their derivation lies once again in the Breit-Wigner formula [1.35] where one assumes that $\phi'_\ell(E) = 0$ and $B_\ell(E) = 0$.

One has

$$f_{\ell \text{ res}}(E) = \frac{A}{\varepsilon - i} \quad [1.39]$$

$$\text{and } \varepsilon = 0 \text{ at } E = E_R. \text{ From eq. [1.34]} \quad \frac{d\varepsilon}{dE} = - \frac{2}{\Gamma_T}. \quad [1.40]$$

From eqs. [1.39] and [1.40], four of the criteria actually used (Plano 1970) to specify the resonance parameters can be derived. We shall consider them alternately. They are:

- at resonance
 - i) $\text{Im } f_\ell(E)$ is maximum
 - ii) $|f_\ell(E)|$ is maximum
 - iii) the velocity of $f_\ell(E)$ on an Argand plot is maximum
 - iv) the elasticity parameter is a minimum.

i) At resonance $\text{Im } f_\ell(E)$ is maximum;

From eqs. [1.39] and [1.40]

$$\text{Im } f_{\ell \text{ res}}(E) = \frac{A}{\varepsilon^2 + 1} \quad [1.42]$$

$$\frac{d \text{Im } f_{\ell \text{ res}}(E)}{dE} = \frac{4A\varepsilon}{\Gamma_T (\varepsilon^2 + 1)^2} = 0 \quad \text{at} \quad E = E_R \quad [1.43]$$

$$\left. \frac{d^2 \text{Im } f_{\ell \text{ res}}(E)}{dE^2} \right|_{E_R} = -\frac{8A}{\Gamma_T^2} < 0 , \quad [1.44]$$

so that from eq. [1.42], the function $\text{Im } f_\ell(E)$ will exhibit a Breit-Wigner shape near resonance. From eqs. [1.43] and [1.44], the point for which the function will be maximum will define the resonance energy. At half height of the peak, from eq. [1.42], $\varepsilon^2 = 1$ and $E = E_R \pm \Gamma_T/2$, so that the width of this peak at half height will specify the resonance width.

ii) At resonance $|f_\ell(E)|$ is maximum;

$$|f_{\ell \text{ res}}(E)| = (f_{\ell \text{ res}}(E) f_{\ell \text{ res}}^*(E))^{1/2} = \frac{A}{(\varepsilon^2 + 1)^{1/2}}$$

[1.45]

$$\frac{d |f_{\ell \text{ res}}(E)|}{dE} = \frac{2A\varepsilon}{\Gamma_T (\varepsilon^2 + 1)^{3/2}} = 0 \quad \text{at} \quad E = E_R \quad [1.46]$$

$$\left. \frac{d^2 |f_{\ell \text{ res}}(E)|}{dE^2} \right|_{E_R} = - \frac{8A}{\Gamma_T^2} < 0 \quad . \quad [1.47]$$

Hence, at resonance, there will be a peak of $|f_{\ell}|$ around the resonance energy. The maximum of the function will define the resonance energy. At half height of the peak, the width of the peak will be equal to $\sqrt{3} \Gamma_T$, since from eq. [1.45] ϵ^2 is then equal to 3 and $E = E_R \pm \sqrt{3} \frac{\Gamma_T}{2}$.

iii) At resonance the velocity of $f_{\ell}(E)$ on an Argand plot is maximum

$$f_{\ell \text{ res}}(E) = \frac{A}{(\epsilon^2 + 1)^{\frac{1}{2}}} e^{i \tan^{-1}(1/\epsilon)}$$

$$\text{and } \arg f_{\ell \text{ res}}(E) = \tan^{-1}(1/\epsilon) \quad [1.48]$$

$$\begin{aligned} \text{velocity of } f_{\ell \text{ res}}(E) &= \text{vel } f_{\ell \text{ res}}(E) = \frac{d \arg f_{\ell \text{ res}}(E)}{dE} \\ &= \frac{2}{\Gamma_T (\epsilon^2 + 1)} \end{aligned} \quad [1.49]$$

$$\frac{d \text{ vel } f_{\ell \text{ res}}(E)}{dE} = \frac{8\epsilon}{\Gamma_T^2 (\epsilon^2 + 1)^2} = 0 \quad \text{at} \quad E = E_R \quad [1.50]$$

$$\left. \frac{d^2 \text{ vel } f_{\ell \text{ res}}(E)}{dE^2} \right|_{E_R} = - \frac{16}{\Gamma_T^3} < 0 \quad . \quad [1.51]$$

Hence, at resonance, there will be a Breit-Wigner peak of vel $f_\ell(E)$. The maximum of this function will specify the resonance energy while from [1.49] the width of the peak at half height will define the resonance width.

iv) At resonance the elasticity parameter is a minimum

This fourth criterion is a little less general than the previous three since it can be applied only to the study of the elastic partial wave amplitude. It is based on the following parametrization for $f_\ell(E)$ namely:

$$f_\ell(E) = \frac{\eta_\ell e^{2i\alpha_\ell} - 1}{2i} \quad [1.52]$$

where η_ℓ and α_ℓ are real and $0 \leq \eta_\ell \leq 1$. [1.53]

η_ℓ is a measure of the amount of inelastic scattering taking place and is called the elasticity parameter; for one channel scattering, from eq. [1.27]

$$\eta_\ell = 1 \quad \text{and} \quad \alpha_\ell = \delta_\ell . \quad [1.54]$$

The existence of the parametrization [1.52] for the elastic scattering amplitude has been shown for any two channel problem governed by a symmetric F-matrix (Dalitz 1962). It satisfies the unitarity condition [1.3] on $F(E)$. Because any n-channel problem can be

reduced to a two-channel one through the definition of an overall reaction channel potential, the parametrization [1.52] will always be possible for an n-channel problem. The only limitation in that case being that the parameter η_ℓ is a measure of the total inelasticity and says nothing about any individual inelastic channel. Obviously, this fourth criterion will also not be applicable to single-channel scattering since in that case η_ℓ is constant as we have seen. This having been said we can now proceed to its derivation.

From eq. [1.52]

$$\eta_\ell = e^{-2i\alpha_\ell} [2i f_\ell(E) + 1] \quad [1.55]$$

and

$$\begin{aligned} \eta_\ell^2 &= |\eta_\ell|^2 = [2i f_\ell(E) + 1] [-2i f_\ell^*(E) + 1] \\ &= \{4|f_\ell(E)|^2 - 4 \operatorname{Im} f_\ell(E) + 1\} . \end{aligned}$$

From eqs. [1.42] and [1.45], near resonance

$$\eta_{\ell \text{ res}}^2 = \frac{4A^2}{\varepsilon^2 + 1} - \frac{4A}{\varepsilon^2 + 1} + 1 = \left(1 - \left|\frac{4A(A-1)}{\varepsilon^2 + 1}\right|\right) \quad [1.56]$$

since from [1.53], A being positive, it must also satisfy $A \leq 1$, for elastic scattering. [1.57]

Then

$$\frac{d\eta_\ell^2}{dE} = - |4A(A-1)| \frac{4}{\Gamma_T} \frac{\epsilon}{(\epsilon^2 + 1)^2} = 0 \quad \text{at} \quad E = E_R \quad [1.58]$$

$$\left. \frac{d^2\eta_\ell^2}{dE^2} \right|_{E_R} = |4A(A-1)| \frac{8}{\Gamma_T^2} > 0 \quad . \quad [1.59]$$

Hence from eq. [1.56] the function η_ℓ^2 will behave like an inverse Breit-Wigner peak at resonance. The maximum of the peak, that is the minimum of η_ℓ^2 or of η_ℓ , will define the resonance position and the width of the inverse peak of η_ℓ^2 , will specify the resonance width.

Let us recall that the criteria [1.41] were derived

- a) from a Breit-Wigner formula [1.60]
- b) for the special case $\phi'_\ell(E) = 0$ and $B_\ell(E) = 0$.

Those two conditions impose severe limitations to the proofs given and restrict considerably the domain over which the criteria will be strictly equivalent to the definitions of the resonance parameters by eqs. [1.30] and [1.31]. In the very special case where

$$f_\ell(E) = f_{\ell \text{ res}}(E) = \frac{A}{\epsilon - i} \quad [1.61]$$

the criterion for energy and width would be exact, since eq. [1.61] satisfies the two conditions [1.60a] and

[1.60b]. Besides this very artificial situation, there is another one for which the two first criteria will specify the resonance energy exactly but for completely different reasons: it is the one-channel case. We have seen that the partial wave amplitude for the single-channel problem can be parametrized as [1.27].

$$f_\ell(E) = \frac{1}{\cotg \delta_\ell - i} = \frac{\cotg \delta_\ell + i}{\cotg^2 \delta_\ell + 1} = \sin \delta_\ell e^{i\delta_\ell} \quad [1.62]$$

and that at resonance $\delta_{E_R} = \pi/2$ (modulo π). Let us now apply the criteria to this amplitude.

$$\text{Im } f_\ell(E) = \frac{1}{\cotg^2 \delta_\ell + 1}$$

$$|f_\ell(E)| = \frac{1}{\cotg^2 \delta_\ell + 1}$$

and those two functions will have their maximum at $\cotg^2 \delta_\ell = 0$ or $\delta_\ell = \pi/2$ (modulo π). On the other hand

$$\text{vel } f_\ell(E) = \frac{d\delta_\ell}{dE}$$

and in general

$$\left. \frac{d^2 \delta_\ell}{dE^2} \right|_{\delta_\ell=\pi/2} \neq 0$$

so that the function vel $f_\ell(E)$ need not have its maximum at $\delta_\ell = \pi/2$.

Hence for the special case of single-channel scattering the first two criteria will specify the resonance energy exactly. On the other hand, the definition of the width of the resonance [eq. 1.26] is accomplished only if the partial wave amplitude is identical to the Breit-Wigner form i.e.

$$f_\ell(E) = f_{\ell\text{res}}(E) = \frac{A}{\varepsilon - i} .$$

This in turn is possible only if the terms of order E^2 and higher in the series expansion of the denominator function in powers of E vanish. For narrow resonances these conditions will almost be realised but not for broad ones.

The resonance recognition criteria have been abstracted from the study of very special cases and would be of no practical use if their domain of applicability cannot be extended. The hope is, of course, that it can be done.

Whether the resonance is narrow or not the resonance energy is given by the condition $\text{Re } \det[D] = 0$ [eq. 1.30]. This, we have adopted as the theoretical definition of the location of the resonance against which the resonance recognition criteria are tested. The resonance energy defined by the condition $\det[D] = 0$ would differ from our definition, particularly for broad resonances.

Aim of the work

From the preceding discussion it is clear that the resonance recognition criteria are based on a Breit-Wigner form of the amplitude and that some of the criteria work exactly for elastic single channel scattering. It is not clear that the criteria will work equally well when other inelastic channels are open. The phase shift analysts however continue to use the criteria in the hope that they are still valid in presence of inelastic channels.

The aim of the present work is to set up exactly soluble models for two channel two body scattering and define the resonance theoretically. Then test the different criteria and see how well they work.

Solution of the general two-channel model

Before solving any particular problem, let us first find the general form of the F-matrix for a two-channel problem; we will consider ℓ -wave scattering and separable potentials. This general problem will contain all the particular cases that will interest us later on. We will thus solve it in some details and will always refer to it to obtain, by direct substitution, the solutions for the particular potentials considered.

The coupled Schrödinger's equations for the problem are the following ones:

$$\frac{d^2 u_{1\ell}(r)}{dr^2} + [k_1^2 - \frac{\ell(\ell+1)}{r^2}] u_{1\ell}(r) = \int_0^\infty v_{11}(r, r') u_{1\ell}(r') dr' + \int_0^\infty v_{12}(r, r') u_{2\ell}(r') dr' \quad [1.63]$$

$$\frac{d^2 u_{2\ell}(r)}{dr^2} + [k_2^2 - \frac{\ell(\ell+1)}{r^2}] u_{2\ell}(r) = \int_0^\infty v_{22}(r, r') u_{2\ell}(r') dr' + \int_0^\infty v_{21}(r, r') u_{1\ell}(r') dr' \quad [1.64]$$

where the units have been taken so that $\hbar = c = 1$;

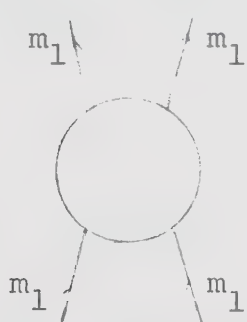
$$k_i^2 = m_i E_i, \quad E_i \text{ being the total center-of-mass kinetic energy in channel } i \quad [1.65]$$

$$k_1^2 = k_o^2 + k_2^2, \quad k_o^2 \text{ being a measure of the inelastic threshold} \quad [1.66]$$

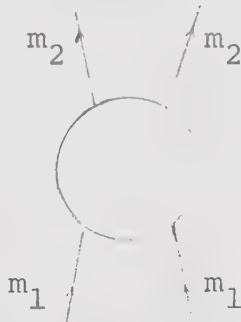
$$V_{ij} = g_{ij} v(r) v(r') \quad (i,j=1,2) \quad [1.67]$$

and where it is assumed that $g_{12} = g_{21}$.

The equations [1.63] and [1.64] represent the scattering of two identical spinless particles of mass m_1 in channel one. Channel two contains two identical spinless particles of mass m_2 . The choice of masses is to be made so that the non-relativistic approximation be valid. Schematically this scattering can be represented by the two following diagrams.



elastic scattering



inelastic scattering

Let us now solve [1.63] and [1.64]. Using [1.66] and [1.67] we get:

$$\frac{d^2 u_{1\ell}(r)}{dr^2} + [k_1^2 - \frac{\ell(\ell+1)}{r^2}] u_{1\ell}(r) = (g_{11} A_{1\ell} + g_{12} A_{2\ell}) v(r) \quad [1.68]$$

$$\frac{d^2 u_{2\ell}(r)}{dr^2} + [k_2^2 - \frac{\ell(\ell+1)}{r^2}] u_{2\ell}(r) = (g_{22} A_{2\ell} + g_{12} A_{1\ell}) v(r) \quad [1.69]$$

where

$$A_{il} = \int_0^\infty v(r') u_{il}(r') dr' . \quad [1.70]$$

Assuming, as required physically, that there is an incoming wave in the first channel only, the solutions of eqs. [1.68] and [1.69] can be written as

$$u_{1l} = r j_l(k_1 r) + (g_{11} A_{1l} + g_{12} A_{2l}) \int G'_{1l}(r, r') v(r') dr' \quad [1.71]$$

$$u_{2l} = (g_{22} A_{2l} + g_{12} A_{1l}) \int G'_{2l}(r, r') v(r') dr' \quad [1.72]$$

where

$$G'_{il}(r, r') = -k_i r_< j_l(k_i r_<) r_> h_l^+(k_i r_>) \quad [1.73]$$

is the Green function satisfying the equation:

$$\frac{d^2 G'_{il}}{dr^2} + [k_i^2 - \frac{l(l+1)}{r^2}] G'_{il} = \delta(r-r') .$$

Substituting [1.73] in [1.71] and [1.72] one can find the asymptotic expressions for $u_{1l}(r)$ and $u_{2l}(r)$.

$$u_{1l}(r) \underset{r \rightarrow \infty}{\sim} \frac{\sin(k_1 r - \frac{l\pi}{2})}{k_1} - e^{i(k_1 r - \frac{l\pi}{2})} (g_{11} A_{1l} + g_{12} A_{2l}) \times \int_0^\infty r' j_l(k_1 r') v(r') dr' \quad [1.74]$$

$$u_{2\ell}(r) \underset{r \rightarrow \infty}{\sim} -e^{i(k_2 r - \frac{\ell\pi}{2})} (g_{22}A_{2\ell} + g_{12}A_{1\ell}) \int_0^{\infty} r' j_{\ell}(k_2 r') v(r') dr' \quad [1.75]$$

And from the definition of the scattering amplitude

$$F_{11} = -k_1 (g_{11}A_{1\ell} + g_{12}A_{2\ell}) \int_0^{\infty} r' j_{\ell}(k_1 r') v(r') dr' \quad [1.76]$$

$$F_{12} = -\sqrt{k_1 k_2} (g_{22}A_{2\ell} + g_{12}A_{1\ell}) \int_0^{\infty} r' j_{\ell}(k_2 r') v(r') dr'. \quad [1.77]$$

To calculate $A_{1\ell}$ and $A_{2\ell}$, multiply [1.71] and [1.72] by $v(r)$ and integrate over r .

$$A_{1\ell} = \int_0^{\infty} r j_{\ell}(k_1 r) v(r) dr + (g_{11}A_{1\ell} + g_{12}A_{2\ell}) \int_0^{\infty} \int G'_{1\ell}(r, r') v(r') v(r) dr' dr \quad [1.78]$$

$$A_{2\ell} = (g_{22}A_{2\ell} + g_{12}A_{1\ell}) \int_0^{\infty} \int G'_{2\ell}(r, r') v(r') v(r) dr' dr. \quad [1.79]$$

Letting

$$\int_0^{\infty} \int G'_{i\ell}(r, r') v(r') v(r) dr' dr = G_{i\ell}$$

and solving [1.78] and [1.79] for $A_{1\ell}$ and $A_{2\ell}$ one gets

$$A_{1\ell} = \frac{\left(\int_0^\infty r j_\ell(k_1 r) v(r) dr \right) (1 - g_{22} G_{2\ell})}{1 - g_{22} G_{2\ell} - g_{11} G_{1\ell} + (g_{22} g_{11} - g_{12}^2) G_{1\ell} G_{2\ell}} \quad [1.80]$$

$$A_{2\ell} = \frac{g_{12} G_{2\ell} \int_0^\infty r j_\ell(k_1 r) v(r) dr}{1 - g_{22} G_{2\ell} - g_{11} G_{1\ell} + (g_{22} g_{11} - g_{12}^2) G_{1\ell} G_{2\ell}} \quad [1.81]$$

Substituting [1.80] and [1.81] in [1.76] and [1.77] one finally gets

$$F_{11} = \frac{-k_1 [g_{11} + (g_{12}^2 - g_{11} g_{22}) G_{2\ell}] \left[\int_0^\infty r v(r) j_\ell(k_1 r) dr \right]^2}{1 - g_{22} G_{2\ell} - [g_{11} + (g_{12}^2 - g_{11} g_{22}) G_{2\ell}] G_{1\ell}} \quad [1.82]$$

$$F_{12} = \frac{-\sqrt{k_1 k_2} g_{12} \left[\int_0^\infty r j_\ell(k_1 r) v(r) dr \right] \left[\int_0^\infty r j_\ell(k_2 r) v(r) dr \right]}{1 - g_{22} G_{2\ell} - [g_{11} + (g_{12}^2 - g_{11} g_{22}) G_{2\ell}] G_{1\ell}} \quad [1.83]$$

where $G_{i\ell}$ is defined by:

$$G_{i\ell} = \iint_0^\infty G'_{i\ell}(r, r') v(r') v(r) dr' dr \quad [1.84]$$

and

$$H_{i\ell} \equiv -k_i \left(\int_0^\infty r v(r) j_\ell(k_i r) dr \right)^2 = \text{Im } G_{i\ell} \text{ for real } k_i, \quad [1.85]$$

more precisely

$$\sqrt{\frac{H_{i\ell}}{k_i}} = i \left| \int_0^\infty r v(r) j_\ell(k_i r) dr \right| .$$

For the asymptotic conditions

$$u_{1\ell}(r) \underset{r \rightarrow \infty}{\sim} \frac{F_{21\ell}}{\sqrt{k_1 k_2}} e^{i(k_2 r - \frac{\ell\pi}{2})} \quad [1.86]$$

$$u_{2\ell}(r) \underset{r \rightarrow \infty}{\sim} \frac{\sin(k_2 r - \frac{\ell\pi}{2})}{k_2} + \frac{F_{22\ell}}{k_2} e^{i(k_2 r - \frac{\ell\pi}{2})} \quad [1.87]$$

one gets similarly

$$F_{22\ell} = \frac{-k_2 [g_{22} + (g_{12}^2 - g_{11}g_{22})G_{1\ell}] [\int_0^\infty r v(r) j_\ell(k_2 r) dr]^2}{1 - g_{22}G_{2\ell} - [g_{11} + (g_{12}^2 - g_{11}g_{22})G_{2\ell}]G_{1\ell}} \quad [1.88]$$

$$F_{21\ell} = \frac{-\sqrt{k_1 k_2} g_{12} [\int_0^\infty r j_\ell(k_2 r) v(r) dr] [\int_0^\infty r j_\ell(k_1 r) v(r) dr]}{1 - g_{22}G_{2\ell} - [g_{11} + (g_{12}^2 - g_{11}g_{22})G_{2\ell}]G_{1\ell}} = F_{12\ell} \quad [1.89]$$

The $[N][D^{-1}]$ representation for the F-matrix

In order to be able to use the preceding formalism, one must define an N-matrix and a D-matrix such that $F = [N][D^{-1}]$ (see paragraph after eq. [1.31]) and that the conditions on the elements of $[N]$ and $[D]$ be met. From the knowledge of $[F]$, [1.82], [1.83], [1.88] and [1.89], one finds:

$$N(k^2) = \begin{pmatrix} g_{11}H_{1\ell} & +g_{12}\sqrt{H_{1\ell}H_{2\ell}} \\ +g_{12}\sqrt{H_{1\ell}H_{2\ell}} & g_{22}H_{2\ell} \end{pmatrix} \quad [1.90]$$

$$D(k^2) = \begin{pmatrix} 1 - g_{11}G_{1\ell} & -g_{12}\sqrt{H_{2\ell}/H_{1\ell}} G_{1\ell} \\ \vdots & \\ -g_{12}\sqrt{H_{1\ell}/H_{2\ell}} G_{2\ell} & 1 - g_{22}G_{2\ell} \end{pmatrix} \quad [1.91]$$

and the potentials must be such that the functions $G_{i\ell}$ and $H_{i\ell}$ have the analytic behaviour required for the elements of $[N]$ and $[D]$.

$$\det[D] = 1 - g_{11}G_{1\ell} - g_{22}G_{2\ell} + (g_{11}g_{22} - g_{12}^2)G_{1\ell}G_{2\ell} \quad [1.92]$$

$$\operatorname{Re} \det[D] = 1 - g_{11} \operatorname{Re} G_{1\ell} - g_{22} \operatorname{Re} G_{2\ell} + (g_{11}g_{22} - g_{12}^2) \times \\ (\operatorname{Re} G_{1\ell} \operatorname{Re} G_{2\ell} - \operatorname{Im} G_{1\ell} \operatorname{Im} G_{2\ell}) \quad [1.93]$$

$$\operatorname{Im} \det[D] = -g_{11} \operatorname{Im} G_{1\ell} - g_{22} \operatorname{Im} G_{2\ell} + (g_{11}g_{22} - g_{12}^2) \times \\ (\operatorname{Re} G_{1\ell} \operatorname{Im} G_{2\ell} + \operatorname{Re} G_{2\ell} \operatorname{Im} G_{1\ell}) \quad [1.94]$$

Techniques

Now that an explicit $[N][D^{-1}]$ solution for the two channel F-matrix has been obtained, we must find some potentials and ℓ -values which will allow resonances to occur and for which it will be possible to perform the integrations [1.84] and [1.85] for $G_{i\ell}$. We have considered the following ones for which we have obtained analytic expressions for $G_{i\ell}$.

a) $v(r) = \delta(r-a)$, $\ell = 0$

b) $v(r) = e^{-mr}$, $\ell = 0$ [1.95]

c) $v(r) = e^{-mr}$, $\ell = 1$.

Because we have proceeded slightly differently in each of those cases, we shall explain later on, in greater detail, how the coupling constants have been determined and how eqs. [1.30] and [1.31] have been solved for E_R and Γ .

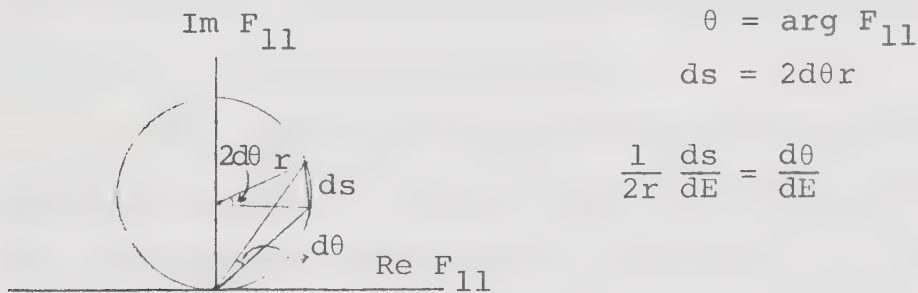
Having obtained the expression for the scattering matrix the IBM 360-67 computer at University of Alberta was used to calculate $\text{Im } F_{11}$, $|F_{11}|$, $\text{vel } F_{11}$ and η over an energy range including E_R . We have restricted our study to the F_{11} matrix-element, that is to the scattering amplitude for the elastic channel. $\text{Im } F_{11}$, $|F_{11}|$ and thus η , were calculated through their exact analytic expressions. However $\text{vel } F_{11}$ was calculated using the formula

$$\text{vel } F_{11} = \frac{[(\text{Re } F_{11a} - \text{Re } F_{11b})^2 + (\text{Im } F_{11a} - \text{Im } F_{11b})^2]^{\frac{1}{2}}}{E_b - E_a}$$

$$= \left| \frac{dF_{11}}{dE} \right| = \frac{ds}{dE} \quad , \quad [1.96]$$

where a and b represent two successive measurements of F_{11} and E . The reason for this choice is that eq. [1.96] is more suitable than $d\theta/dE$ to analyse experimental data (Phillips and Ringland 1969). When the resonant circle is not distorted, the two procedures are equivalent (see the following diagram). It was then possible to apply the four criteria to find the resonance energy as defined by each of them and to compare those values with the theoretical one.

Resonant circle showing the equivalence between $\frac{ds}{dE}$ and $\frac{d\theta}{dE}$



r being a constant when the resonant circle is not distorted \rightarrow equivalence of the two procedures. For single channel scattering $r = 1/2$ and $d\theta/dE = ds/dE$.

CHAPTER II

A. S-wave scattering from a δ -function potential

The first model that we have chosen to look at is specified by

$$v(r) = \delta(r-a), \quad l = 0. \quad [2A.1]$$

In this case the separable potential becomes local. In the case of the δ -function potential resonances can be produced in $l = 0$ state for both positive (repulsive potential) and negative (attractive potential) strengths of the potential (McVoy 1967). For the δ -function potential with a positive strength one obviously has a trapping mechanism to generate standing wave pattern in the region $0 \leq r \leq a$. For a potential with a negative strength, the rapid variation of the potential at $r = a$ imparts violent enough velocity change to the wave function to produce the right boundary condition to sustain a standing wave pattern.

The problem now is to determine the coupling constants which will allow those resonances to occur. The procedure is as follows. Setting $g_{12} = 0$ and $g_{22} = 0$, one first looks at the single channel problem. Requiring that the conditions [1.25], [1.26] and [1.28], [1.29] be satisfied, a domain of the plane (g_{11} vs k^2) over which a resonance can be forced is determined. A

particular choice (g_{11}, k^2) is then made such that for this one channel problem $(g_{11}, k^2) = (g_{11}, k_R^2)$ where k_R^2 is the resonance energy. Switching on the coupling to the second channel, a g_{12} value is chosen to produce an appropriate shift of the resonance position. The computer is then used to calculate the new resonance energy and width. This concludes the first part of the work. One now knows E_R and Γ for the single channel and the two channel problem. The shift of the resonance due to the presence of a reaction channel can be evaluated and the resonance recognition criteria can be tested using the method that has already been described in the first chapter. This is the second part of the work.

Before looking at the single channel problem and starting the analysis that has just been outlined, let us first evaluate the integrals [1.84] and [1.85] for the G_{il} functions and find the N and D matrices for the special case defined by [2A.1].

Substituting $\ell = 0$, $v(r) = \delta(r-a)$ and $v(r') = \delta(r'-a)$ in eqs. [1.84] and [1.85], and using eq. [1.73] one gets

$$\begin{aligned}
 G_{io} &= \frac{-1}{k_i} \int_0^\infty \left[\sin k_i r \right] e^{ik_i r'} \delta(r'-a) \delta(r-a) dr' dr \\
 &= \frac{-1}{k_i} \int_0^\infty \sin k_i r \delta(r-a) \int_r^\infty e^{ik_i r'} \delta(r'-a) dr' dr - \\
 &\quad - \frac{1}{k_i} \int_0^\infty e^{ik_i r} \delta(r-a) \int_0^r \sin k_i r' \delta(r'-a) dr' dr \\
 &= \frac{-1}{k_i} \sin k_i a e^{ik_i a}
 \end{aligned}
 \tag{2A.2}$$

so that

$$\operatorname{Re} G_{io} = -\frac{\sin 2k_i a}{2k_i} \text{ and } \operatorname{Im} G_{io} = -\frac{\sin^2 k_i a}{k_i} \text{ for real } k_i .$$

[2A.3]

From eq. [1.85]

$$H_{il} = -k_i \left(\int_0^\infty r \frac{\delta(r-a) \sin k_i r dr}{k_i r} \right)^2 = -\frac{\sin^2 k_i a}{k_i} \quad [2A.4]$$

From [1.90] and [1.91] and [2A.2], [2A.3], [2A.4]

$$N = \begin{pmatrix} -\frac{g_{11} \sin^2 k_1 a}{k_1} & -\frac{g_{12} \sin k_1 a \sin k_2 a}{\sqrt{k_1} \sqrt{k_2}} \\ -\frac{g_{12} \sin k_1 a \sin k_2 a}{\sqrt{k_1} \sqrt{k_2}} & -\frac{g_{22} \sin^2 k_2 a}{k_2} \end{pmatrix} \quad [2A.5]$$

$$D = \begin{pmatrix} \frac{1 + g_{11} \sin k_1 a e^{ik_1 a}}{k_1} & \frac{g_{12} \sin k_2 a e^{ik_1 a}}{\sqrt{k_1 k_2}} \\ \frac{g_{12} \sin k_1 a e^{ik_2 a}}{\sqrt{k_1 k_2}} & \frac{1 + g_{22} \sin k_2 a e^{ik_2 a}}{k_2} \end{pmatrix} \quad [2A.6]$$

$$\text{and } F = [N][D^{-1}] .$$

[2A.7]

One channel problem

Letting $g_{22} = 0$ and $g_{12} = 0$ in [2A.5], [2A.6] and [2A.7], one gets:

$$N = - \frac{g_{11} \sin^2 ka}{k} \quad [2A.8]$$

$$D = \frac{1 + g_{11} \sin ka e^{ika}}{k} \quad [2A.9]$$

$$F = \frac{N}{D} = - \frac{\frac{g_{11} \sin^2 ka}{k}}{1 + g_{11} \frac{\sin ka}{k} e^{ika}} . \quad [2A.10]$$

From eq. [2A.9]

$$\operatorname{Re} D = \frac{1 + g_{11} \sin 2ka}{2k} , \quad \operatorname{Im} D = \frac{g_{11} \sin^2 ka}{k} \quad [2A.11]$$

$$\begin{aligned} \frac{d \operatorname{Re} D}{dE} &= \frac{1}{2k} \frac{d \operatorname{Re} D}{dk} = \frac{1}{2k} \left(\frac{g_{11}}{2k^2} \right) (2ka \cos 2ka - \sin 2ka) \\ &= \frac{g_{11} \alpha(k)}{4k^3} . \end{aligned} \quad [2A.12]$$

To satisfy condition [1.25], one must have $\operatorname{Re} D = 0$ or

$$g_{11} = - \frac{2k_R}{\sin 2k_R a} \quad \text{where } k_R = \sqrt{E_R} \quad \text{and } E_R \text{ is the resonance energy.} \quad [2A.13]$$

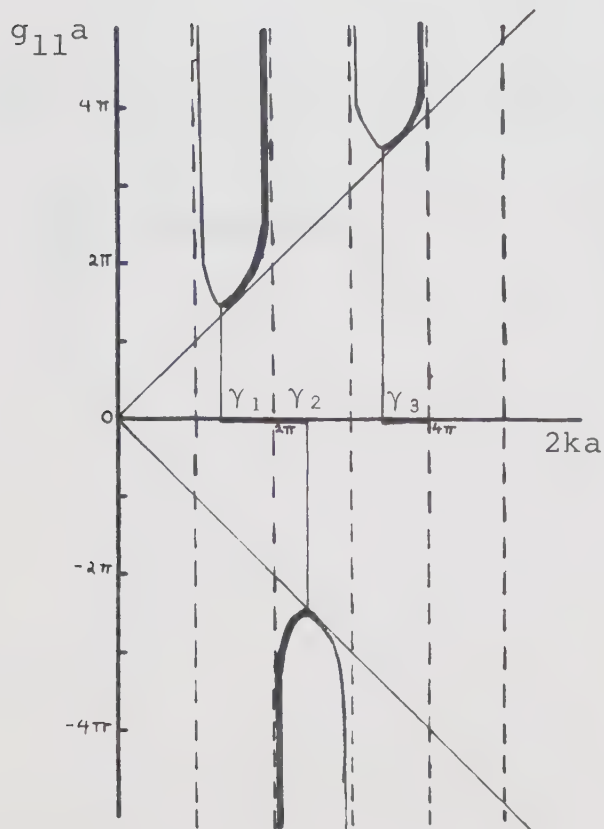
To satisfy condition [1.26], one must have

$$\left. \frac{\text{Im } D}{\frac{d}{dE} \text{Re } D} \right|_{E_R} = \frac{\Gamma}{2} > 0 ,$$

or

$$\left. \frac{4k^2 \sin^2 ka}{\alpha(k)} \right|_{E_R} = \frac{4k_R^2 \sin^2 k_R a}{\alpha(k_R)} = \frac{\Gamma}{2} > 0 \Rightarrow \alpha(k_R) > 0 . \quad [2A.14]$$

The following graph shows the regions where it is possible to have a resonance according to conditions [1.25] and [1.26].



The heavy lines represent the potential strength and energy values for which a resonance is possible.

The points $\gamma_1, \gamma_2, \gamma_3$ are determined by the relation $\alpha(k_R) = 0$.

The values of $g_{11}a$ are given by the relation $g_{11}a = -2ka/\sin 2ka$.

The behaviour of the phase shift is as follows:

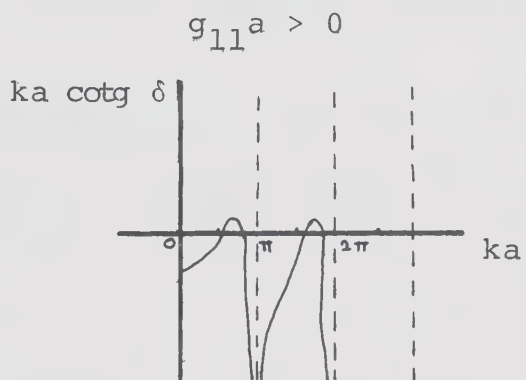
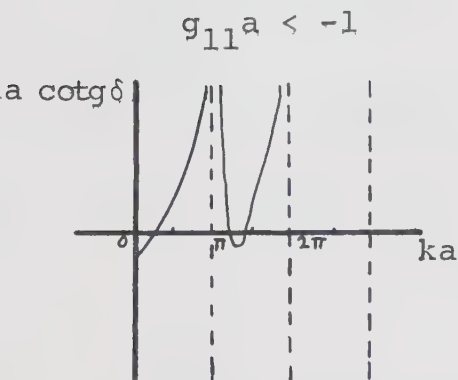
$$ka \cotg \delta = ka \left(\frac{1 + g_{11} a \frac{\sin ka}{ka} \cos ka}{-g_{11} a \frac{\sin^2 ka}{ka}} \right) \quad [2A.15]$$

and as $k \rightarrow 0$ one gets

$$\lim_{k \rightarrow 0} ka \cotg \delta \rightarrow \frac{1 + g_{11} a}{-g_{11} a} \quad [2A.16]$$

so that for $g_{11} a > 0$ and $g_{11} a < -1$, the two regions where resonances are possible, $ka \cotg \delta$ starts negative.

Let us sketch the shape of $ka \cotg \delta$ in each of those regions.



In order to draw the graph for the phase shift with respect to k , we first find the number of bound states possible in the model. We have seen [1.9] that a bound state is defined by

$$D(E) = 0 \quad \text{for } E < 0 \quad [2A.17]$$

that is

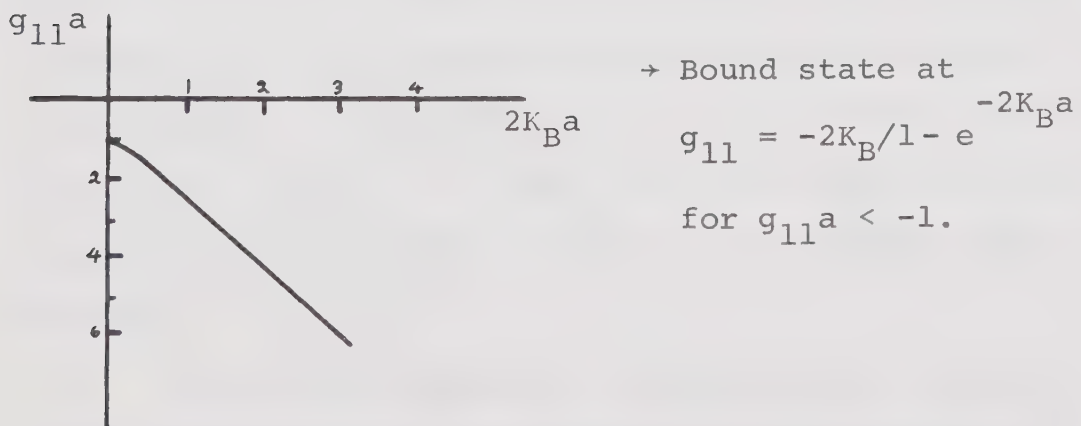
$$D(-K^2) = \frac{1 + g_{11} \sinh 2Ka}{2K} - \frac{g_{11} \sinh^2 Ka}{K} = 0 \quad \text{where } k = iK.$$

There will thus exist bound states for

$$g_{11}a = -\frac{\frac{2K_B a}{-2K_B a}}{1 - e} \quad [2A.18]$$

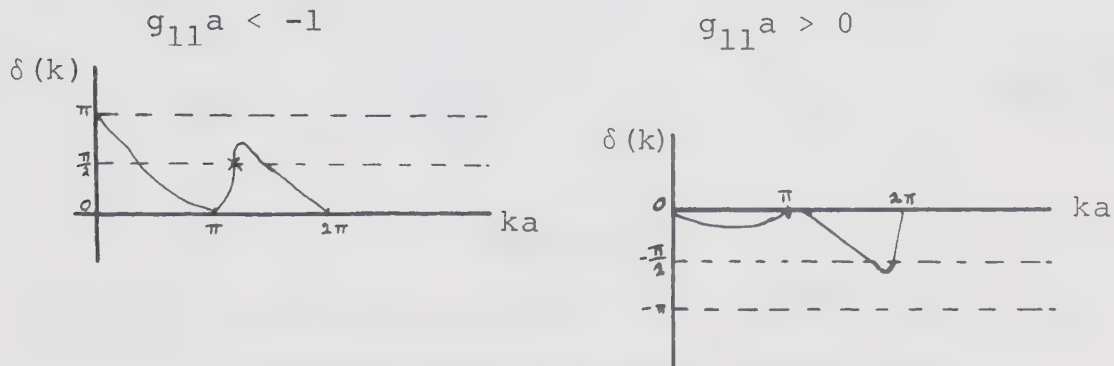
where we have set $K = K_B$, the binding energy of the bound state.

The following graph shows the bound state region. One can see that there is no bound state for $g_{11}a > -1$.



Since $D(z) \rightarrow 1$ and $D(z) \rightarrow z^c$ with $c = 0$, from
 $\underset{z \rightarrow \infty}{z} \underset{z \rightarrow 0}{}$
Levinson's theorem $\delta(0) = N\pi$ where N is the number of bound states. For $g_{11}a < -1$ there will be one bound state possible so that $\delta(0) = \pi$. For $g_{11}a > 0$ there is no bound state and $\delta(0) = 0$.

The following graphs show the phase shift behaviour with respect to ka .



* indicate resonances

As was previously seen, the passage of the phase shift through $\pi/2$ (modulo π) from below, will produce a pole of $f(k^2)$ on the second Riemann sheet and hence a resonance. A resonance will thus be possible for $g_{11}a > 0$ or for $g_{11}a < -1$ when the conditions previously mentioned are satisfied. There is no resonance possible for $-1 < g_{11}a < 0$.

To find the numerical values for $g_{11}a$, some k -values were picked in the intervals where resonances

possible (see diagram on page 44), both for positive and negative g_{11}^a , and the corresponding coupling constant g_{11}^a were calculated from eq. [2A.13]. The results are shown in table 2A.1. The parameter b was set equal to $\pi/3.2$ to simplify the calculation and a was left arbitrary. The following transformations were used:

$$k'_R = \frac{a}{b} k_R , \quad g'_{ij} = \frac{a}{b} g_{ij} , \quad b = \frac{\pi}{3.2} .$$

In terms of g'_{11} , k'_R and b , eq. [2A.13] reads:

$$g'_{11} = - \frac{2k'_R}{\sin 2k'_R b} . \quad [2A.19]$$

Table 2A.1

Resonance positions and the corresponding coupling constants for the single channel case

k_R	k'_R	g'_{11}
$14\pi/16a$	2.8	7.92
$30\pi/16a$	6.0	16.97
$36\pi/32a$	3.6	-10.18
$33\pi/32a$	3.3	-33.83

Two channel problem

From eqs. [2A.7], [2A.5] and [2A.6] we can write

$$F_{11} = \frac{N_{11}D_{22} - N_{12}D_{21}}{\det[D]} \quad [2A.20]$$

$$\begin{aligned} F_{11} &= \frac{-g_{11} \frac{\sin^2 k_1 a}{k_1} + (g_{12}^2 - g_{11}g_{22}) \times}{ik_1 a} \times \\ &\quad \frac{1+g_{11}\sin k_1 ae}{k_1} + \frac{g_{22}\sin k_2 ae}{k_2} + \\ &\quad \times \frac{\sin^2 k_1 a}{k_1} \frac{\sin k_2 a}{k_2} e^{ik_2 a} \\ &\quad + (g_{11}g_{22} - g_{12}^2) \frac{\sin k_1 a}{k_1} \frac{\sin k_2 ae}{k_2} e^{ik_2 a} \end{aligned} \quad [2A.21]$$

where

$$k_2^2 = k_1^2 - k_0^2 . \quad [2A.22]$$

For simplicity we shall let $g_{22} = 0$, i.e. no elastic potential in channel 2. From eqs. [1.30], [1.93], [2A.3] and [2A.4], the position of the resonance is determined by

$$\begin{aligned} \operatorname{Re} \det[D] = 0 &= 1 + \frac{g_{11} \sin 2k_1 a}{2k_1} \\ &- g_{12}^2 \left(\frac{\sin 2k_1 a}{2k_1} \frac{\sin 2k_2 a}{2k_2} - \frac{\sin^2 k_1 a}{k_1} \frac{\sin^2 k_2 a}{k_2} \right) \end{aligned} \quad [2A.23]$$

Choosing a g_{11} such that there is a resonance in the single channel case for a certain value of $k = k_R$, eq. [2A.23] for $g_{12}^2 \neq 0$ will then define a new position $k = k'_{1R}$ for the resonance which will be shifted because of the presence of the reaction channel. The threshold energy, k_o^2 , is so chosen that the resonances could be generated both below and above the inelastic threshold (see diagram on page 44). By trial and error the value of the inter-channel coupling constant g_{12}^2 is determined so that there is a significantly noticeable shift in the resonance position as a result of the channel coupling.

Using table 2A.1 as a guide we have thus taken for g'_{11} the values given in table 2A.2 and the computer was used to calculate $k'^2_{1R} = E'_R$ from eq. [2A.23] for $g'^2_{12} = 0$ and $g'^2_{12} = 16$. The results appear in table 2A.2. It can be seen that for large enough g'_{11} , two resonances are possible in the energy range considered. This was expected (see diagram on page 44).

The width of the resonances for the single and the two channel problems (see eqs. [1.26] and [1.31]) was also calculated in the following approximation:

$$\begin{aligned} \frac{\Gamma}{2} &= \left. \frac{\text{Im det}[D]}{\frac{d}{dE} \text{Re det}[D]} \right|_{E_R} = \left. \frac{1}{\frac{d}{dE} \left(\frac{\text{Re det}[D]}{\text{Im det}[D]} \right)} \right|_{E_R} \\ &\approx \frac{E_b - E_a}{\left[\frac{\text{Re det}[D]}{\text{Im det}[D]} \right]_b - \left[\frac{\text{Re det}[D]}{\text{Im det}[D]} \right]_a} \quad [2A.24] \end{aligned}$$

where a and b represent two successive measurements of E and $(\text{Re } \det[D]/\text{Im } \det[D])$. The results are shown in table 2A.3.

Table 2A.2

Resonance positions defined by $\text{Re } \det[D] = 0$.

For the two channel case $g_{12}'^2 = 16$ and $k_o'^2 = 11.56$. $E_R' = k_R'^2$ and $b = \pi/3.2$.

g_{11}'	one channel E_R' between	two channel E_R' between	E_R' shift under the coupling
8.17	7.9	5.8	left
	8.0	5.9	
16.94	9.0	8.6	left
	9.1	8.7	
	35.9	35.5	left
	36.0	35.6	
-9.82	13.1	11.3	left
	13.2	11.4	
-33.34	10.9	10.7	left
	11.0	10.8	
	43.6	43.8	right
	43.7	43.9	

Note: The values of g_{11}' are slightly different from those of table 2A.1. The resonance energy could have been determined more accurately but it was not considered necessary to do so since the resonance energy was shifted in the two-channel case by an amount much bigger than the uncertainty in its location.

Table 2A.3

Resonance widths defined by $\frac{\Gamma'}{2} = \frac{a^2}{b^2} \frac{\Gamma}{2}$ and eq. [2A.14]

For the two channel case $g_{12}'^2 = 16$ and $k_0'^2 = 11.56$. $b = \pi/3.2$.

g_{11}'	one channel	two channel	change in $\Gamma'/2$ under the coupling
8.17	.862	6.18	increase
16.94	.230	.384	increase
	2.43	6.34	increase
-9.82	2.19	.126	decrease
-33.34	.0929	.0354	decrease
	.611	.862	increase

Note: The large changes in width under the coupling, for $g_{11}' = 8.17$ and $g_{11}' = -9.82$, can be understood from fig. 2A.7.

Table 2A.4

Resonance positions as given by the various resonance
recognition criteria

Single channel problem $g_{12}^{\prime 2} = 0$. $E_R' = k_R'^2$ and $b = \pi/3.2$.

g_{11}'	$\text{Re } D = 0$ E_R' between	$\text{Max Im } F$ E_R' between	$\text{Max } F $ E_R' between	$\text{Max vel } F$ E_R' between
8.17	7.9	7.8	7.8	8.2
	8.0	8.0	8.0	8.4
16.94	9.0	9.0	9.0	9.1
	9.1	9.2	9.2	9.3
	35.9	35.9	35.9	36.9
	36.0	36.1	36.1	37.1
-9.82	13.1	13.0	13.0	12.3
	13.2	13.2	13.2	12.4
-33.34	10.9	10.8	10.8	10.8
	11.0	11.0	11.0	11.0
	43.6	43.6	43.6	43.4
	43.7	43.8	43.8	43.6

Table 2A.5

Resonance positions as given by the various resonance recognition criteria

Two channel problem $g_{12}^{'2} = 16$, $k_O^{'2} = 11.56$. $E_R' = k_R^{'2}$ and $b = \pi/3.2$.

g_{11}'	Re det[D]=0 E_R' between	Max Im F E_R' between	Max F E_R' between	Max vel F E_R' between	Min η E_R' between
8.17	5.8 5.9	5.8 6.0	5.8 6.0	7.2 7.4	-
16.94	8.6	8.6	8.6	8.8	
	8.7	8.8	8.8	9.0	-
-9.82	35.5 35.6	ill defined	ill defined	37.4 37.6	36.6 36.8
	11.3 11.4	11.3 11.5	11.3 11.5	11.3 11.5	-
-33.34	10.7	10.7	10.7	10.7	
	10.8	10.9	10.9	10.9	-
	43.8 43.9	43.7 43.9	43.8 44.0	43.5 43.7	43.5 43.7

Note: The appellation "ill defined" means that the data in in this case does not show a well defined maximum. This can be seen from fig. 2A.3.

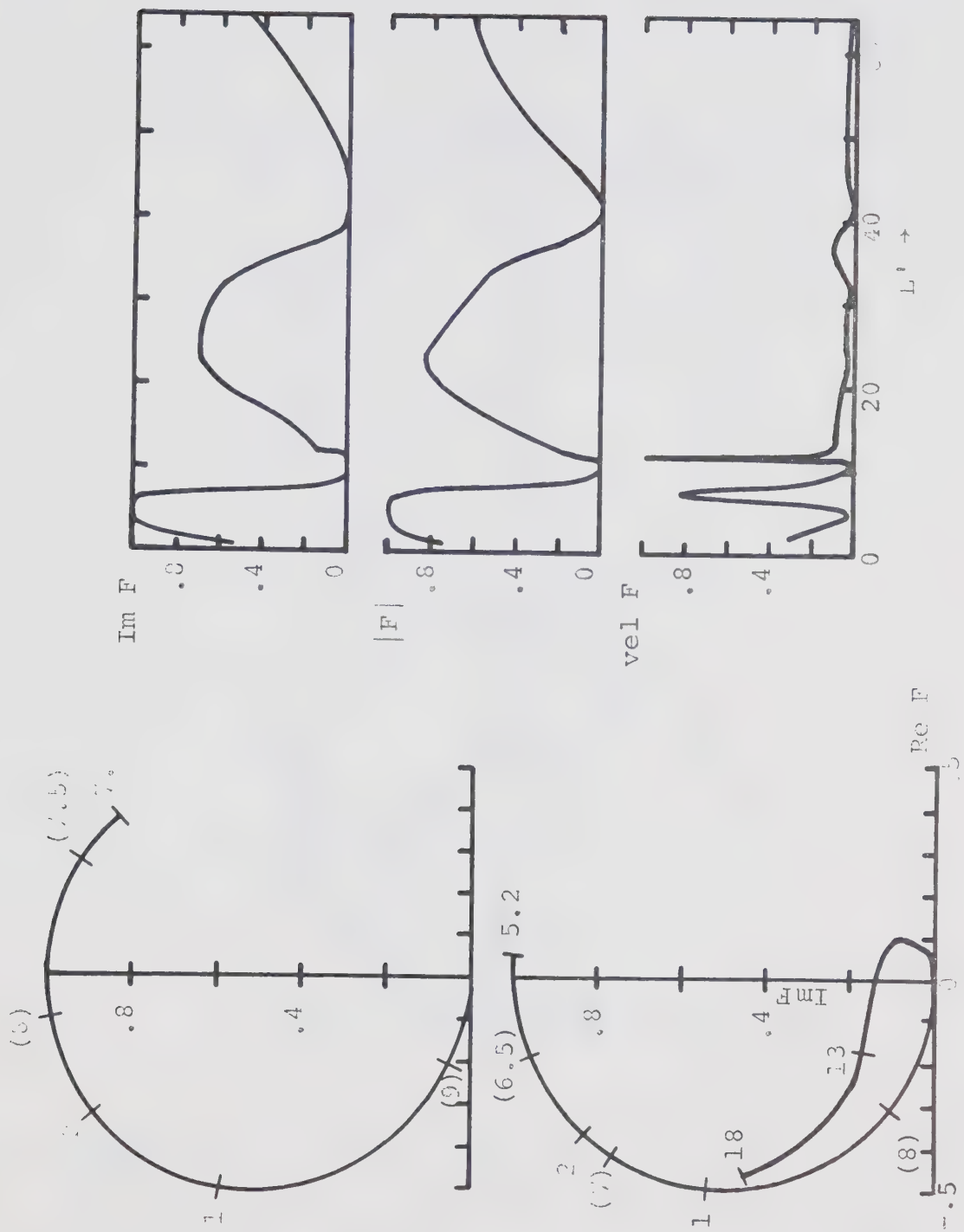


Figure 2A.1. $\text{Im } F$, $|F|$ and $\text{vel } F$ for $g_{11}'=8.17$, $g_{12}'^2=16$ and $k_0'^2=11.56$. $E'=\left(\frac{a}{b} k\right)^2$ as defined in the text. Argand diagrams for $g_{12}'^2=0$ (top) and 16 (bottom). Some energy values are plotted on the Argand diagrams, the parenthesis indicates a counter motion of F on a previous loop. The second peak in $\text{vel } F$ was not studied but appears to be a highly inelastic resonance.

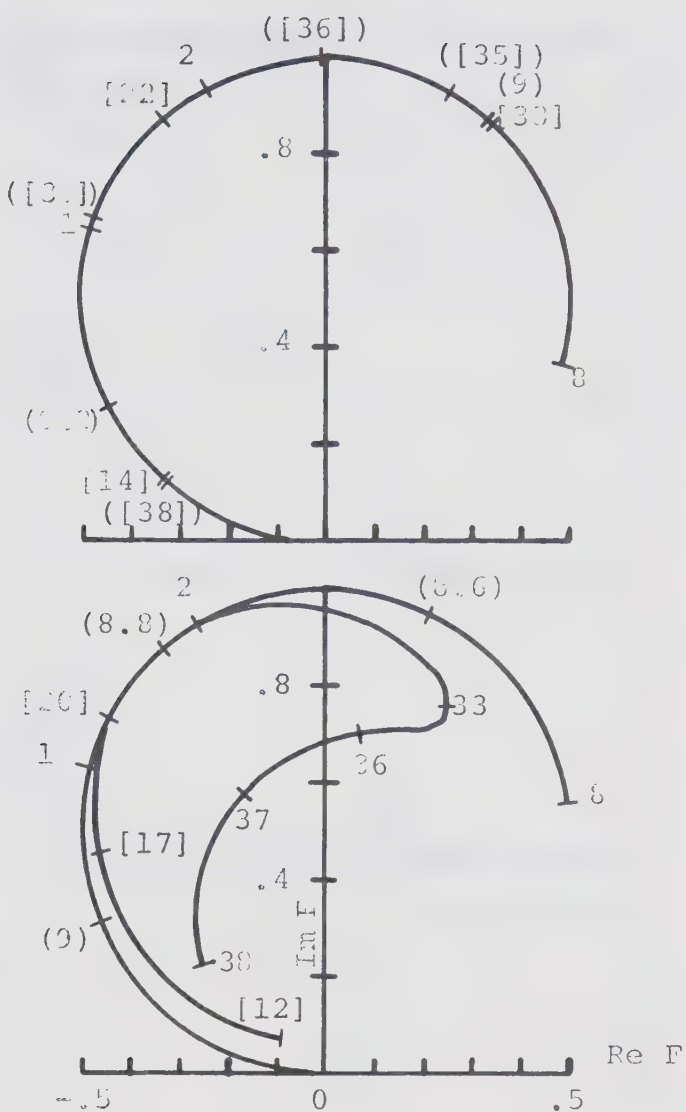


Figure 2A.2. Argand diagrams for $g_{11}^2 = 16.94$, $k_0^2 = 11.56$, $g_{12}^2 = 0$ (top) and 16 (bottom). The Argand diagrams oscillate back and forth, on or inside the unitary circle. The energies in parenthesis of kind (), () and ([]) respectively represent higher repetitions of these oscillations.

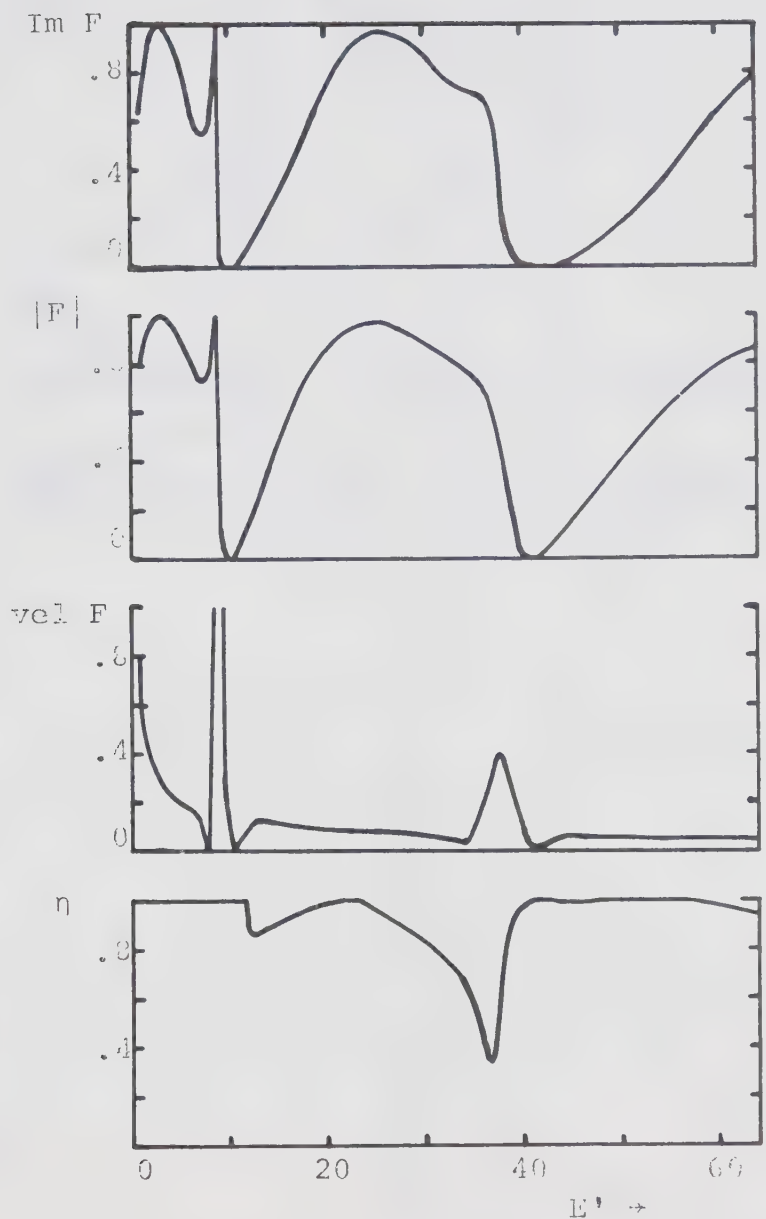


Figure 1A.3. $\text{Im } F$, $|F|$, $\text{vel } F$ and η for
 $g_{11}^{(1)} = 16.54$, $g_{12}^{(2)} = 16$ and $v_0^{(2)} = 11.56$.

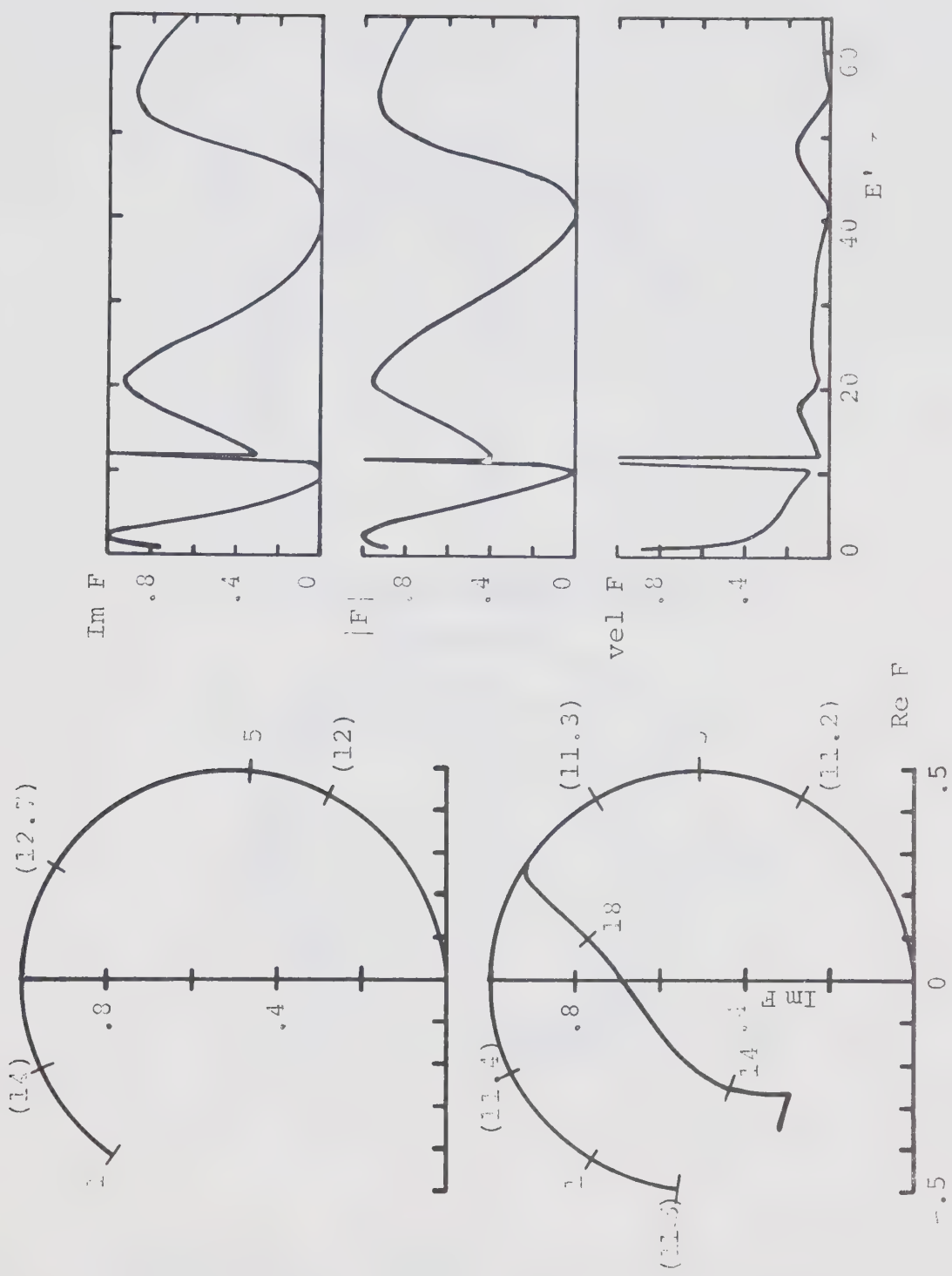


Figure 20. $\text{Im } F$, $|F|$, and $\text{Re } F$ for $g_{11}^{(2)} = -11.62$,
 $g_{12}^{(2)} = 11.62$, $k_{11}^{(2)} = 11.56$, $\Delta \mu = 0$, $\alpha = 0$,
 $(\alpha_1, \alpha_2) = (11, 11)$.

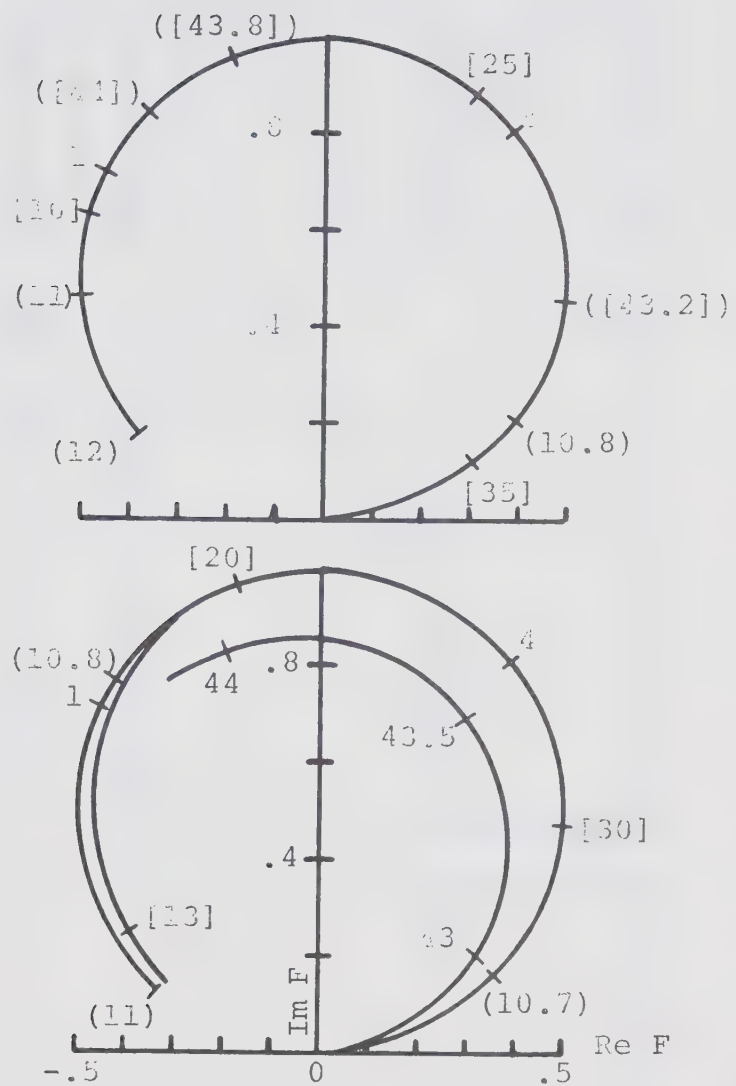


Figure 2A.5. Argand diagrams for $g_{11}' = -33.34$, $g_{12}^{(1)} = 11.56$. $g_{12}^{(2)} = 0$ (top) and 16 (bottom).

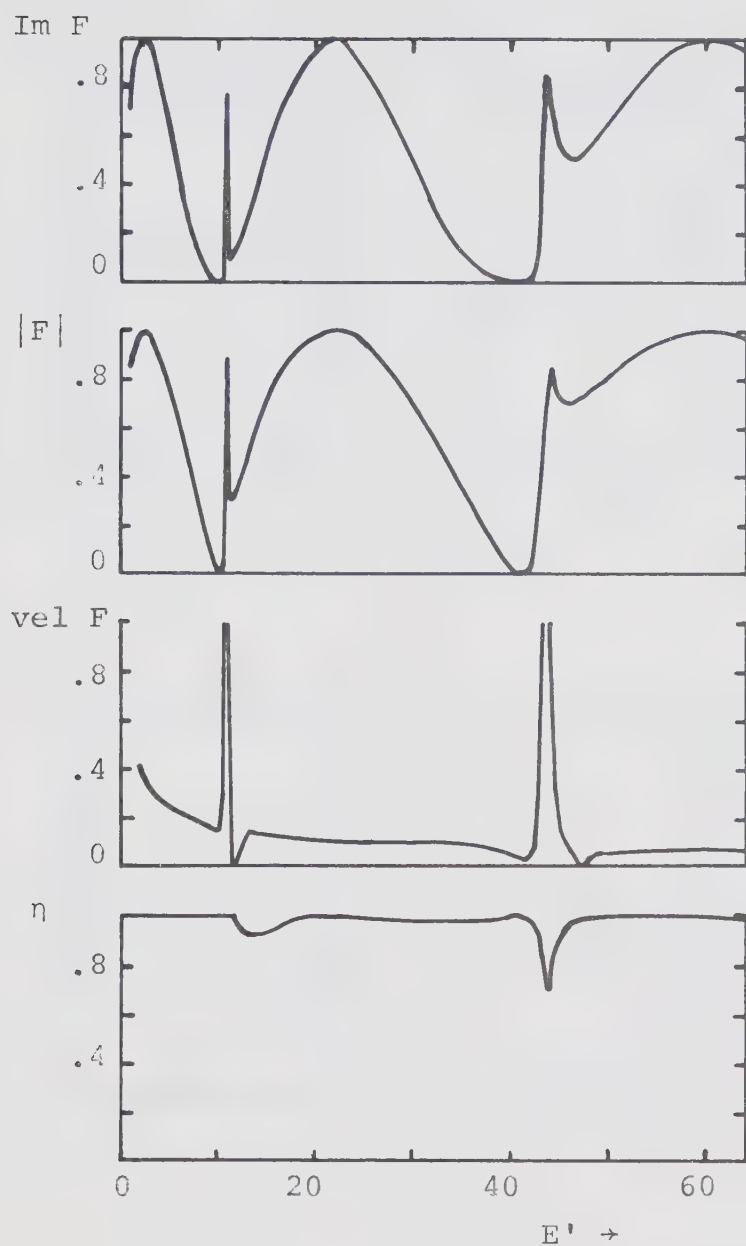


Figure 2A.6. $\text{Im } F$, $|F|$, $\text{vel } F$ and η for
 $g_{11}' = -33.34$, $g_{12}'^2 = 16$ and $k_o'^2 = 11.56$.

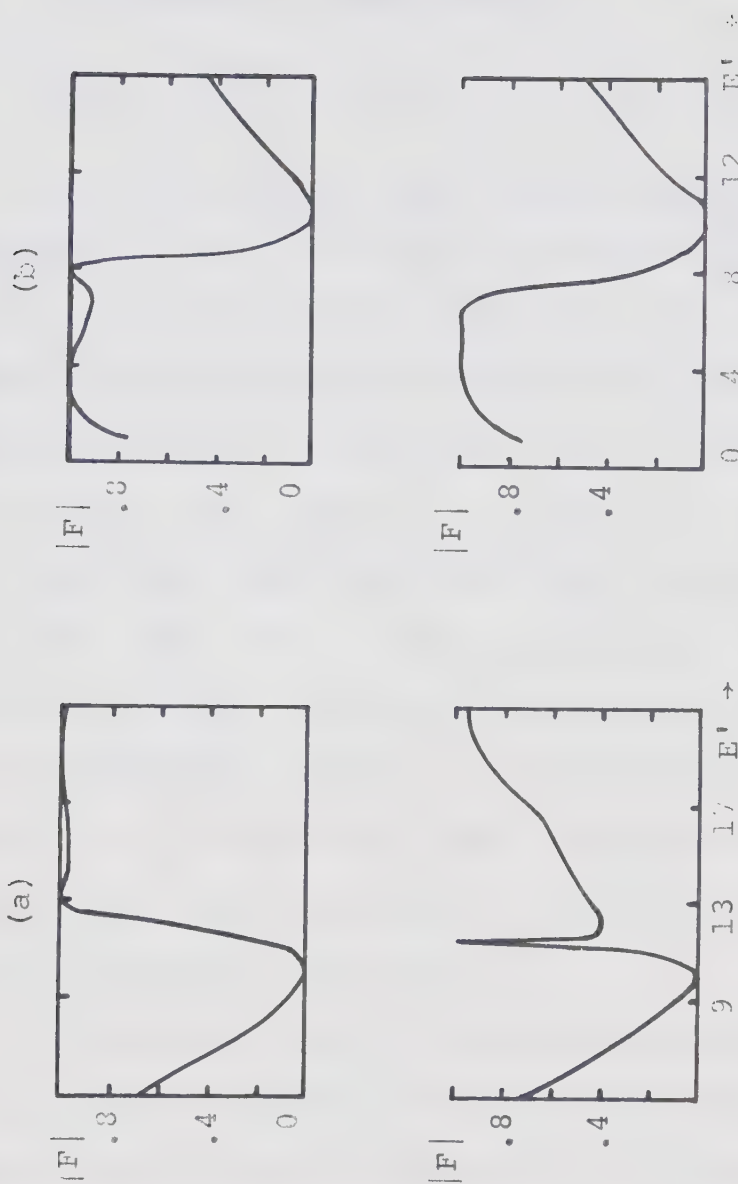


Figure 2A.7. The absolute value of the scattering amplitude for a) $g'_{11} = -9.82$, $g'_{12}^2 = 0$ (top), 16 (bottom). b) $g'_{11} = 3.17$, $g'_{12}^2 = 0$ (top), 16 (bottom). From this figure the large changes in the single channel resonance widths under the coupling to the second channel can be understood (see table 2A.3).

B. S-wave scattering from an exponential potential

This model is specified by

$$v(r) = e^{-mr}, \quad l = 0. \quad [2B.1]$$

In this model we have looked at two types of resonances. The first type of resonance is generated, surprisingly, by a highly repulsive potential. If the potential is sufficiently repulsive the phase shift passes through -90° from above. But as the phase shift has to return to 0° for $k^2 \rightarrow \infty$ (this will not be true for a hard core - but we do not have a hard core) it will cross -90° from below at some energy k_R^2 . This phase shift has all the features of a resonance i.e. it satisfies the resonance criteria set out in eqs. [1.28] and [1.29]. It is clear that there being no centrifugal barrier one would not be able to generate resonances with an attractive potential.

The second type of resonance studied here is one which is a bound state of channel 2 in the continuum of channel 1 but appears, through the interchannel coupling, as a resonance in channel 1.

Before looking at the two models that we want to study, let us evaluate the integrals [1.84] and [1.85] to get the G_{il} functions for a separable exponential potential in s-wave. Using eq. [1.73] one gets

$$\begin{aligned}
G_{io} &= - (k_i)^{-1} \iint_0^\infty \sin k_i r e^{ik_i r} e^{-mr} e^{-mr'} dr' dr \\
&= - (k_i)^{-1} \int_0^\infty \sin k_i r e^{-mr} \int_r^\infty e^{ik_i r'} e^{-mr'} dr' dr \\
&\quad - (k_i)^{-1} \int_0^\infty e^{ik_i r} e^{-mr} \int_0^r \sin k_i r' e^{-mr'} dr' dr \\
&= - \frac{(m + ik_i)}{k_i(m^2 + k_i^2)} \int_0^\infty \sin k_i r e^{-2mr} e^{ik_i r} dr \\
&\quad - \frac{m}{k_i(m^2 + k_i^2)} \int_0^\infty \sin k_i r e^{-2mr} e^{ik_i r} dr \\
&\quad + \frac{1}{(m^2 + k_i^2)} \int_0^\infty \cos k_i r e^{-2mr} e^{ik_i r} dr - \frac{1}{(m^2 + k_i^2)} \int_0^\infty e^{ik_i r} e^{-mr} dr \\
&= \frac{1}{(m^2 + k_i^2)} \int_0^\infty e^{-2mr} dr - \frac{1}{(m^2 + k_i^2)} \int_0^\infty e^{-(m-ik_i)r} dr \\
G_{io} &= \frac{1}{2m(m^2 + k_i^2)} - \frac{(m + ik_i)}{(m^2 + k_i^2)^2} = - \frac{(m+ik_i)^2}{2m(m^2 + k_i^2)^2} = - \frac{1}{2m(m-ik_i)^2}
\end{aligned}$$

[2B.2]

so that for $k_i^2 > 0$

$$\operatorname{Re} G_{io} = \frac{k_i^2 - m^2}{2m(m^2 + k_i^2)^2} \quad \text{and} \quad \operatorname{Im} G_{io} = \frac{-k_i}{(m^2 + k_i^2)^2}. \quad [2B.3]$$

From eq. [1.85]

$$\begin{aligned}
 H_{io} &= -k_i \left(\int_0^{\infty} r e^{-mr} \frac{\sin k_i r}{k_i r} dr \right)^2 \\
 &= -\frac{1}{k_i} \left(\int_0^{\infty} e^{-mr} \sin k_i r dr \right)^2 = -\frac{k_i}{(m^2 + k_i^2)^2} \quad [2B.4]
 \end{aligned}$$

From [1.90], [1.91], [2B.2], [2B.3] and [2B.4] one also gets:

$$N = \begin{cases} -\frac{g_{11}k_1}{(m^2 + k_1^2)^2} & -\frac{g_{12}\sqrt{k_1 k_2}}{(m^2 + k_1^2)(m^2 + k_2^2)} \\ -\frac{g_{12}\sqrt{k_1 k_2}}{(m^2 + k_1^2)(m^2 + k_2^2)} & -\frac{g_{22}k_2}{(m^2 + k_2^2)^2} \end{cases} \quad [2B.5]$$

$$D = \begin{cases} 1 + \frac{g_{11}}{2m(m-ik_1)^2} & \frac{g_{12}}{2m} \sqrt{\frac{k_2}{k_1}} \frac{(m^2 + k_1^2)}{(m^2 + k_2^2)(m-ik_1)^2} \\ \frac{g_{12}}{2m} \sqrt{\frac{k_1}{k_2}} \frac{(m^2 + k_2^2)}{(m^2 + k_1^2)(m-ik_2)^2} & 1 + \frac{g_{22}}{2m(m-ik_2)^2} \end{cases} \quad [2B.6]$$

$$\text{and } F = [N][D^{-1}] \quad [2B.7]$$

Single channel problem

Letting $g_{22} = 0$ and $g_{12} = 0$ in [2B.5], [2B.6] and [2B.7], one gets:

$$N = - \frac{g_{11}k}{(m^2+k^2)^2} \quad [2B.8]$$

$$D = 1 + \frac{g_{11}(m^2-k^2)}{2m(m^2+k^2)^2} + i \frac{g_{11}k}{(m^2+k^2)^2} \quad [2B.9]$$

$$F = \frac{N}{D} = \frac{-g_{11}k/(m^2+k^2)^2}{1 + \frac{g_{11}(m^2-k^2)}{2m(m^2+k^2)^2} + i \frac{g_{11}k}{(m^2+k^2)^2}} \quad [2B.10]$$

From eq. [2B.9]

$$\text{Re } D = 1 + \frac{g_{11}(m^2-k^2)}{2m(m^2+k^2)^2}, \quad \text{Im } D = \frac{g_{11}k}{(m^2+k^2)^2} \quad [2B.11]$$

$$\frac{d \text{Re } D}{dE} = \frac{g_{11}}{2m} \frac{(k^2 - 3m^2)}{(k^2 + m^2)^3}. \quad [2B.12]$$

To satisfy the conditions [1.25] and [1.26] it must be required that

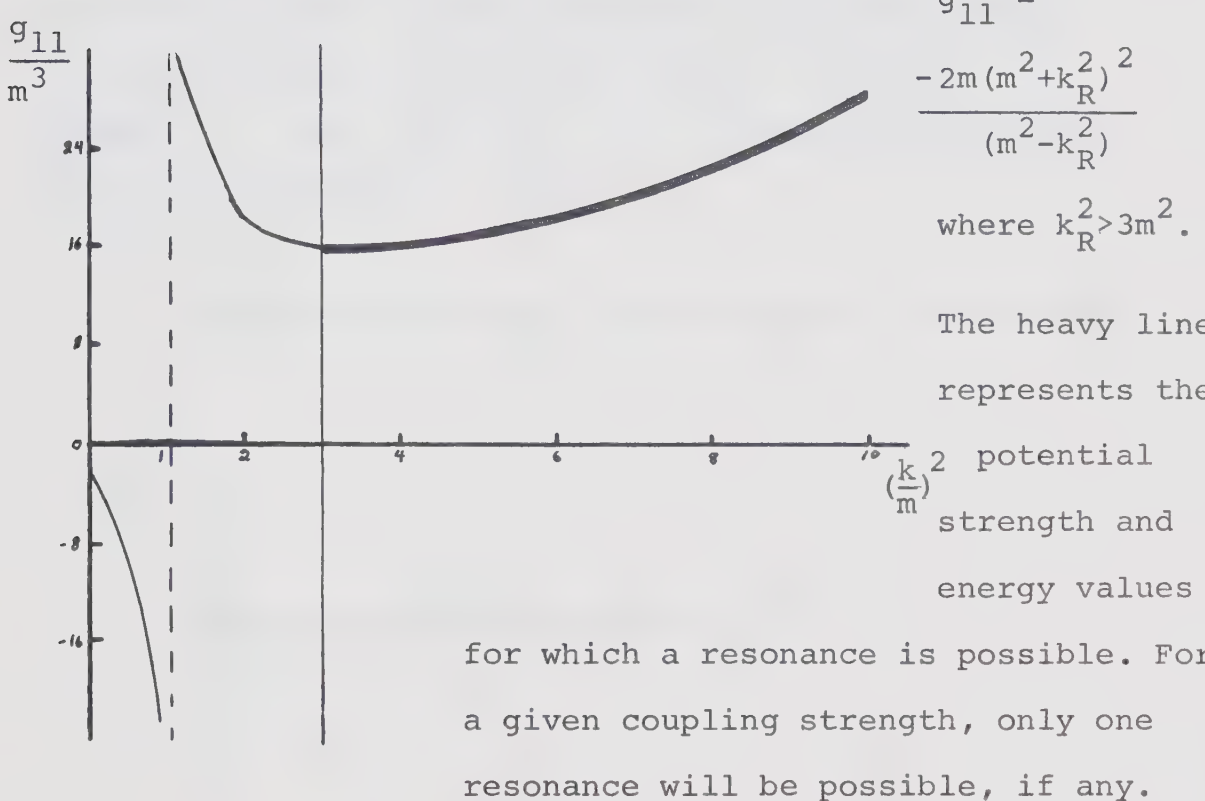
$$\text{Re } D = 0 \quad \text{or} \quad g_{11} = - \frac{2m(m^2+k_R^2)^2}{(m^2 - k_R^2)} \quad [2B.13]$$

where $k_R^2 = E_R$ is the resonance energy, and

$$\left. \frac{\text{Im } D}{\frac{d}{dE} \text{Re } D} \right|_{E_R} = \frac{\Gamma}{2} > 0 \quad \text{or} \quad \frac{2m k_R (k_R^2 + m^2)}{(k_R^2 - 3m^2)} = \frac{\Gamma}{2} \Rightarrow k_R^2 > 3m^2 .$$

[2B.14]

The following graph shows the resonance regions defined by the conditions [2B.13] and [2B.14].

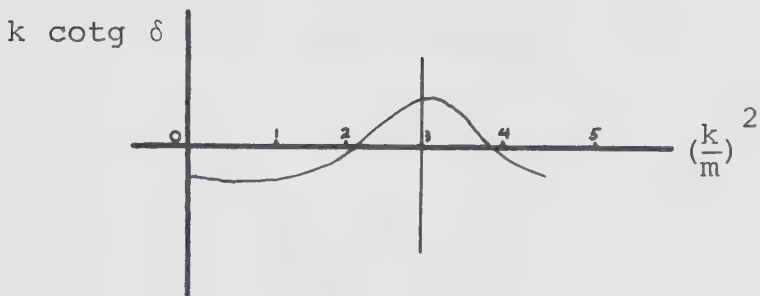


Let us verify that the conditions [1.28] and [1.29] on the phase shift are satisfied in the resonance region determined on this graph.

$$\begin{aligned}
 k \cotg \delta &= \frac{k \operatorname{Re} D(k^2)}{k^2 \rightarrow 0 \quad N(k^2)} = \lim_{k^2 \rightarrow 0} \frac{\frac{k(1 + \frac{(m^2 - k^2)}{(m^2 + k^2)^2} \frac{g_{11}}{2m})}{(m^2 + k^2)^2}}{-\frac{g_{11} k}{(m^2 + k^2)^2}} \\
 &= \frac{1 + \frac{g_{11}}{2m^3}}{-\frac{g_{11}}{m^4}} .
 \end{aligned} \tag{2B.15}$$

Hence for $g_{11} > 16m^3$, the region where a resonance is possible, $k \cotg \delta$ starts negative. In this region $k \cotg \delta$ will go through zero twice, first for $(k/m)^2 < 3$, then for $(k/m)^2 > 3$, and one gets the following graph for $k \cotg \delta$.

Behaviour of $k \cotg \delta$ with respect to the energy



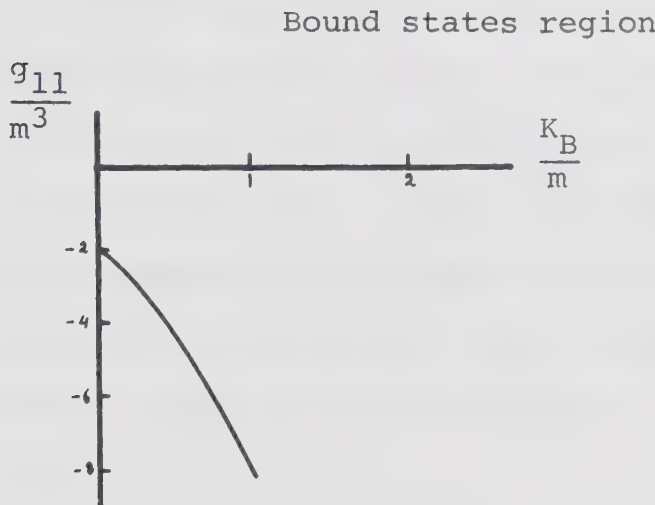
Looking for the possible bound states one has, from [1.9], $D(E) = 0$ for $E < 0$. Letting $k = iK$ with $K > 0$, one gets from eq. [2B.9]

$$D(-K^2) = 1 + \frac{g_{11}(m^2 + K^2)}{2m(m^2 - K^2)^2} - \frac{g_{11}K}{(m^2 - K^2)^2} = 1 + \frac{g_{11}}{2m(m+K)^2} = 0$$

so that the bound states will be determined by

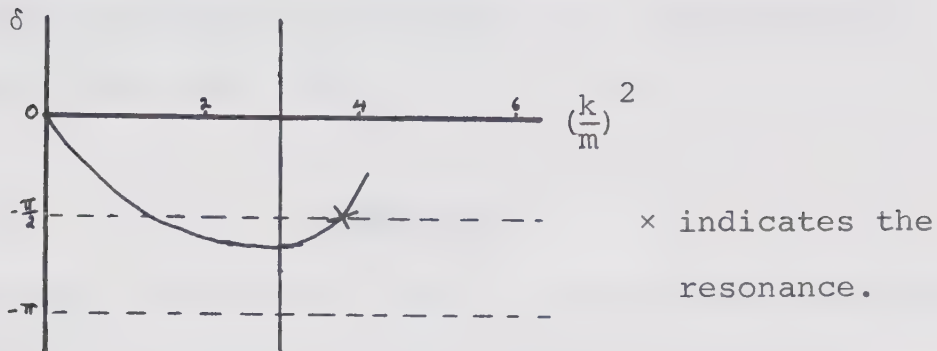
$$g_{11} = -2m(m+K_B)^2 \quad \text{where } K_B > 0 . \quad [2B.16]$$

The following diagram shows the bound states region. One can see that there is no bound state for $g_{11} > -2m^3$. Since $dg_{11}/dK_B = -4m(m+K_B)$ is a decreasing function of K_B , there will be only one bound state for a given g_{11} .



From this graph, it can be seen that there is no bound state possible for $g_{11} > 16m^3$, so that from Levinson's theorem $\delta(0)=0$, and the behaviour of the phase shift is as sketched below.

Behaviour of the phase shift with respect to the energy



Since δ crosses $-\pi/2$ from below, a resonance is possible for $g_{11} > 16m^3$ and $(k/m)^2 > 3$. As it has already been said, it is somehow surprising to find an S-wave resonance for the exponential potential and the question which immediately arises is, how good will the resonance recognition criteria be in this case?

To answer that question we have looked at a particular potential, $g_{11} = 18m^3$, for which the previous study has established the existence of a resonance. This resonance is expected to be at the value of $(k/m)^2$ which will solve the equation $\text{Re } D = 0$, namely from [2B.13],

$$\left[1 + \left(\frac{k_R}{m}\right)^2\right]^2 + \left[1 - \left(\frac{k_R}{m}\right)^2\right] \frac{g_{11}}{2m^3} = 0$$

$$\left(\frac{k_R}{m}\right)^4 - 7\left(\frac{k_R}{m}\right)^2 + 10 = 0 ,$$

$$\text{that is } \left(\frac{k_R}{m}\right)^2 = 5 \quad \text{or} \quad \left(\frac{k_R}{m}\right)^2 = 2 .$$

Since from [2B.14] $(k_R/m)^2$ must be greater than 3, the resonance position is at $(k_R/m)^2 = 5$. The resonance recognition criteria give the following results (see table 2B.1).

Table 2B.1

Resonance positions as given by the various resonance recognition criteria and as defined by $\text{Re } D = 0$.

$$E'_R = (k_R/m)^2.$$

$\frac{g_{11}}{m^3}$	$\text{Re } D = 0$ E'_R at	Max Im F E'_R between	Max F' E'_R between	Max vel F E'_R between
18	5	4.5 5.5	4.5 5.5	no maximum

Notice that the velocity of F in the Argand diagram does not show a maximum. It was emphasized that this resonance is produced by a large repulsive potential and therefore the mechanism of production is somewhat unusual.

Two channel problem

Study of a resonance induced in the first channel by the presence of a bound state in the second channel.

It is possible to induce a resonance by coupling one channel to a second already supporting a bound state. This is a new type of resonance, namely one produced by the coupling mechanism between two channels and it is worthwhile to test the resonance recognition criteria in this model. Since it will help us to interpret the results and because it happens to give simple mathematical expressions, the variation in position and width of the resonance with respect to the value of the interchannel coupling strength g_{12}^2 will also be studied analytically.

Let us choose a g_{22} such that there is a bound state in the uncoupled second channel. Letting $g_{11} = 0$ and $g_{12} = 0$ in eqs. [2B.5], [2B.6] and [2B.7], one can write

$$F_{22} = \frac{-\frac{g_{22}k_2}{(m^2+k_2^2)^2}}{1 + \frac{(m^2-k_2^2)}{(m^2+k_2^2)^2} \frac{g_{22}}{2m} + i \frac{g_{22}k_2}{(m^2+k_2^2)^2}} . \quad [2B.17]$$

From the previous study (see diagram on page 68) a bound state is known to exist for

$$g_{22} = -2m(m + K_B)^2, \quad K_B > 0. \quad [2B.18]$$

We now couple this second channel to the first and look for resonances. For simplicity we will let $g_{11} = 0$. g_{22} is chosen to satisfy eq. [2B.18]. From [2B.5], [2B.6] and [2B.7] one gets:

$$F_{11} = \frac{\frac{g_{12}^2 k_1}{2m(m-ik_2)^2 (m^2+k_1^2)^2}}{1 + \frac{g_{22}}{2m(m-ik_2)^2} - \frac{g_{12}^2}{(2m)^2 (m-ik_1)^2 (m-ik_2)^2}}. \quad [2B.19]$$

From [2B.6]

$$\det[D] = 1 + [g_{22} - \frac{g_{12}^2 (m^2 - k_1^2)}{2m(m^2 + k_1^2)^2}] \frac{1}{2m(m+K_2)^2} - i \frac{g_{12}^2 k_1}{(m^2 + k_1^2)^2 2m(m+K_2)^2}$$

where $k_2 = iK_2$ was used below the inelastic threshold since for small enough interchannel coupling strength, it is expected that the value of k_2 will stay imaginary.

From [1.30] the resonance energy is determined by

$$\operatorname{Re} \det[D] = 1 - \frac{1}{2m(m+K_{2R})^2} [|g_{22}| + \frac{g_{12}^2 (m^2 - k_{1R}^2)}{2m(m^2 + k_{1R}^2)^2}] = 0 \quad [2B.20]$$

where g_{22} is given by eq. [2B.18] and can be written as $g_{22} = -|g_{22}|$. From eq. [1.31] the resonance width is

$$\frac{\Gamma}{2} = \left. \frac{\text{Im } \det[D]}{\frac{d}{dE} \text{Re } \det[D]} \right|_{E_R} > 0$$

$$\text{Im } \det[D] = -\frac{k_1 g_{12}^2}{2m(m+k_2)^2(m^2+k_1^2)^2} < 0 \quad [2B.21]$$

so that $\frac{d \text{Re } \det[D]}{dE} \Big|_{E_R} < 0$ at the resonance energy.

From eq. [2B.20]

$$\begin{aligned} \frac{d \text{Re } \det[D]}{dE} &= -\left(|g_{22}| + \frac{g_{12}^2(m^2-k_1^2)}{2m(m^2+k_1^2)^2}\right) \frac{1}{2mK_2(m+k_2)^3} \\ &\quad + \frac{g_{12}^2}{4m^2(m+k_2)^2} \left(\frac{(m^2+k_1^2)+2(m^2-k_1^2)}{(m^2+k_1^2)^3}\right). \end{aligned} \quad [2B.22]$$

Substituting eq. [2B.20] in [2B.22] to evaluate the derivative at E_R the following condition is obtained:

$$-\frac{1}{K_2(m+K_{2R})} + \frac{g_{12}^2}{4m^2(m+K_{2R})^2} \left(\frac{3m^2-k_{1R}^2}{(m^2+k_{1R}^2)^3}\right) < 0. \quad [2B.23]$$

For $k_{1R}^2 > 3m^2$, this condition [2B.23] will certainly be satisfied, without any restriction on the threshold value k_o^2 . The bound state in the second channel will thus induce a resonance in the first since the conditions [1.30] and [1.31] can be satisfied. To test the resonance recognition criteria in this model, we chose $g_{22} =$

$-18m^3$ so that $k_{1R}^2 > 3m^2$ and we take $k_o^2 = 8m^2$. The results appear in table 2B.2.

Variation of the position and width of the resonance with respect to the coupling parameter g_{12}^2 .

For $g_{12}^2 \rightarrow 0$, the resonance is expected to be very close to the energy producing the bound state in the second uncoupled channel, that is

$$k_{1R} \approx \sqrt{k_o^2 - k_B^2} .$$

Let us now write [2B.20] in the following way:

$$4m^2(m+k_{2R})^2 + g_{12}^2 \frac{(k_{1R}^2 - m^2)}{(m^2 + k_{1R}^2)^2} - 2m|g_{22}| = 0 . \quad [2B.24]$$

Since

$$\frac{d[2B.24]}{dg_{12}^2} = \frac{\partial[2B.24]}{\partial g_{12}^2} + \left(\frac{\partial[2B.24]}{\partial k_{1R}^2} + \frac{\partial[2B.24]}{\partial k_{2R}^2} \right) \frac{dk_{2R}^2}{dk_{1R}^2} \frac{dk_{1R}^2}{dg_{12}^2} = 0 ,$$

taking the total derivative of eq. [2B.24] with respect to g_{12}^2 and using the fact that $dk_{2R}^2/dk_{1R}^2 = -1$, one can solve for dk_{1R}^2/dg_{12}^2 and obtain

$$\frac{dk_{1R}^2}{dg_{12}^2} = \frac{\frac{k_{1R}^2 - m^2}{(m^2 + k_{1R}^2)^2}}{g_{12}^2 \frac{(k_{1R}^2 - 3m^2)}{(m^2 + k_{1R}^2)^3} + \frac{4m^2(m+k_{2R})}{k_{2R}}} \quad [2B.25]$$

and since

$$k_{1R}^2 > 3m^2, \quad dk_{1R}^2/dg_{12}^2 > 0, \quad k_{1R}^2 \text{ increases with } g_{12}^2. \quad [2B.26]$$

Hence the resonance is moved towards the right with increasing value of the coupling strength g_{12}^2 .

The width of the resonance is given by the expression [1.31]. From [2B.21] and [2B.23] one can write

$$\begin{aligned} \Gamma &= -\frac{2k_{1R}g_{12}^2}{2m(m+K_2)^2(m^2+k_{1R}^2)^2} \left[\frac{1}{\frac{-1}{K_{2R}(m+K_{2R})} + \frac{g_{12}^2(3m^2-k_{1R}^2)}{4m^2(m+K_{2R})^2(m^2+k_{1R}^2)^3}} \right] \\ &= \frac{g_{12}^2 k_{1R}}{m(m^2+k_{1R}^2)^2} \left[\frac{1}{\frac{(m+K_{2R})}{K_{2R}} + \frac{g_{12}^2(k_{1R}^2-3m^2)}{4m^2(m^2+k_{1R}^2)^3}} \right] \end{aligned} \quad [2B.27]$$

The variation in width with respect to g_{12}^2 is given by

$$\frac{d\Gamma}{dg_{12}^2} = \frac{\partial \Gamma}{\partial g_{12}^2} + \left(\frac{\partial \Gamma}{\partial k_{1R}^2} + \frac{\partial \Gamma}{\partial K_{2R}^2} \right) \frac{dk_{1R}^2}{dk_{1R}^2} \frac{dk_{1R}^2}{dg_{12}^2}. \quad [2B.28]$$

Calculating each term on the right hand side of eq. [2B.28], one gets:

$$\frac{\partial \Gamma}{\partial g_{12}^2} = \frac{k_{1R}}{m(m^2+k_{1R}^2)^2} \frac{1}{\kappa(k_{1R})} \left(1 - \frac{g_{12}^2 (k_{1R}^2 - 3m^2)}{\kappa(k_{1R}) 4m^2 (m^2+k_{1R}^2)^3} \right) \quad [2B.29]$$

where

$$\kappa(k_{1R}) = \left(\frac{(m+K_{2R})}{K_{2R}} + \frac{g_{12}^2 (k_{1R}^2 - 3m^2)}{4m^2 (m^2+k_{1R}^2)^3} \right) \quad [2B.30]$$

$$\frac{dK_{2R}^2}{dk_{1R}^2} = -1 \quad [2B.31]$$

$$\frac{\partial \Gamma}{\partial K_{2R}^2} = \frac{g_{12}^2 k_{1R}}{2K_{2R}^3 (m^2+k_{1R}^2)^2} \frac{1}{\{\kappa(k_{1R})\}^2} \quad [2B.32]$$

$$\begin{aligned} \frac{\partial \Gamma}{\partial k_{1R}^2} &= \frac{g_{12}^2}{m(m^2+k_{1R}^2)^3} \frac{1}{\kappa(k_{1R})} \left\{ \frac{(m^2 - 3k_{1R}^2)}{2k_{1R}} + \frac{g_{12}^2 k_{1R} (k_{1R}^2 - 5m^2)}{2m^2 (m^2+k_{1R}^2)^3} \times \right. \\ &\quad \left. \times \frac{1}{\kappa(k_{1R})} \right\} \quad [2B.33] \end{aligned}$$

$$\frac{dk_{1R}^2}{dg_{12}^2} = \frac{(k_{1R}^2 - m^2)}{4m^2 (m^2+k_{1R}^2)^2} \frac{1}{\kappa(k_{1R})} \quad [2B.34]$$

and for small g_{12}^2 , neglecting terms containing this factor, one gets:

$$\frac{d\Gamma}{dg_{12}^2} = \frac{k_{1R} K_{2R}}{m(m^2+k_{1R}^2)^2 (m+K_{2R})} > 0 \quad . \quad [2B.35]$$

Hence for small g_{12}^2 , the resonance width increases with increasing value of g_{12}^2 . It is shown in Appendix 1 that this conclusion is borne out in the special case studied.

Table 2B.2

Resonance positions as given by the various resonance recognition criteria and as defined by $\text{Re det}[D] = 0$.

The inelastic threshold value is $(k_0/m)^2 = 8$, $g_{22}/m^3 = -18$ and $g_{11}/m^3 = 0$, $E'_R = (k_R/m)^2$.

$\frac{g_{12}^2}{m^6}$	$\text{Re det}[D]=0$ E'_R between	Max Im F E'_R between	Max F E'_R between	Max vel F E'_R between
1	4.01	4.01	4.01	4.02
	4.02	4.03	4.03	4.04
9	4.17	4.17	4.17	4.19
	4.18	4.19	4.19	4.21
16	4.31	4.30	4.30	4.34
	4.32	4.32	4.32	4.36

One notices from this table that as g_{12}^2 is increased the resonance is shifted to the right.

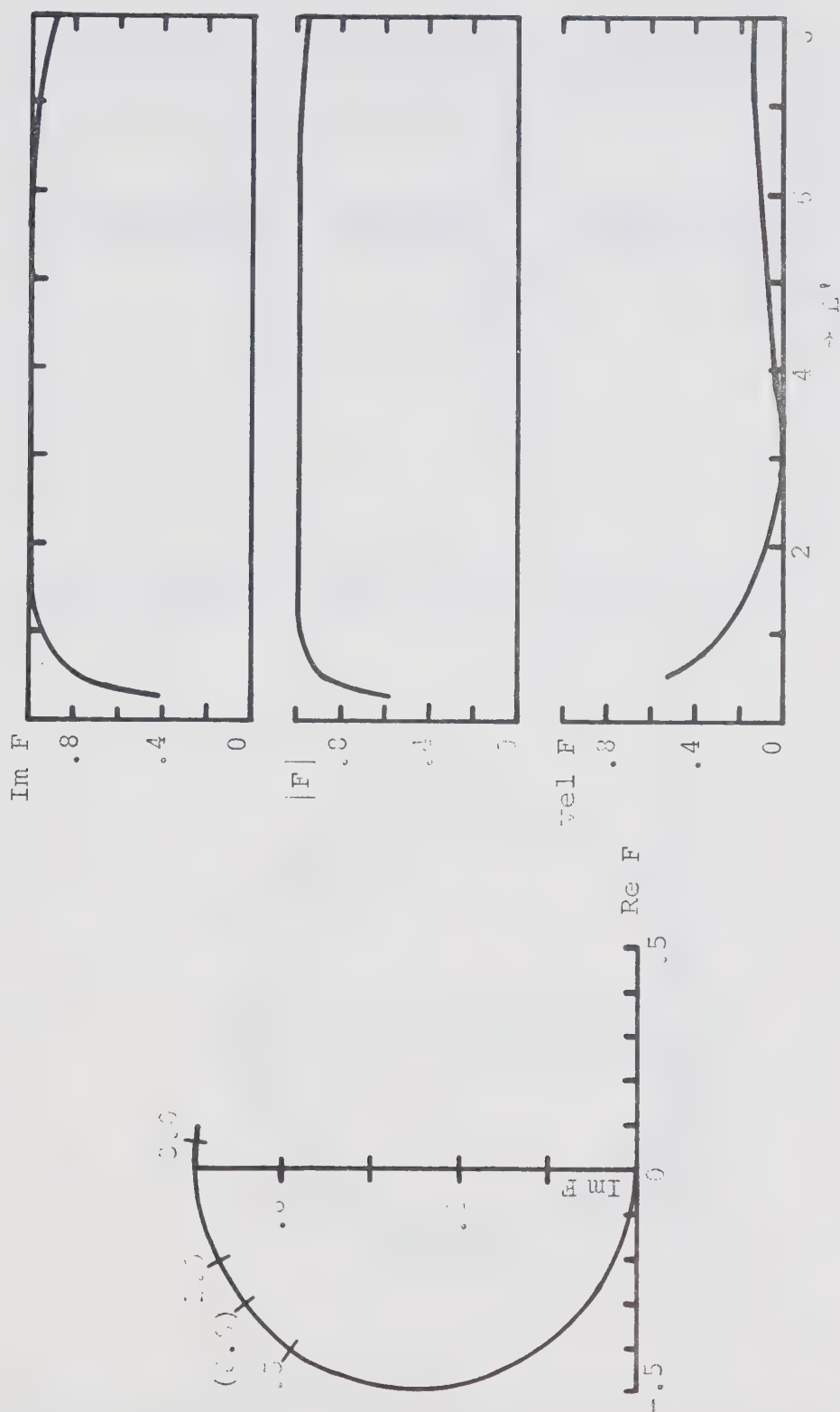


Figure 2B.1. Argand diagram, $\text{Im } F$, $|F|$ and $\text{vol } F$ for $g_{11} = 2 \times 10^5 \text{ m}^{-3}$ and $g_{21}^{(2)} = 2 \times 10^2 \text{ (J/m)}^2$ as defined in the text. Some energy values are plotted on the Argand diagram; those in parentheses indicate a counter motion of F or a level in 3000.

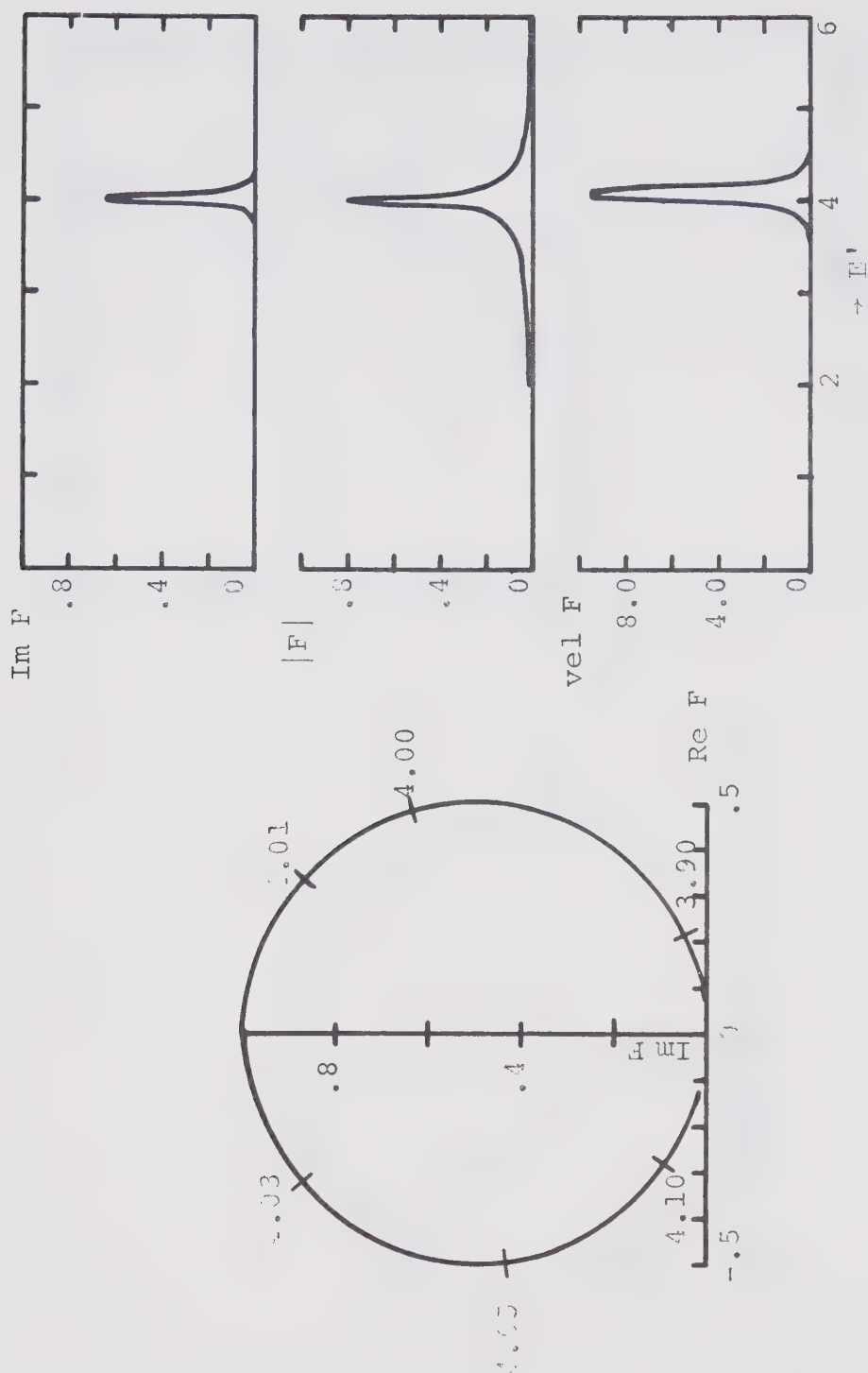


Figure 2B.2. Argand diagram, $\text{Im } F$, $|F|$ and $\text{vel } F$ for
 $g_{11} = 0$, $g_{22} = -15 \text{ m}^3$, $g_{12}^2 = 1 \text{ m}^6$ and $(\omega/\text{m})^2 = 8$.

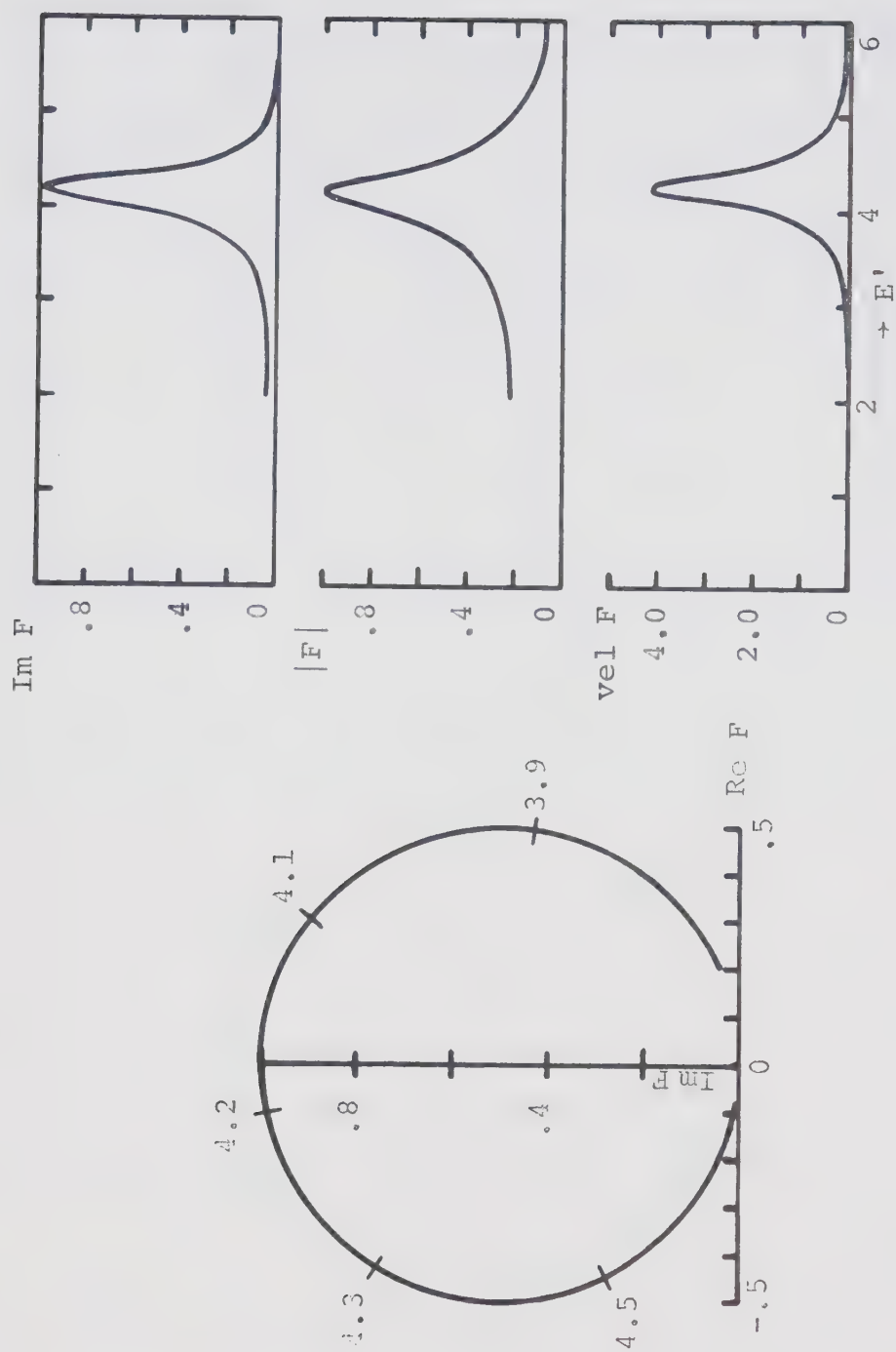


Figure 2B.5. Argand diagram, $\text{Im } F$, $|F|$ and $\text{vel } F$ for $g_{11} = 0$, $g_{22} = -10 \text{ m}^3$, $g_{12}^2 = 3 \text{ m}^6$ and $(k_0/m)^2 = 8$.

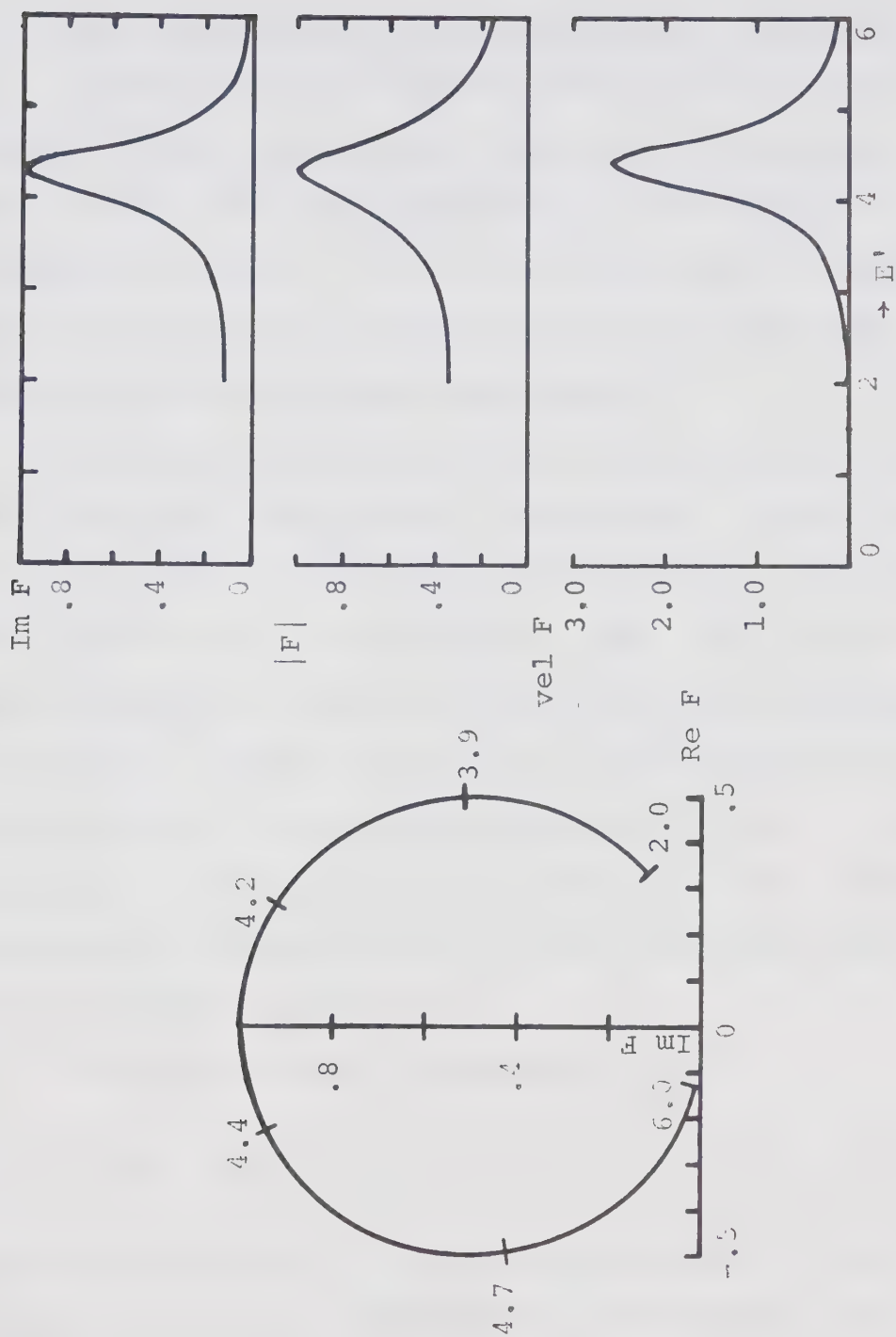


Figure 2B.4. Argand diagram, $\text{Im } F$, $|F|$ and $\text{vel } F$ for $g_{11} = 0$, $g_{22} = -10 \text{ m}^3$, $g_{12}^2 = 16 \text{ m}^6$ and $(k_c/m)^2 = 8$.

C. P-wave scattering from an exponential potential

Contrary to the S-wave resonances the P-wave resonances are generated by the more "conventional" means of the trapping mechanism provided by the centrifugal barrier. In this section a model has been set up for the P-wave resonances and the resonance recognition criteria have been tested.

This model is studied in a similar way as was the δ -function S-wave model (section 2A). Some potential strengths g_{11} are determined such that resonances are forced in the single channel case. This channel is then coupled to a second one for which the threshold energy is so chosen that some of the resonances are above and some below the inelastic threshold $(k_0/m)^2$. The new positions of the resonances are found and the resonance recognition criteria are tested for both the single and the two-channel problems.

The model taken is specified by

$$v(r) = e^{-mr} , \quad \ell = 1 . \quad [2C.1]$$

As it will be seen, the expression for the F_{11} matrix element is far more complicated in the P-wave than in the S-wave case so that the problem had to be programmed on the computer even for the single channel calculations.

Let us evaluate the integrals [1.84] and [1.85] for the G_{il} functions for the special case which is now under study.

Substituting $\ell = 1$, $v(r) = e^{-mr}$ and $v(r') = e^{-mr'}$ in eq. [1.84] and [1.85] and using eq. [1.73] one gets:

$$G_{il} = \iint_0^\infty G''_{il}(r, r') e^{-mr} e^{-mr'} dr' dr - ik_i \left[\int_0^\infty r e^{-mr} j_1(k_i r) dr \right]^2$$

where $G''_{il}(r, r') \equiv -k_i r < j_1(k_i r) r > n_1(k_i r)$. The last integral can be evaluated easily. One gets (Gradshteyn and Ryzhik 1965)

$$H_{il} = -\frac{4}{9m^3} \left(\frac{k_i}{m} \right)^3 {}_2F_1^2 \left(\frac{3}{2}, 2; \frac{5}{2}; -\left(\frac{k_i}{m} \right)^2 \right) = \text{Im } G_{il} \text{ for real } k_i,$$

$$\text{Re}(m+ik_i) > 0 . \quad [2C.2]$$

The evaluation of the first integral requires a lengthy calculation which is given in Appendix 2. The result is

$$\begin{aligned} G_{il} = & \frac{1}{m^3} \left\{ \frac{1}{2} \left(\frac{m}{k_i} \right)^2 + \frac{1}{\left[1 + \left(\frac{k_i}{m} \right)^2 \right]^2} + \frac{\left(2 \ln 2 - \frac{1}{2} \right) \left(\frac{m}{k_i} \right)^2}{\left[1 + \left(\frac{k_i}{m} \right)^2 \right]} \right. \\ & - 2 \ln 2 \left(\frac{m}{k_i} \right)^3 \tan^{-1} \left(\frac{k_i}{m} \right) - \frac{\left(\frac{m}{k_i} \right)^2 \ln \left(1 + \left(\frac{k_i}{m} \right)^2 \right)}{\left[1 + \left(\frac{k_i}{m} \right)^2 \right]} \\ & \left. + 2 \left(\frac{m}{k_i} \right)^3 L(\tan^{-1} \left(\frac{k_i}{m} \right)) \right\} + iH_{il} . \quad [2C.3] \end{aligned}$$

The hypergeometric function [2C.2] can also be expressed in terms of elementary functions. One gets

$${}_2F_1\left(\frac{3}{2}, 2; \frac{5}{2}; -\left(\frac{k_i}{m}\right)^2\right) = \frac{3}{2\left(\frac{k_i}{m}\right)^2} \left(\frac{\tan^{-1}\left(\frac{k_i}{m}\right)}{\left(\frac{k_i}{m}\right)} - \frac{1}{[1 + \left(\frac{k_i}{m}\right)^2]} \right)$$

[2C.4]

Single channel problem

Letting $g_{12} = 0$ and $g_{22} = 0$, and using eqs. [2C.2] and [2C.4] in [1.90] and [1.91], one has,

$$N = -\frac{g_{11}}{m^3} \left(\frac{m}{k}\right)^3 \left(\tan^{-1}\left(\frac{k}{m}\right) - \frac{\frac{k}{m}}{[1 + \left(\frac{k}{m}\right)^2]} \right)^2 \quad [2C.5]$$

and

$$D = 1 - g_{11} G_{11}\left(\frac{k}{m}\right) = 1 - g_{11} \operatorname{Re} G_{11}\left(\frac{k}{m}\right) - i g_{11} \operatorname{Im} G_{11}\left(\frac{k}{m}\right)$$

[2C.6]

where $\operatorname{Re} G_{11}$ and $\operatorname{Im} G_{11}$ are given by eq. [2C.3]. Also $F_{11} = N/D$. From eqs. [1.25] and [1.26] the two following conditions will define the resonance parameters,

$$\operatorname{Re} D = 0 = 1 - g_{11} \operatorname{Re} G_{11}\left(\frac{k}{m}\right) \quad [2C.7]$$

$$\text{and } \frac{\Gamma}{2} = \left. \frac{\operatorname{Im} D}{\frac{d}{dE} \operatorname{Re} D} \right|_{E_R} > 0 \quad . \quad [2C.8]$$

Since the function $\text{Re } G_{11}(k/m)$ (see eq. [2C.3]) is difficult to handle, the computer was used to evaluate it for some k^2 values over an energy range starting at $k^2=0$. We have plotted $m^3 \text{Re } G_{11}$ vs $(k/m)^2$ in figure 2C.1. As the function is always negative it implies that the eq. [2C.7] will have a solution only for negative g_{11} . From figure 2C.1 it is known that two values of the energy will give the same $\text{Re } G_{11}$, for the smaller k^2 , $d \text{Re } G_{11}/dk^2 < 0$ and for the larger k^2 , $d \text{Re } G_{11}/dk^2 > 0$. Eq. [2C.8] will determine which one of these two values will be the resonance energy.

From eqs. [2C.6] and [2C.8] we have

$$\frac{\Gamma}{2} = \left. \frac{\text{Im } G_{11}(\frac{k}{m})}{\frac{d}{dE} \text{Re } G_{11}} \right|_{E_R} \quad \text{and from eq. [2C.2], } \text{Im } G_{11} < 0 . \quad [2C.9]$$

This implies that $d \text{Re } G_{11}/dE < 0$ and it is the smaller k^2 which will solve eq. [2C.7] for $g_{11} < 0$, which will be the resonance energy.

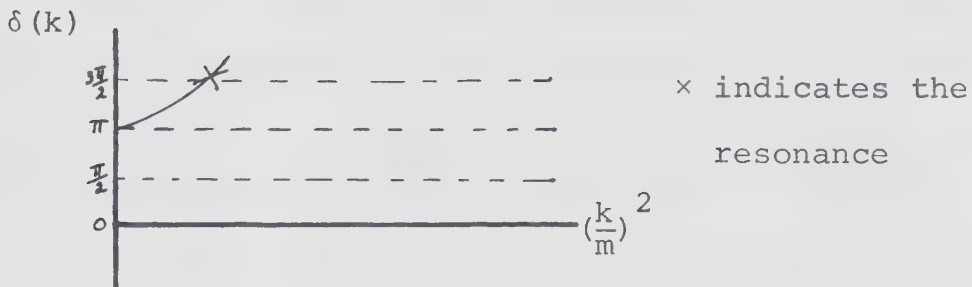
One can also check that the phase shift has the right behaviour by looking at $(k/m)^3 \cotg \delta$.

$$\begin{aligned} \left(\frac{k}{m} \right)^3 \cotg \delta &= \lim_{k^2 \rightarrow 0} \frac{\text{Re } D}{N} = \lim_{k^2 \rightarrow 0} \frac{\left(\frac{k}{m} \right)^3 (1 - g_{11} \text{Re } G_{11}(\frac{k}{m}))}{\frac{-4g_{11}}{9m} \left(\frac{k}{m} \right)^3 {}_2F_1(\frac{3}{2}, 2; \frac{5}{2}, -(\frac{k}{m})^2)} \\ &= \frac{1 - g_{11} \text{Re } G_{11}(0)}{\frac{-4g_{11}}{9m} \left(\frac{k}{m} \right)^3} > 0 . \end{aligned}$$

Hence $(k/m)^3 \cotg \delta$ starts positive and one has:



and this implies the following behaviour for δ :



This would be the graph for one bound state $N = 1$, but the results would be the same for any number of bound states, including $N = 0$. From this graph, one can see unambiguously that there is a resonance at the first zero of [2C.7] for $g_{11} < 0$. From figure 2C.1 we have thus chosen four energy values and have found the corresponding $\text{Re } G_{11}(k/m)$ such that there would be a resonance in the single channel case. The choice of those energy values was made keeping in mind that some of the resonances should be below and some above the inelastic threshold for the two channel

problem. The value of the coupling strength g_{11} was then calculated from eq. [2C.7], that is:

$$g_{11} = \frac{1}{\operatorname{Re} G_{11} \left(\frac{k_R}{m} \right)}$$

for those chosen values of $(k_R/m)^2$. The results obtained are as follows (see table 2C.1).

Table 2C.1

Resonance energies and corresponding coupling strengths for the single channel case

$(k_R/m)^2$	$m^3 \operatorname{Re} G_{11} (k_R/m)$	g_{11}/m^3
.03	-.096	-10.42
.08	-.102	-9.80
.05	-0.098723	-10.129
.15	-0.10672	-9.3700

Note: The number of significant figures in the different entries of table 2C.1 can be explained as follows. For the first two lines $m^3 \operatorname{Re} G_{11}$ was read off from figure 2C.1 and are accurate to $\pm .0005$. For each one of those two extreme values of $m^3 \operatorname{Re} G_{11}$ for a given $(k_R/m)^2$, a potential strength was calculated from Eq. [2C.7]; their approximate average value was chosen for g_{11}/m^3 . For the last two lines of table 2C.1, the values of $m^3 \operatorname{Re} G_{11}$ had already been computed for the chosen values of $(k_R/m)^2$ in order to draw figure 2C.1, this explains the higher accuracy to which both $m^3 \operatorname{Re} G_{11}$ and g_{11}/m^3 are known.

Two channel problem

Once the interchannel coupling is switched on, $g_{12}^2 \neq 0$, the resonance position is given by the solution of the equation (see eq. [1.93])

$$1 - g_{11} \operatorname{Re} G_{11} \left(\frac{k_1}{m} \right) - g_{12}^2 \left[\operatorname{Re} G_{11} \left(\frac{k_1}{m} \right) \operatorname{Re} G_{21} \left(\frac{k_2}{m} \right) - \operatorname{Im} G_{11} \left(\frac{k_1}{m} \right) \operatorname{Im} G_{21} \left(\frac{k_2}{m} \right) \right] = 0 \quad [2C.10]$$

where $G_{11}(k_1/m)$ and $G_{21}(k_2/m)$ are given in eqs. [2C.2]

and [2C.3]. g_{22} is set equal to zero for simplicity.

The threshold energy was so chosen that some of the resonances were generated below the inelastic threshold and some above it, so that the resonance recognition criteria could be tested for both these situations. The value $(g_{12}/m^3)^2 = 1.2$ was taken as the interchannel coupling strength.

* The interchannel coupling strength was chosen such that it would produce a shift of the resonance position of about $\Delta(k_R/m)^2 \approx .02$. To find the required value for $(g_{12}/m^3)^2$, eq. [2C.10] was solved roughly for a two channel problem below the inelastic threshold with $g_{11} \approx -10$. In this case eq. [2C.10] becomes:

$$1 - [g_{11} + g_{12}^2 G_{21} \left(\frac{k_2}{m} \right)] \operatorname{Re} G_{11} \left(\frac{k_1}{m} \right) = 0$$

since $\operatorname{Im} G_{21} = 0$ and $\operatorname{Re} G_{21} = G_{21}$ for $(k_1/m)^2 < (k_o/m)^2$.

Assuming that $G_{21}(k_2/m)$ is of the order of $\operatorname{Re} G_{11}(k_1/m)$, we let $m^3 G_{21}(k_2/m) \approx .09$. From table 2C.1, one can see that for $\Delta(g_{11}/m^3) \approx .76$, $\Delta(k_R/m)^2 \sim .1$ so that a change of about .15 in the coupling strength is needed to produce the desired $\Delta(k_R/m)^2 \sim .02$. Hence one needs:

$$g_{12}^2 G_2(k^2/m) \approx .15$$

which implies $(g_{12}/m^3)^2 \approx 1.6$. We have taken $(g_{12}/m^3)^2 = 1.2$.

As previously, the resonance energy and width are found for the single and the two channel cases (tables 2C.2 and 2C.3) and (tables 2C.4 and 2C.5). The resonance recognition criteria are tested for the model (tables 2C.6, 2C.7 and 2C.8). Because the η criterion was ill defined for $(g_{12}/m^3)^2 = 1.2$, due to a weak inelasticity (η not much different from 1), the value of the interchannel coupling strength was increased for some of the calculations (tables 2C.3, 2C.5, 2C.8).

Table 2C.2

Resonance positions defined by $\text{Re } \det[D] = 0$.

For the two channel case $(g_{12}/m^3)^2 = 1.2$ and $(k_o/m)^2 = .05$.
 $E'_R = (k_R/m)^2$.

$\frac{g_{11}}{m^3}$	one channel E'_R between	two channel E'_R between	E'_R shift under the coupling
-10.420	.0300	.0225	left
	.0325	.0250	
-9.800	.0775	.0675	left
	.0800	.0700	

For the two channel case $(g_{12}/m^3)^2 = 1.2$ and $(k_o/m)^2 = .10$

-10.129	.050 .055	.040 .045	left
-9.370	.150 .155	.120 .125	left

Table 2C.3Resonance positions defined by $\text{Re } \det[D] = 0$ For the two channel case $(k_O/m)^2 = .005$. $E'_R = (k_R/m)^2$.

$\frac{g_{11}}{m^3}$	$(\frac{g_{12}}{m^3})^2$	one channel E'_R between	two channel E'_R between	E'_R shift under the coupling
-10.420	4	.0300 .0325	.0100 .0125	left
-9.800	6	.0775 .0800	.0325 .0350	left

For the two channel case $(k_O/m)^2 = .01$.

-10.129	4	.050 .055	.025 .030	left
-9.370	6	.150 .155	.060 .065	left

Table 2C.4

Resonance widths defined by eq.[1.31]

For the two channel case $(g_{12}/m^3)^2 = 1.2$ and $(k_o/m)^2 = .05$.

$\frac{g_{11}}{m^3}$	one channel	two channel	change in $\Gamma/2m^2$ under the coupling
-10.420	.0162	.00951	decrease
-9.800	.0824	.0631	decrease

For the two channel case $(g_{12}/m^3)^2 = 1.2$ and $(k_o/m)^2 = .10$.

-10.129	.0407	.0257	decrease
-9.370	.483	.228	decrease

Table 2C.5

Resonance widths defined by eq. [1.31]

For the two channel case $(k_0/m)^2 = .005$

$\frac{g_{11}}{m^3}$	$\left(\frac{g_{12}}{m^3}\right)^2$	one channel	two channel	change in $\Gamma/2m^2$ under the coupling
-10.420	4	.0162	.00336	decrease
-9.800	6	.0824	.0179	decrease

For the two channel case $(k_0/m)^2 = .01$

-10.129	4	.0407	.0137	decrease
-9.370	6	.483	.0509	decrease

Table 2C.6

Resonance positions as given by the various resonance
recognition criteria

Single channel problem $E'_R = (k_R/m)^2$.

g_{11}/m^3	Re D = 0 E'_R between	Max Im F E'_R between	Max F E'_R between	Max vel F E'_R between
-10.420	.0300 .0325	.0275 .0325	.0275 .0325	.0225 .0275
-9.800	.0775 .0800	.0775 .0825	.0775 .0825	.0450 .0500
-10.129	.050 .055	.045 .055	.045 .055	.030 .040
-9.370	.150 .155	.145 .155	.145 .155	.055 .070

Table 2C.7

Resonance positions as given by the various resonance recognition criteria

For the two channel problem $(g_{12}/m^3)^2 = 1.2$ and $(k_o/m)^2 = .05$.
 $E'_R = (k_R/m)^2$.

g_{11}/m^3	Re det[D]=0 E'_R between	Max Im F E'_R between	Max F E'_R between	Max vel F E'_R between	Min η E'_R between
-10.420	.0225	.0225	.0225	.0175	-
	.0250	.0275	.0275	.0225	
-9.800	.0675	.0650	.0650	.0425	ill defined
	.0700	.0700	.0700	.0475	

For the two channel problem $(g_{12}/m^3)^2 = 1.2$ and $(k_o/m)^2 = .10$.

	.040	.040	.040	.030	
-10.129	.045	.050	.050	.040	-
	.120	.120	.115	.055	
-9.370	.125	.130	.125	.065	ill defined

Note: In the ill defined cases η decreases slowly with energy without displaying a minimum.

Table 2C.8

Resonance positions as given by the various resonance
recognition criteria

For the two channel problem $(k_o/m)^2 = .005$. $E'_R = (k_R/m)^2$.

$\frac{g_{11}}{m^3}$	$(\frac{g_{12}}{m^3})^2$	Re det[D]=0 E'_R between	Max E'_R Im F between	Max F E'_R between	Max vel F E'_R between	Min η E'_R between
-10.420	4	.0100 .0125	.0075 .0125	.0075 .0125	.0075 .0125	.0075 .0125
-9.800	6	.0325 .0350	.0300 .0350	.0300 .0350	.0250 .0300	.0325 .0375

For the two channel problem $(k_o/m)^2 = .01$.

-10.129	4	.025 .030	.020 .030	.020 .030	.020 .030	.025 .035
-9.370	6	.060 .065	.060 .070	.060 .070	.040 .050	.065 .075

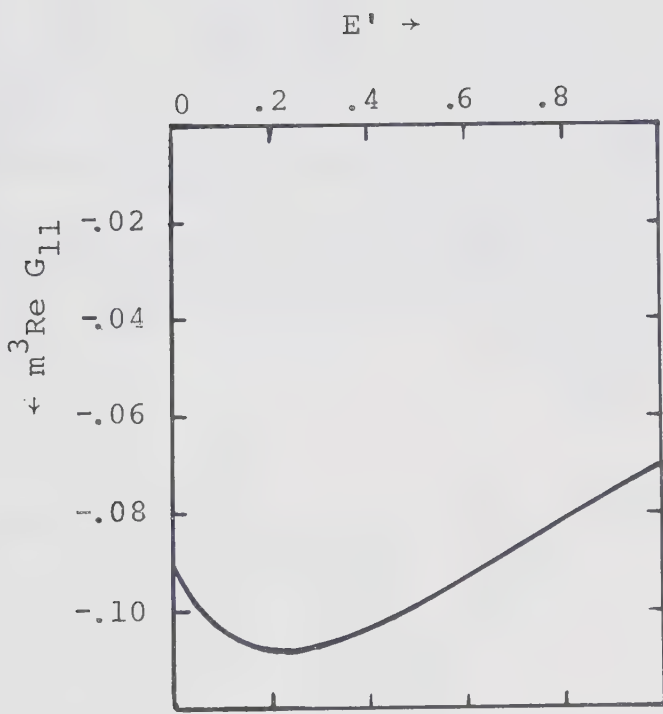


Figure 2C.1. $m^3 \operatorname{Re} G_{11}$ vs $E' \equiv \left(\frac{k}{m}\right)^2$.

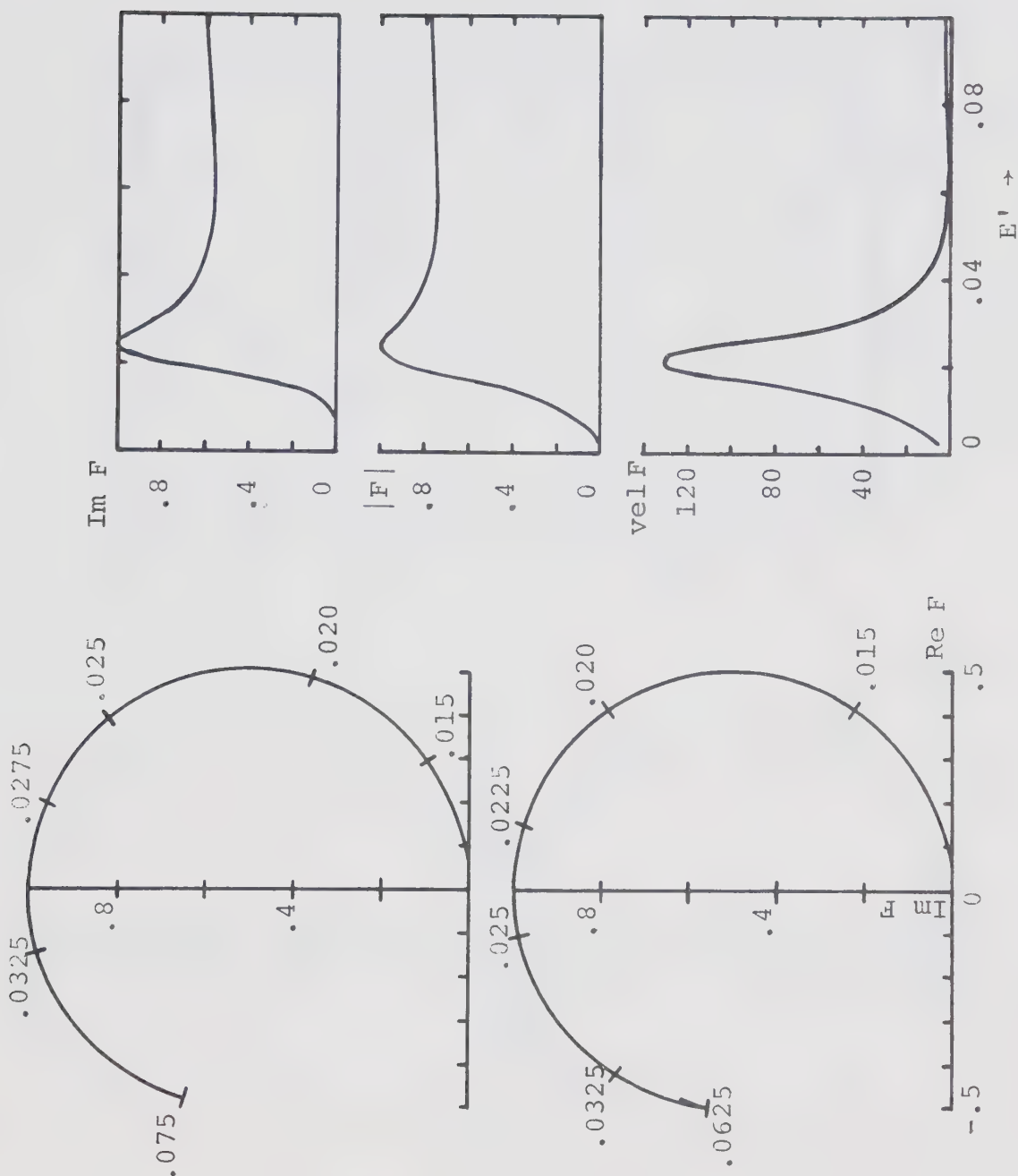


Figure 2C.2. $\text{Im } F$, $|F|$ and $\text{vel } F$ for $g_{11} = -10.420 \text{ m}^3$, $g_{12}^2 = 1.2 \text{ m}^6$ and $(k_c/m)^2 = .05$. $E' = (k/m)^2$ as defined in the text. Argand diagrams for $g_{12}^2 = 0$ (top) and 1.2 m^6 (bottom). Some energy values are plotted on the Argand diagrams.

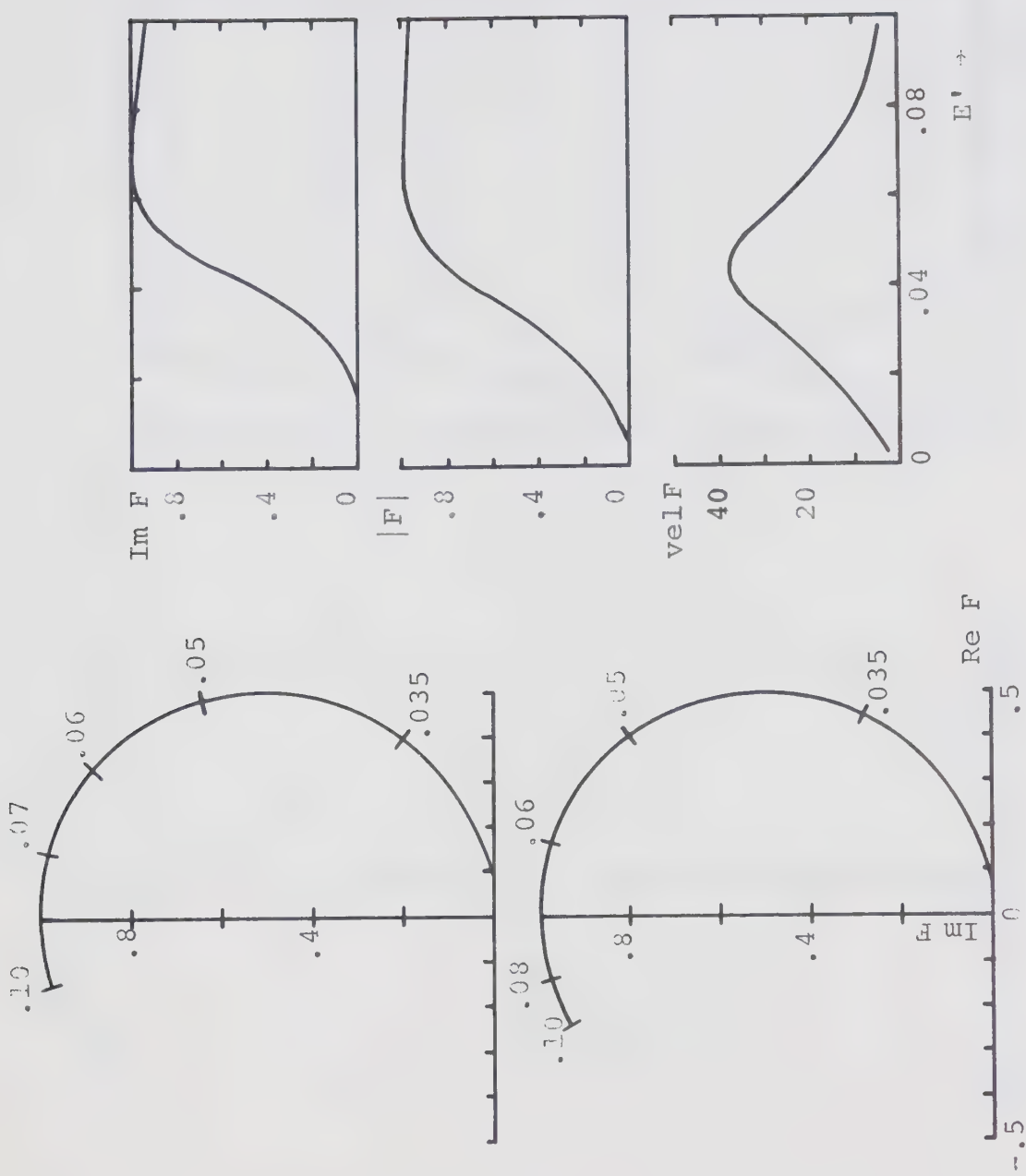


Figure 2C.3. $\text{Im } F$, $|F|$ and $\text{vel } F$ for $g_{11} = -9,800 \text{ m}^3$,
 $g_{12}^2 = 1.2 \text{ m}^6$ and $(k_0/m)^2 = .05$. Argand diagrams for
 $g_{12} = -1.2 \text{ m}^6$ (top) and 1.2 m^6 (bottom).

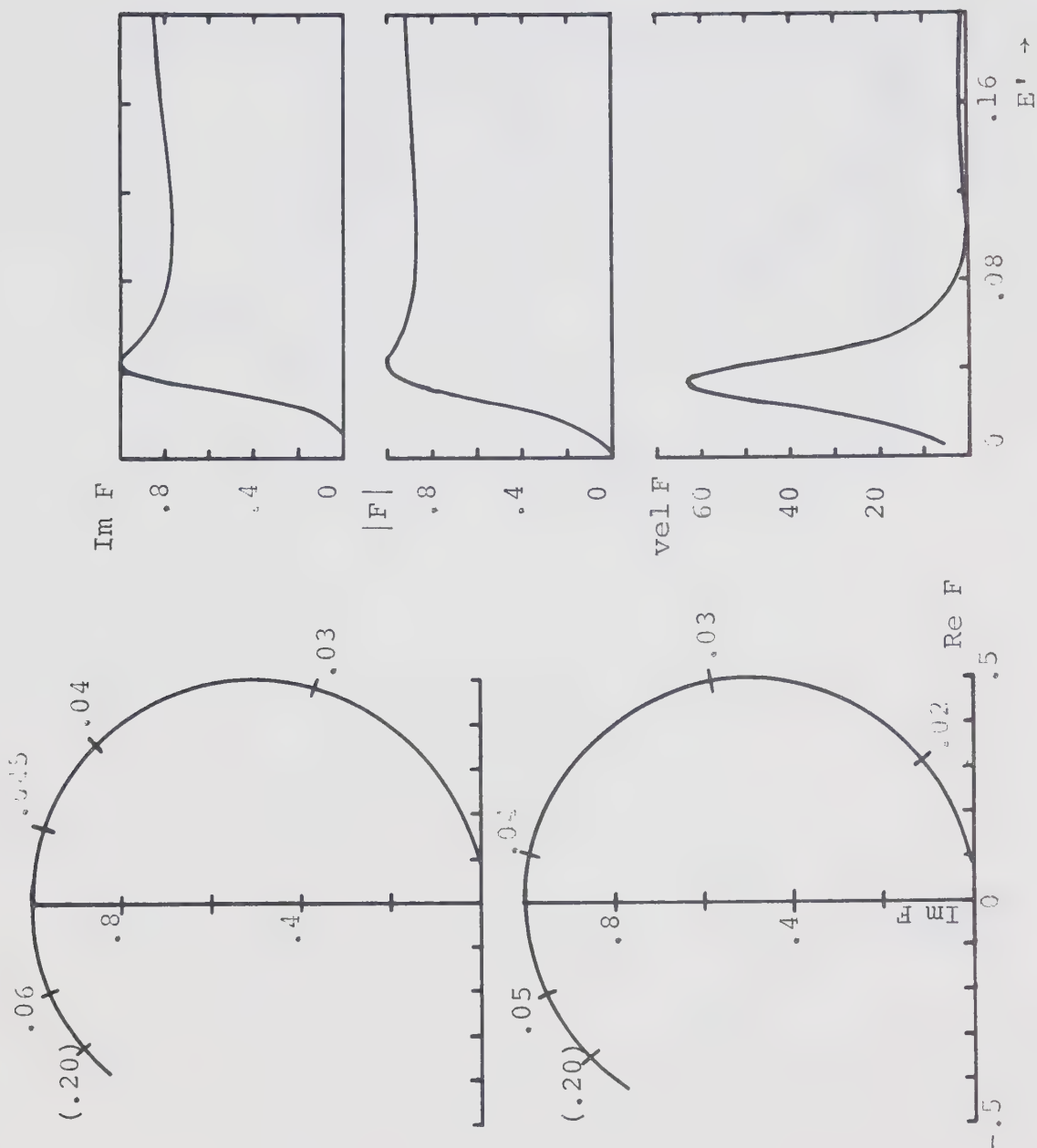


Figure 2C.4. $\text{Im } F$, $|F|$ and $\text{vel } F$ for $g_{11} = -10.129 \text{ m}^3$,
 $g_{12}^2 = 1.2 \text{ m}^6$ and $(k_0/m)^2 = .10$. Argand diagrams
for $g_{12}^2 = 0$ (top) and 1.2 m^6 (bottom).

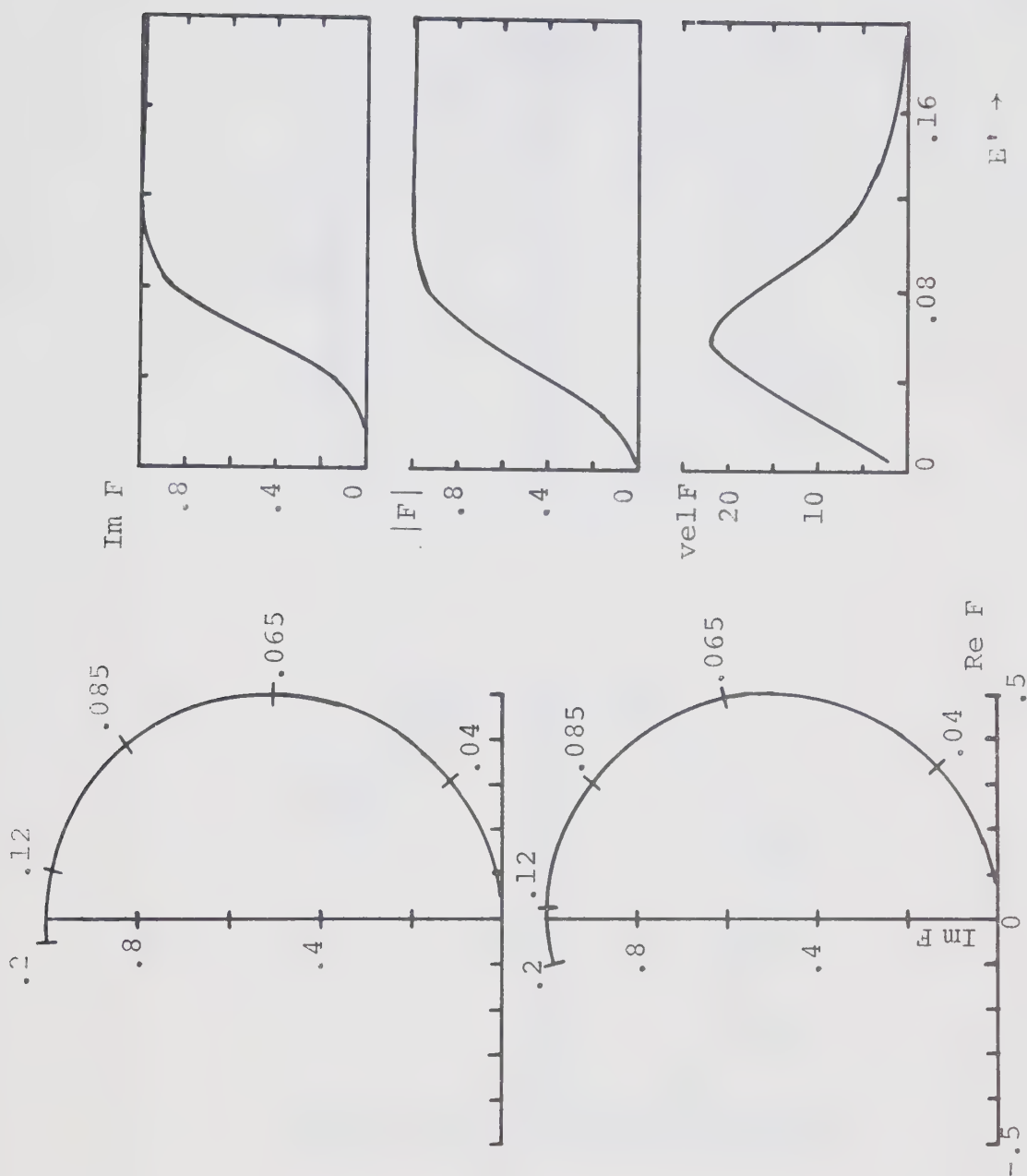


Figure 2C.5. $\text{Im } F$, $|F|$ and $\text{vel } F$ for $g_{11} = -9.370 \text{ m}^3$, $g_{12}^2 = 1.2 \text{ m}^6$ and $(k_0/m)^2 = .10$. Argand diagrams for $g_{12}^2 = 0$ (top) and 1.2 m^6 (bottom).

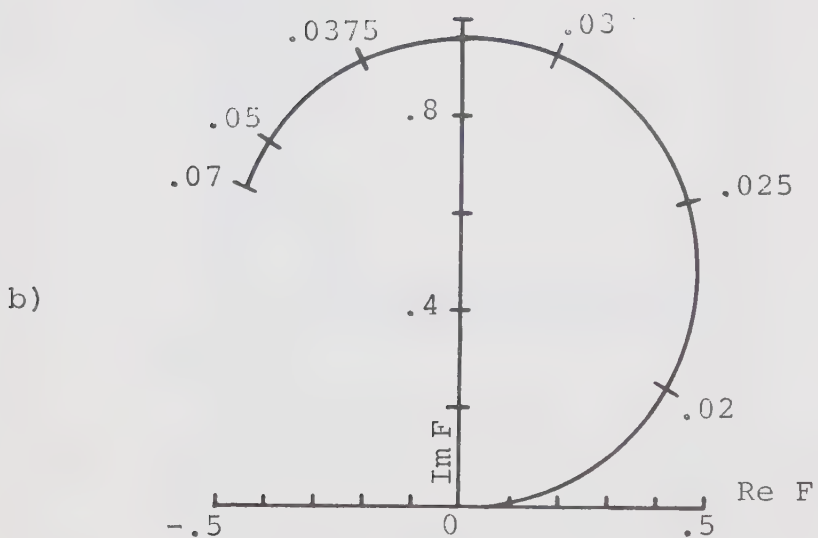
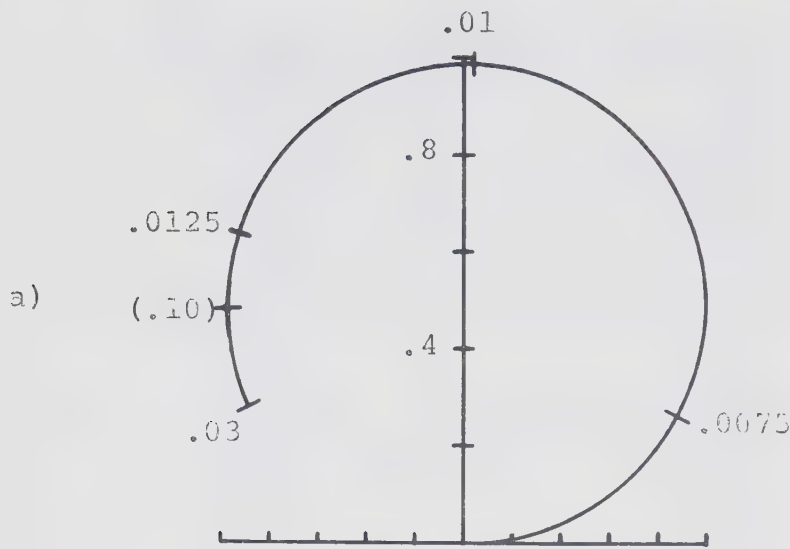


Figure 2C.6. a) Argand diagram for $g_{11} = -10.420 \text{ m}^3$,
 $g_{12}^2 = 4 \text{ m}^6$ and $(k_O/m)^2 = .005$.

b) Argand diagram for $g_{11} = -9.800 \text{ m}^3$,
 $g_{12}^2 = 6 \text{ m}^6$ and $(k_O/m)^2 = .005$.

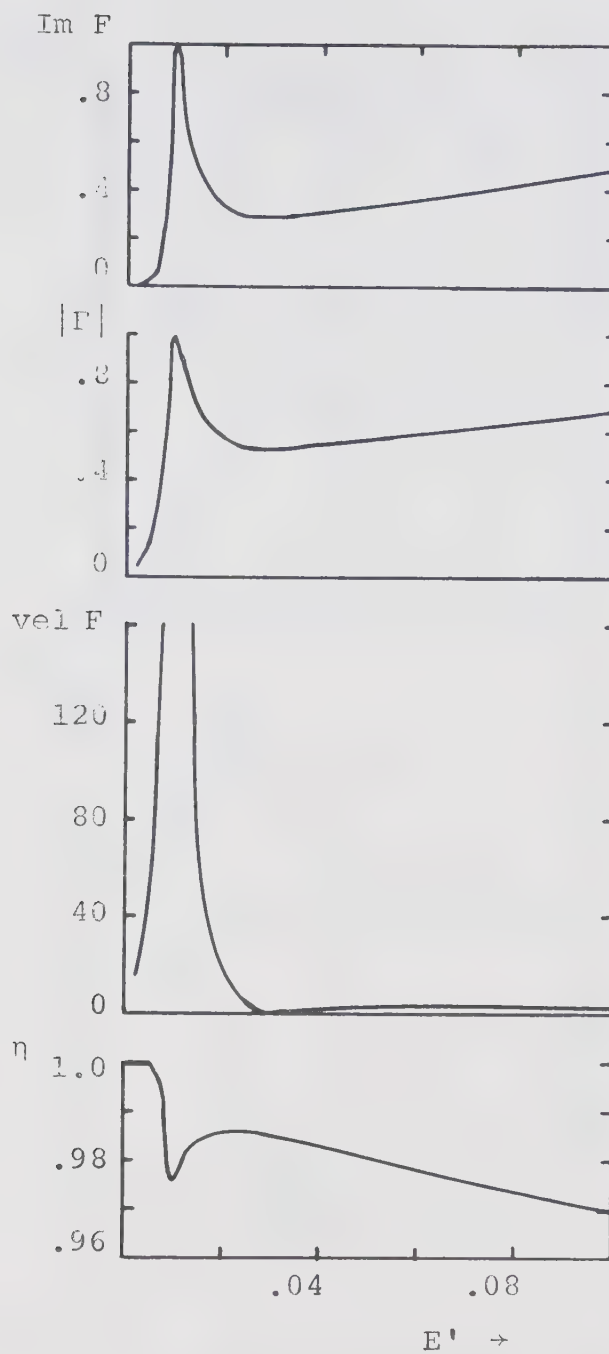


Figure 2C.7. $\text{Im } F$, $|F|$, $\text{vel } F$ and η for
 $g_{11} = -10.420 \text{ m}^3$, $g_{12}^2 = 4 \text{ m}^6$ and $(k_O/m)^2 = .005$.

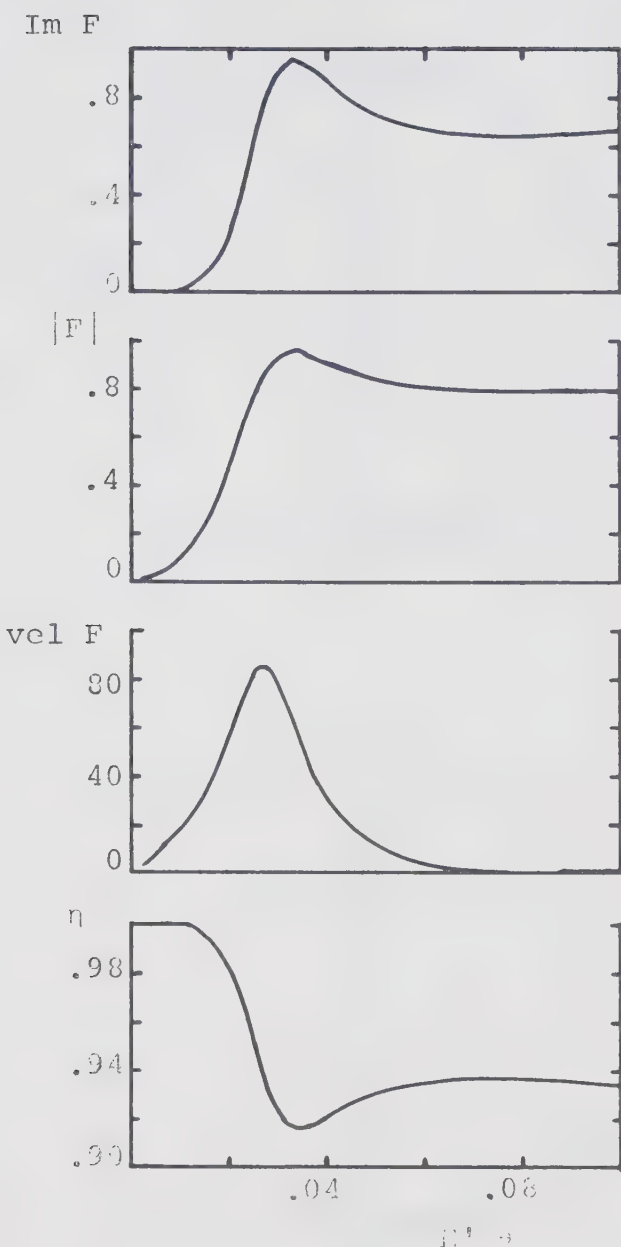


Figure : BC.8. $\text{Im } F$, $|F|$, $\text{vel } F$ and η for
 $g_{11} = -9.800 \text{ m}^3$, $g_{12}^2 = 6 \text{ m}^6$ and $(k_\infty/m)^2 = .005$.

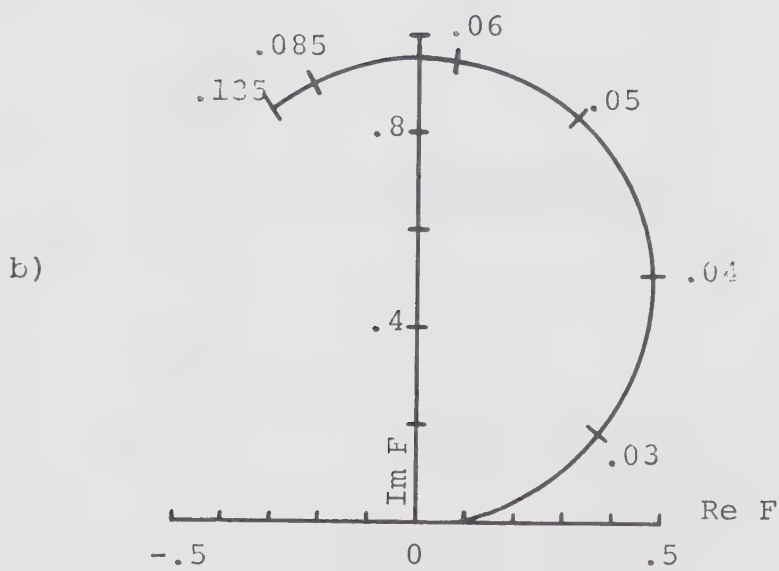
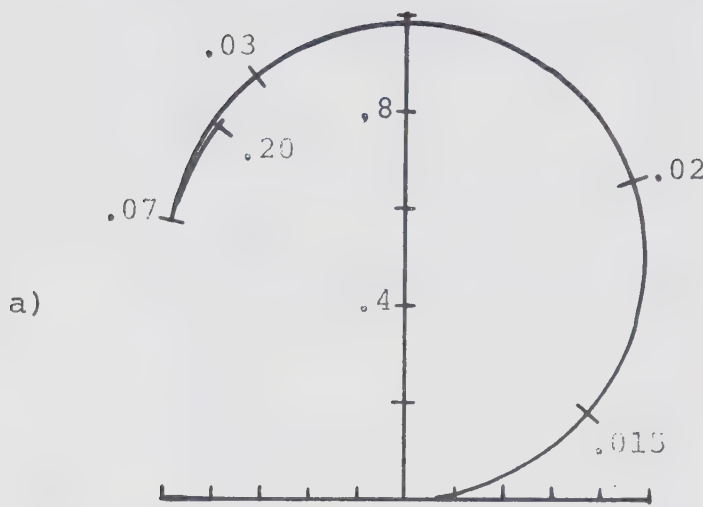


Figure 2C.9. a) Argand diagram for $g_{11} = -10.129 \text{ m}^3$,
 $g_{12}^2 = 4 \text{ m}^6$ and $(k_O/m)^2 = .01$.

b) Argand diagram for $g_{11} = -9.370 \text{ m}^3$,
 $g_{12}^2 = 6 \text{ m}^6$ and $(k_O/m)^2 = .01$.

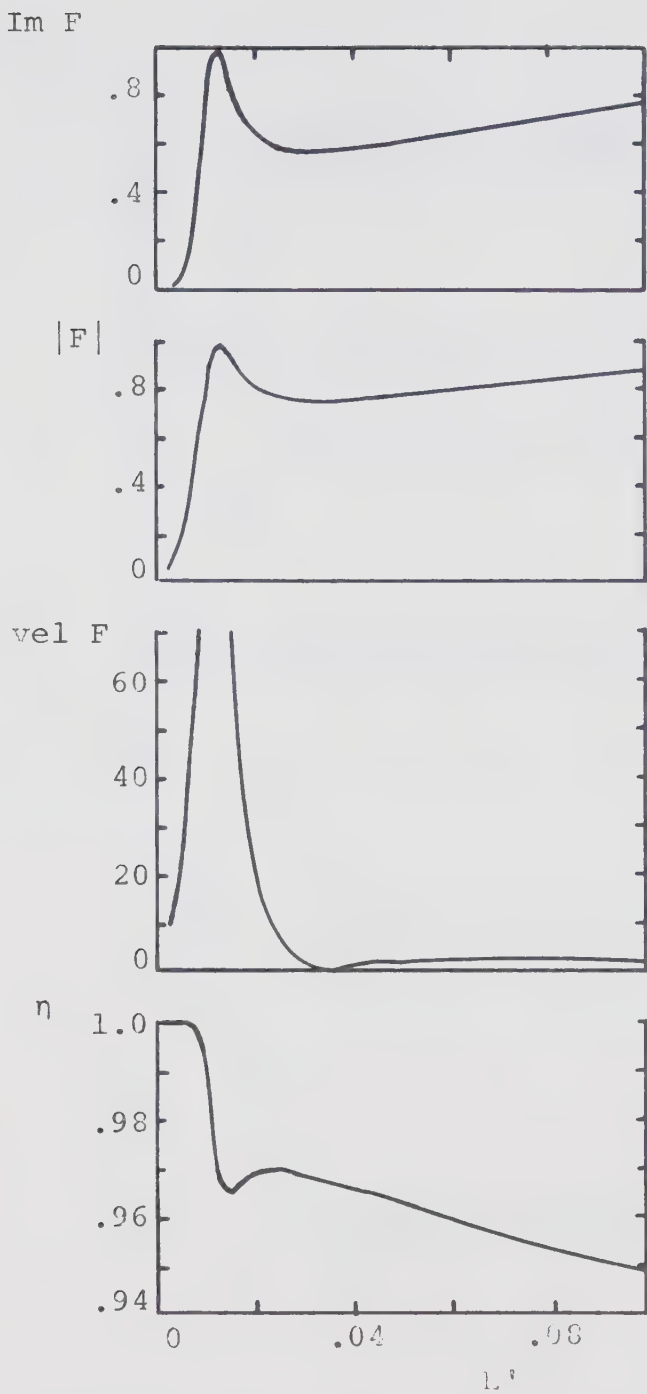


Figure 2C.10. $\text{Im } F$, $|F|$, $\text{vel } F$ and η for
 $g_{11} = -10.129 \text{ m}^3$, $g_{12}^2 = 4 \text{ m}^6$ and $(k_o/m)^2 = .01$.

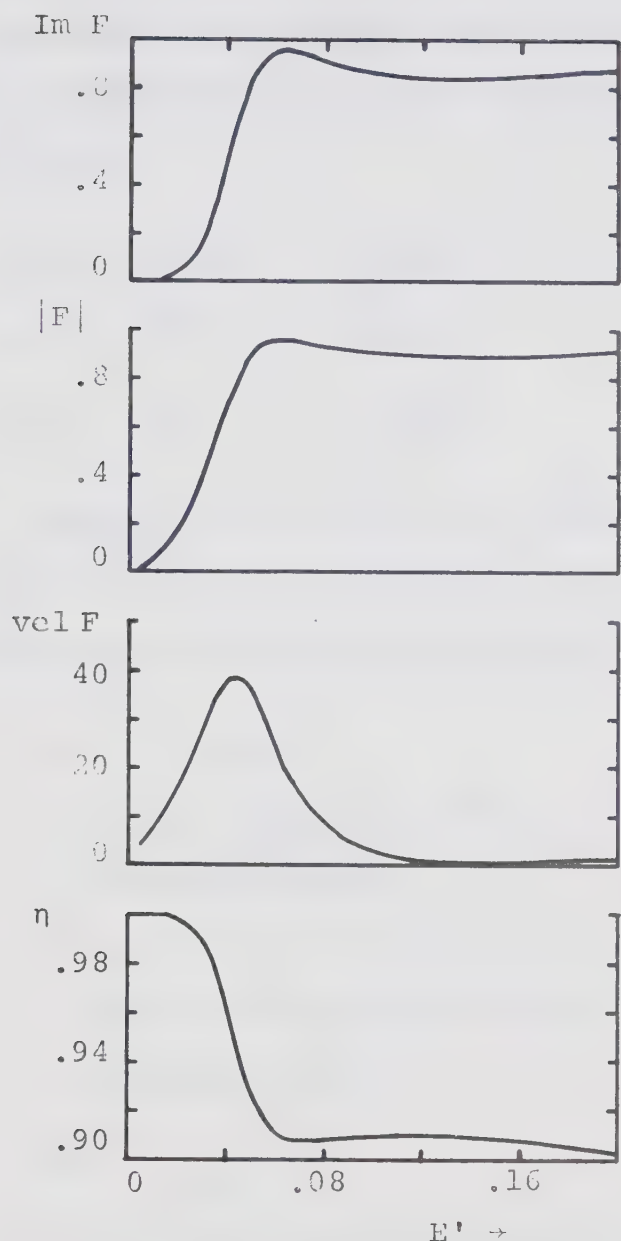


Figure 2C.11. $\text{Im } F$, $|F|$, $\text{vel } F$ and n for
 $g_{11} = -9.370 \text{ m}^3$, $g_{12}^2 = 6 \text{ m}^6$ and $(k_o/m)^2 = .01$.

Summary

The resonance recognition criteria were tested in three different models with potentials $v_{ij}(r,r') = g_{ij}v(r)v(r')$,

- A. $v(r) = \delta(r-a)$, S-wave
- B. $v(r) = e^{-mr}$, S-wave
- C. $v(r) = e^{-mr}$, P-wave .

In each of the above three cases exact solutions were obtained for the scattering amplitude. Resonances were produced by different mechanisms listed below:

- A. $\delta(r-a)$, S-wave
 - 1) $g_{11} > 0$, trapping mechanism provided by the potential barrier.
 - 2) $g_{11} < 0$, standing wave produced by the double velocity change occurring at the sharp edges of the potential.
- B. e^{-mr} , S-wave
 - 1) Sufficiently repulsive potential in the first channel ($g_{11} > 0$) such that the phase shift crosses -90° at some energy and crosses -90° again while returning to zero value for large energies. It is the second crossing of $\delta = -90^\circ$ line which has all the properties of a resonance.

2) Bound state in the second channel seen in the first channel as a resonance, through inter-channel coupling.

C. e^{-mr} , P-wave

1) $g_{11} < 0$ trapping mechanism provided by the centrifugal barrier.

For each one of the above cases the values of $\text{Im } F_{11}$, $|F_{11}|$, $\text{vel } F_{11}$ and η (where applicable) were obtained both for the un-coupled and the coupled cases. The resonances were then identified through the criteria

- i) $\max \text{Im } F_{11}$
- ii) $\max |F_{11}|$
- iii) $\max \text{vel } F_{11}$
- iv) $\min \eta$.

The resonance energy was then compared with the theoretically defined location of resonance, namely, $\text{Re } \det[D] = 0$. The plots of $\text{Im } F_{11}$, $|F_{11}|$, $\text{vel } F_{11}$ and η as functions of energy signalled presence of resonances through their maxima or minima, as the case may be. The locations of the resonances were read out from the computer printouts of these quantities. The results can be summarized as follows.

Max Im F_{11} and max $|F_{11}|$

The similarities between these two criteria render it simpler to discuss them both together. One should recall that those criteria are exact for resonances lying below the inelastic threshold. For resonances lying above the inelastic threshold they are also very good in all the cases studied if the "ill defined" case of table [2A.5] is excepted.

The relative failure of these criteria in showing the resonance in certain cases, especially in the δ -function model, can be understood from the fact that the functions Im F_{11} and $|F_{11}|$ are bounded by unitarity. Because the partial wave amplitude happens to have reached its unitarity bound very near the resonance energy, the two successive maxima overlap and the resonance recognition is difficult (see figure 2A.1). Above the inelastic threshold this problem still exists (see figure 2A.3).

Even though the precision with which the results are presented is not high enough to allow us to discriminate between these two criteria, the last cases of tables 2A.5 and 2C.7 seem to suggest some differences in the resonance energies determined from each of them.

Max vel F_{11}

The velocity criterion appears to be working well only for the few cases where $\text{Im } F_{11}$ and $|F_{11}|$ show very sharp resonance peaks, independently of the particular model considered [see table 2A.5 ($g'_{11} = -9.82, -33.34$), table 2B.2 ($g_{12}^2/m^6 = 1$), table 2C.8 ($g_{11}/m^3 = -10.420, -10.129$) and the corresponding figures]. The energy parameter determined by the velocity criterion is otherwise usually farther away from the exact energy value than the energy produced by the $\text{Im } F_{11}$ and $|F_{11}|$ criteria; this is of course even more so for the single channel problem.

For the δ -function model, there does not seem to be any definite trend for the velocity criterion to produce resonance energies always higher or always lower than the exact ones, but the shift in resonance energy, when it exists, remains on the same side of the exact value for both the single and the corresponding two channel case (see tables 2A.4 and 2A.5). For the two channel exponential S-wave model, the energies produced are always higher than the exact ones and the discrepancy seems to grow with g_{12}^2/m^6 (see table 2B.2), while for the exponential P-wave model the energies are always lower than the exact ones (see tables 2C.6 and 2C.7). Again the same observation on the energy shift can be made for the P-wave model as for the δ -function model.

The velocity criteria, on the other hand, turns out to be very good at signalling the presence of resonances. The fact that it relies on the behaviour of an unbounded function could explain the presence of sharper peaks in vel F_{11} than in $\text{Im } F_{11}$ and $|F_{11}|$. This is particularly true of the P-wave case. However, it must be remembered that in one of the cases studied, namely the S-wave problem with an exponential potential, the velocity criterion failed completely. The total absence of any peak in the velocity plot of figure 2B.1 can be explained from the fact that the partial wave amplitude is almost constant in energy for this case. But it must be remembered that the velocity criterion will always fail in similar situations.

Min η

The η criterion works usually well for the P-wave problem (see table 2C.8) but it seems to indicate slightly higher resonance energies than the max $\text{Im } F_{11}$ and max $|F_{11}|$ criteria. Even if our results are not precise enough to determine which one is the best of these three, they do indicate that the η criterion might be better than the velocity criterion.

For the δ -function model, the resonance energy produced by the η criterion is much too high in one of

the cases (see table 2A.5, $g'_{11} = 16.94$), however, it is nearer to the exact value than the resonance energy determined from the velocity criterion. It should be noted that the max $\text{Im } F_{11}$ and max $|F_{11}|$ criteria also fail in this particular case (table 2A.5, $g'_{11} = 16.94$). Looking at the same table 2A.5 it can be seen that, for $g'_{11} = -33.34$, the resonance energy produced is slightly too low and comparable to the one determined by the velocity criterion.

It is also obvious that for small inelasticity the η criterion will fail, as was the case for some of the P-wave problems (see table 2C.7). Needless to say this criterion is also restricted to resonances lying above the inelastic threshold.

As far as the Argand diagrams are concerned, they turn out to indicate systematically the presence of resonances without any failure; but it must be remembered that the facility with which they can be used to identify resonances in the models studied comes from the fact that the resonant circles are not very much distorted, which is not always the case for diagrams produced from phase shift analyses of experimental data.

Considering the overall problem, it is very difficult to point out the best criterion. For sharp resonances, all four criteria work usually well (see

figures 2A.4, 2A.6, 2C.7, 2C.10 and the corresponding tables). The velocity criterion was the best one for showing the presence of resonances although it failed in one case (see figure 2B.1); it did not seem to be very good in producing the resonance location which is more accurately given by the $\max \operatorname{Im} F_{11}$ and $\max |F_{11}|$ criteria. It is difficult to draw conclusions from our results on the $\min \eta$ criterion and the question remains open whether it could turn out to be convenient for locating highly inelastic resonances.

REFERENCES

- Bertero M., Talenti G. and Viano G.A.: Nucl. Phys., A115, 395 (1968).
- Bjorken J.D.: Phys. Rev. Letters, 4, 473 (1960).
- Burkhardt H.: Dispersion Relation Dynamics. North-Holland (1969).
- Coleman S.: in Theory and Phenomenology in Particle Physics. Editor A. Zichichi, Academic Press (1969) p.658.
- Collins P.D.B., Ross G.G. and Squires E.J.: Nucl. Phys. B10, 475 (1967).
- Dalitz R.H.: Strange-Particles and Strong Interactions. Oxford U. Press (1962).
- Dalitz R.H.: Annual Review of Nuclear Science. Volume 13, p.339 (1963).
- de Alfaro V. and Regge T.: Potential Scattering. North-Holland (1965).
- Donnachie A., Kirsopp R.G. and Lovelace C.: Phys. Letters, 26B, 161 (1968).
- Donnachie A.: Modern Developments in Hadron Physics. Proceedings of the CERN School of Physics, Loma-Koli, Finland (1970).
- Frautschi S.C.: Regge Poles and S-Matrix Theory. W.A. Benjamin Inc. (1963).
- Goldberger M.L. and Watson K.M.: Collision Theory. John Wiley and Sons Inc., Third printing (1967).

- Gradshteyn I.S. and Ryzhik: Tables of Integrals, Series, and Products. Academic Press (1965).
- McVoy K.W., Heller L. and Bolsterli M.: Rev. Mod. Phys., 39, 245 (1967).
- Messiah A.: Mécanique Quantique. Tome II, Dunod (1964).
- Murphy P.G.: Proceedings of the XIII International Conference on High Energy Physics. Berkeley (1966), U. of California Press (1967) p.175.
- Newton R.G.: Scattering Theory of Waves and Particles. McGraw-Hill (1966).
- Phillips R.J.N. and Ringland G.: Nucl. Phys., B13, 274 (1969).
- Plano R.: High Energy Physics. Proceedings of the XV International Conference. Kiev 1970. Naukova Dumka publishers Kiev 1972, p.148.
- Salmeron R.A.: in Subnuclear Phenomena. Editor A. Zichichi, Academic Press (1970) p.366.
- Zachariasen F. and Zemach C.: Phys. Rev. 128, 849 (1962).

Appendix 1

It is shown that for $g_{22}/m^3 = -18$, $g_{11}/m^3 = 0$, $(k_o/m)^2 = 8$ and $(g_{12}/m^3)^2 \leq 16$, the conclusion 2B.35 is true. In this case (see table 2B.2)

$$3.5 < k_{1R}^2 < 5 \quad \text{and} \quad 1.7 < K_{2R} < 2.5 \quad . \quad [1]$$

From eqs. [2B.32] and [2B.33]

$$\begin{aligned} - \left| \frac{\partial \Gamma}{\partial K_{2R}^2} \frac{dk_{1R}^2}{dg_{12}^2} \right| &= \left| - \frac{k_{1R}}{m(m^2+k_{1R}^2)^2} \frac{1}{\kappa(k_{1R})} \left(\frac{g_{12}^2 (k_{1R}^2 - m^2)}{2\{\kappa(k_{1R})\}^2 K_{2R}^3 4m(m^2+k_{1R}^2)^2} \right) \right. \\ &\left. < \frac{k_{1R}}{m(m^2+k_{1R}^2)^2} \frac{1}{\kappa(k_{1R})} \left(\frac{16(4)}{8\{\kappa(k_{1R})\}^2 (1.7)^3 (4.5)^2} \right) \right]. \end{aligned}$$

From [2B.30] and [1]

$$\kappa(k_{1R}) > 1 \quad [2]$$

so that

$$< \frac{k_{1R}}{m(m^2+k_{1R}^2)^2} \frac{1}{\kappa(k_{1R})} \frac{1}{10} \quad . \quad [3]$$

From eqs. [2B.33] and [2B.34]

$$\begin{aligned} \left| \frac{\partial \Gamma}{\partial k_{1R}^2} \frac{dk_{1R}^2}{dg_{12}^2} \right| &= \frac{k_{1R}}{m(m^2+k_{1R}^2)^2} \frac{1}{\kappa(k_{1R})} \left(\frac{g_{12}^2}{(m^2+k_{1R}^2)k_{1R}} \times \right. \\ &\left. \times \left(\frac{m^2-3k_{1R}^2}{2k_{1R}} + \frac{g_{12}^2 k_{1R} (k_{1R}^2 - 5m^2)}{2m^2 (m^2+k_{1R}^2)^3 \kappa(k_{1R})} \right) \frac{(k_{1R}^2 - m^2)}{4m^2 (m^2+k_{1R}^2)^2} \frac{1}{\kappa(k_{1R})} \right) \Big| \end{aligned}$$

and from [1] and [2]

$$\begin{aligned}
 & < \frac{k_{1R}}{m(m^2+k_{1R}^2)^2} \frac{1}{\kappa(k_{1R})} \left(\frac{16}{4.5\sqrt{3.5}} \left(\frac{14}{2\sqrt{3.5}} + \frac{16\sqrt{3.5}(1.5)}{2(4.5)^3} \right) \frac{4}{4(4.5)^2} \right) \\
 & < \frac{k_{1R}}{m(m^2+k_{1R}^2)^2} \frac{1}{\kappa(k_{1R})} \frac{5}{10} \quad . \tag{4}
 \end{aligned}$$

From [2B.29]

$$\frac{\partial \Gamma}{\partial g_{12}^2} = \frac{k_{1R}}{m(m^2+k_{1R}^2)^2 \kappa(k_{1R})} \left(1 - \frac{g_{12}^2 (k_{1R}^2 - 3m^2)}{\kappa(k_{1R}) 4m^2 (m^2+k_{1R}^2)^3} \right)$$

and since

$$\begin{aligned}
 \frac{g_{12}^2 (k_{1R}^2 - 3m^2)}{4m^2 (m^2+k_{1R}^2)^3} & < \frac{16(2)}{4(4.5)^3} < \frac{1}{10} \\
 \frac{\partial \Gamma}{\partial g_{12}^2} & > \frac{k_{1R}}{m(m^2+k_{1R}^2)^2} \frac{1}{\kappa(k_{1R})} \left[1 - \frac{1}{10} \right] \quad . \tag{5}
 \end{aligned}$$

Substituting [3], [4] and [5] in [2B.28] one gets:

$$\begin{aligned}
 \frac{d\Gamma}{dg_{12}^2} & > \frac{k_{1R}}{m(m^2+k_{1R}^2)^2} \frac{1}{\kappa(k_{1R})} \left[\frac{9}{10} - \frac{5}{10} - \frac{1}{10} \right] \\
 & > \frac{k_{1R}}{m(m^2+k_{1R}^2)^2} \frac{1}{\kappa(k_{1R})} \frac{3}{10} > 0 \quad .
 \end{aligned}$$

Hence $d\Gamma/dg_{12}^2 > 0$ and the resonance width increases with increasing value of g_{12}^2 in the special case studied.

Appendix 2

Evaluation of the integral

$$I = \iint_0^\infty G_1''(r, r') e^{-mr} e^{-mr'} dr' dr$$

where

$$G_1'' = -kr < j_1(kr) r > n_1(kr) .$$

$$\begin{aligned} I &= \int_0^\infty \int_r^\infty -kr' n_1(kr') r j_1(kr) e^{-mr} e^{-mr'} dr' dr \\ &\quad + \int_0^\infty \int_0^r -kr' j_1(kr') r n_1(kr) e^{-mr'} e^{-mr} dr' dr \\ &= - \int_0^\infty \int_0^\infty kr' n_1(kr') r j_1(kr) e^{-mr} e^{-mr'} dr' \theta(r' - r) dr \\ &\quad - \int_0^\infty \int_0^\infty kr' j_1(kr') r n_1(kr) e^{-mr} e^{-mr'} \theta(r - r') dr' dr \\ &= -2 \int_0^\infty kr n_1(kr) e^{-mr} \int_0^r r' j_1(kr') e^{-mr'} dr' dr . \end{aligned}$$

In order to evaluate this integral let us write

$$I = \int_{\infty}^m \frac{dI}{dm} dm \quad [6]$$

and calculate dI/dm .

$$\begin{aligned}
 \frac{dI}{dm} &= 2k \int_0^\infty r^2 n_1(kr) e^{-mr} \int_0^r r' j_1(kr') e^{-mr'} dr' dr \\
 &\quad + 2k \int_0^\infty r n_1(kr) e^{-mr} \int_0^r r'^2 j_1(kr') e^{-mr'} dr' dr \\
 &= 2k \int_0^\infty \int_0^\infty r^2 n_1(kr) e^{-mr} r' j_1(kr') e^{-mr'} dr' \theta(r-r') dr \\
 &\quad + 2k \int_0^\infty r n_1(kr) e^{-mr} \int_0^r r'^2 j_1(kr') e^{-mr'} dr' dr \\
 &= 2k \int_0^\infty r' j_1(kr') e^{-mr'} \int_{r'}^\infty r^2 n_1(kr) e^{-mr} dr dr' \\
 &\quad + 2k \int_0^\infty r n_1(kr) e^{-mr} \int_0^r r'^2 j_1(kr') e^{-mr'} dr' dr . \quad [7]
 \end{aligned}$$

Substituting

$$n_1(kr) = \frac{\cos kr}{(kr)^2} + \frac{\sin kr}{kr} \quad \text{and} \quad j_1(kr') = \frac{\sin kr'}{(kr')^2} - \frac{\cos kr'}{kr'}$$

in [7], the integrals can be split into the following ones:

$$\begin{aligned}
 \frac{dI}{dm} &= 2k \int_0^\infty r' j_1(kr') e^{-mr'} \int_{r'}^\infty \frac{1}{k^2} \cos kr e^{-mr} dr dr' \\
 &\quad + 2k \int_0^\infty r' j_1(kr') e^{-mr'} \int_{r'}^\infty \frac{1}{k} r \sin kr e^{-mr} dr dr' \\
 &\quad + 2k \int_0^\infty r n_1(kr) e^{-mr} \int_0^r \frac{1}{k^2} \sin kr' e^{-mr'} dr' dr \\
 &\quad - 2k \int_0^\infty r n_1(kr) e^{-mr} \int_0^r \frac{1}{k} r' \cos kr' e^{-mr'} dr' dr .
 \end{aligned}$$

Each one of these indefinite integrals can be evaluated easily with the help of standard tables (see for example Gradshteyn and Ryzhik 1965).

Using the relations

$$\cos kr j_1(kr) = \sin kr n_1(kr) - \frac{1}{kr}$$

$$\sin kr j_1(kr) = -\cos kr n_1(kr) + \frac{1}{(kr)^2}$$

one gets, after simplification:

$$\begin{aligned}
 \frac{dI}{dm} &= -\frac{2}{m^2+k^2} \int_0^\infty e^{-2mr'} r' dr' - \frac{4m}{(m^2+k^2)^2} \int_0^\infty e^{-2mr'} dr' \\
 &\quad + \frac{4k}{(m^2+k^2)^2} \int_0^\infty \sin kr e^{-mr} dr \\
 &\quad + \frac{2m^2}{k^2(m^2+k^2)^2} \int_0^\infty \frac{e^{-2mr'} dr'}{r'} - \frac{2(m^2+k^2)}{k^2(m^2+k^2)^2} \int_0^\infty \frac{e^{-2mr'} dr'}{r'} \\
 &\quad - \frac{2}{(m^2+k^2)^2} \int_0^\infty \frac{e^{-2mr'} dr'}{r'} + \frac{4}{(m^2+k^2)^2} \int_0^\infty \frac{\cos k_1 r e^{-mr} dr}{r} \\
 &= -\frac{2}{(m^2+k^2)^2} - \frac{1}{2m^2(m^2+k^2)} + \frac{4k^2}{(m^2+k^2)^3} + \frac{4}{(m^2+k^2)^2} \times \\
 &\quad \int_0^\infty \frac{-e^{-2mr} + e^{-mr}}{r} dr - \frac{4}{(m^2+k^2)^2} \int_0^\infty \frac{e^{-mr}(1-\cos kr) dr}{r} \\
 &= -\frac{2}{(m^2+k^2)^2} - \frac{1}{2m^2(m^2+k^2)} + \frac{4k^2}{(m^2+k^2)^3} \\
 &\quad - \frac{2}{(m^2+k^2)^2} \ln \left(\frac{m^2+k^2}{m^2} \right) + \frac{4 \ln 2}{(m^2+k^2)^2} . \quad [8]
 \end{aligned}$$

Substituting [8] in [6], and performing elementary calculations this yields:

$$I = \frac{1}{2k^2 m} + \frac{m}{(k^2 + m^2)^2} + \frac{(4 \ln 2 + 1)m}{2k^2 (k^2 + m^2)} + \frac{(4 \ln 2 + 2)(\tan^{-1}(\frac{m}{k}) - \frac{\pi}{2})}{2k^3}$$

$$- 2 \int_{\infty}^{m'} \frac{\ln(\frac{m'^2 + k^2}{m'^2}) dm'}{(m'^2 + k^2)^2}. \quad [9]$$

To integrate the last term of eq. [9], let us write

$$I_1 = -2 \int_{\infty}^{m'} \frac{\ln(\frac{m'^2 + k^2}{m'^2}) dm'}{(m'^2 + k^2)^2}. \quad [10]$$

Letting $z = k/m'$, $dz = -d(m'/k)/(m'/k)^2$ and substituting in [10], one has

$$I_1 = + \frac{2}{k^3} \int_0^{k/m} \frac{\ln(1+z^2) z^2 dz}{(1+z^2)^2}.$$

Integrating by parts with

$$u = \ln(1+z^2) \quad du = \frac{2z \ dz}{1+z^2}$$

$$dv = \frac{z^2 dz}{(1+z^2)^2} \quad v = -\frac{z}{2(1+z^2)} + \frac{\tan^{-1} z}{2}$$

one gets

$$\begin{aligned}
 I_1 &= \frac{2}{k^3} \left(\ln(1+z^2) \left(-\frac{z}{2(1+z^2)} + \frac{1}{2} \tan^{-1} z \right) \right|_0^{k/m} \\
 &- \int_0^{k/m} \left(-\frac{z}{2(1+z^2)} + \frac{1}{2} \tan^{-1} z \right) \frac{2z dz}{1+z^2} \\
 &= -\frac{1}{mk^2} \frac{\{\ln(1+(\frac{k}{m})^2) + 1\}}{1 + (\frac{k}{m})^2} + \frac{1}{k^3} \tan^{-1}(\frac{k}{m}) \\
 &+ \frac{1}{k^3} \int_0^{k/m} \frac{\ln(1+z^2) dz}{1+z^2} . \quad [11]
 \end{aligned}$$

To integrate the last term of eq. [11], let us make the change of variable $z = \tan \theta$. Then $dz = \sec^2 \theta d\theta$, and

$$\begin{aligned}
 I_2 &= \frac{1}{k^3} \int_0^{\tan^{-1}(k/m)} \ln(\sec^2 \theta) \frac{\sec^2 \theta d\theta}{\sec^2 \theta} \\
 &= \frac{1}{k^3} \int_0^{\tan^{-1}(k/m)} \ln(\frac{1}{\cos^2 \theta}) d\theta \\
 &= -\frac{2}{k^3} \int_0^{\tan^{-1}(k/m)} \ln(\cos \theta) d\theta \\
 &= \frac{2}{k^3} L(\tan^{-1}(\frac{k}{m})) . \quad [12]
 \end{aligned}$$

where $L(x)$ is the Lobachevskiy function.

Substituting [12] in [11] and [11] in [9], one finally gets:

$$\begin{aligned}
 I &= \frac{1}{m^3} \left(\frac{1}{2} \left(\frac{m}{k} \right)^2 + \frac{1}{[1 + (\frac{k}{m})^2]^2} + \frac{\left(2 \ln 2 - \frac{1}{2} \right) \left(\frac{m}{k} \right)^2}{[1 + (\frac{k}{m})^2]} \right. \\
 &\quad \left. - 2 \ln 2 \left(\frac{m}{k} \right)^3 \tan^{-1} \left(\frac{k}{m} \right) - \frac{\left(\frac{m}{k} \right)^2 \ln \left(1 + \left(\frac{k}{m} \right)^2 \right)}{[1 + (\frac{k}{m})^2]} \right. \\
 &\quad \left. + 2 \left(\frac{m}{k} \right)^3 L \left(\tan^{-1} \left(\frac{k}{m} \right) \right) \right)
 \end{aligned}$$

B30073